THE ROLE OF ATF4 IN MEDIATING SKELETAL MUSCLE FUNCTION IN RESPONSE TO ACUTE CONTRACTILE ACTIVITY

VICTORIA C. SANFRANCESCO

A THESIS SUBMITTED TO THE FACULTY OF GRADUATE STUDIES IN PARTIAL FULFILLMENT OF THE REQUIREMENTS FOR THE DEGREE OF

MASTER OF SCIENCE

GRADUATE PROGRAM IN KINESIOLOGY AND HEALTH SCIENCE

YORK UNIVERSITY

TORONTO, ONTARIO

AUGUST 2023

ABSTRACT

To maintain homeostatic conditions under cellular stress, mitochondria possess the ability to initiate a nuclear retrograde signaling response to counteract the initial stressor and restore optimal organellar functioning. The Integrated Stress Response (ISR) is a newfound mitochondrial quality control stress mechanism that is activated in the face of intraorganellar stress and is capable of transducing various transcriptional responses in a manner dependent on the activating transcription factor 4 (ATF4). Mitochondrial homeostatic conditions can be challenged by acute contractile activity/exercise, activating the ISR. Using a mouse model, we sought to determine the responsiveness of the ISR and ATF4 to acute contractile activity of hindlimb muscle. Our data suggest that both the ISR and its effector, ATF4, are activated with contractile activity-induced stress at various stages. However, the precise mitochondrial stress that occurs with contractile activity and leads to the activation of the ISR and ATF4, remains to be elucidated.

ACKNOWLEDGEMENTS

I'd like to dedicate my MSc degree to my late grandfather, Nonno Frank, who left us in 2021. Thank you for being my advocate and teaching me to be diligent and courageous.

To my parents, thank you. You have both supported me throughout my university experience and gave me the confidence to pursue the path that I have chosen. You believed in me even in times when I couldn't believe in myself. I couldn't be here without the help from you both, and I only hope to make you proud.

To my partner Robert, thank you for being undoubtably by my side throughout this process and keeping me grounded in stressful times. You always reaffirm the reasons why I'm meant to take this path in life and help me acknowledge my own strengths in times when I can't recognize them. I truly am lucky to have you in my life.

To my supervisor Dr. David Hood, thank you. Your mentorship, guidance, and unwavering support has helped me garner the skills and confidence I have today. I truly am excited to continue to grow as a scientist in my PhD work with you.

To my lab colleagues, past and present, I thank you all for your willingness to help and support me throughout this degree. To Jonathan, thank you for teaching me everything I know to this point in my academic career. I aspire to obtain your level of critical thinking and intelligence one day. To Neushaw, Mikhaela, Jenna, Sabrina, Priyanka and Kate, I appreciate every single one of you for not only being outstanding lab mates, but also incredible friends. I will cherish the bond that we have developed indefinitely. I look forward to seeing you all thrive in your future endeavours.

TABLE OF CONTENTS

LIST OF FIGURES

CHAPTER 1: REVIEW OF LITERATURE

CHAPTER 2: MANUSCRIPT

APPENDIX B: ADDITIONAL DATA

LIST OF TABLES

CHAPTER 2: MANUSCRIPT

APPENDIX A: DATA AND STATISTICAL ANALYSIS

LIST OF ABBREVIATIONS

AARE	Amino acid response element
ADP	Adenosine diphosphate
AIF	Apoptosis-inducing factor
AMP	Adenosine monophosphate
AMPK	AMP-activated protein kinase
ANOVA	Analysis of variance
ARE	Antioxidant response element
ATF2	Activating transcription factor 2
ATF4	Activating transcription factor 4
ATF5	Activating transcription factor 5
ATFS-1	Activating transcription factor associated with stress-1
ATP	Adenosine triphosphate
BiP	Binding immunoglobin protein
C/EBP	CCAAT-enhancer binding protein $\alpha/\beta/\gamma/\delta$
Ca^{2+}	Calcium ion
CaMK	Ca^{2+}/calmodulin-dependent protein kinase
cAMP	cyclic AMP
CARE	C/EBP-ATF response element
CDS	Coding DNA sequence
ChaC1	ChaC glutathione specific gamma-glutamylcyclotransferase 1
CHOP	C/EBP homologous protein
ClpP	Caseinolytic mitochondrial matrix peptidase proteolytic subunit
Cpn10	10kDa chaperonin, mitochondrial
CRE	cAMP response element
CREB	cAMP response element-binding protein
DHPR	Dihydrogen pyridine receptor
E-box	Enhancer box
eIF2B	Eukaryotic translation initiation factor 2B subunit alpha
eIF2α	Eukaryotic translation-initiation factor-2 alpha
EM	Electron microscopy
EndoG	Endonuclease G
ER	Endoplasmic reticulum
ERR	Estrogen related receptor
ETC	Electron transport chain
FAD^+	Flavin adenine dinucleotide
$FADH_2$	Flavin adenine dinucleotide (reduced)
FTR	Fast-twitch red
FTW	Fast-twitch white
GCN2	General control nonderepressible 2 (serine/threonine protein kinase)
GDP	Guanine diphosphate
GEF	Guanine exchange factor
GTP	Guanine triphosphate
H^+	Hydrogen ion
H_2O_2	Hydrogen peroxide

HDAC	Histone deacetylase
HRI	Heme-regulated inhibitor
HSP10	10 kDa heat shock protein
HSP60	60 kDa heat shock protein
HSP70	70 kDa heat shock protein
HSP90	90 kDa heat shock protein
IM	Intermembrane
IMF	Intermyofibrillar
IMM	Inner mitochondrial membrane
IMS	Intermembrane space
ISR	Integrated stress response
JNK	c-jun N-terminal kinase
LC3	Microtubule-associated proteins 1A/1B light chain 3A
LonP	Lon protease
MAPK	Mitogen-activated protein kinase
MEF2	Myocyte enhancer factor 2
MHC	Myosin heavy chain
MPP	Mitochondrial processing peptidase
MQC	Mitochondrial quality control
mRNA	Messenger RNA
MSF	Mitochondrial import stimulation factor
mtDNA	Mitochondrial DNA
mtHSP70	75 kDa mitochondrial heat shock protein
mTORC1	Mammalian/mechanistic target of rapamycin complex 1
mtPTP	Mitochondrial permeability transition pore
MTS	Mitochondrial targeting sequence
MURE	UPRmt response element
NAD^+	Nicotinamide adenine dinucleotide
NADH	Nicotinamide adenine dinucleotide (reduced)
NRF-1/2	Nuclear respiratory factor-1 and -2
NuGEMPs	Nuclear genes encoding mitochondrial proteins
OM	Outer membrane
OMA1	Optic atrophy 1
OMM	Outer mitochondrial membrane
OXPHOS	Oxidative phosphorylation
P-AMPK	Phospho-AMPK
P-CaMK	Phospho-CaMK
P-P38 MAPK	Phospho-p38 MAPK
P-JNK	Phospho-JNK
P21	Cyclin-dependent kinase inhibitor 1 or CDK-interacting protein 1
P300	E1A-associated protein p300
P38 MAPK	38kDa mitogen-activated protein kinase
P53	Tumor Suppressor protein 53
p62/SQSTM1	Sequestosome 1
PAM	Presequence translocase-associated motor
PERK	Protein kinase R-like ER kinase

PGC-1α	PPAR gamma coactivator 1 alpha
PHD	Prolyl-4-hydroxylase domain
PIC	Preinitiation complex
PIM	Protein import machinery
PINK1	PTEN-induced kinase 1
PKR	Protein kinase RNA-activated
PP1	Protein phosphatase 1
PPARs	Peroxisome proliferator-activated receptors (alpha, beta, gamma)
PUMA	p53 upregulated modulator of apoptosis
qPCR	Quantitative polymerase chain reaction
REs	Response elements
RNA	Ribonucleic acid
ROS	Reactive oxygen species
rRNA	ribosomal RNA
RyR	Ryanodine receptor
SAM	Sorting and assembly machinery
SCF	SKP1, CUL1, F-box protein (SCF) complex
SCI	Spinal cord injury
SIRT1	Sirtuin 3
SS	Subsarcolemmal
STR	Slow-twitch red
TAD	Transactivation domain
TC	Ternary complex
Tfam	Mitochondrial transcription factor A
TIM	Translocase of the inner membrane
TOM	Translocase of the outer membrane
tRNA	Transfer RNA
ULK-1	Unc-51 like kinase 1
uORF	Upstream open reading frame
UPRmt	Mitochondrial unfolded protein response
USF-1	Upstream stimulatory factor 1
YME1L1	YME1 Like 1 ATPase
β-TrCP	β-transducin repeat-containing protein
Δp	Proton motive force
$\Delta\Psi$	Mitochondrial membrane potential

CHAPTER 1:

REVIEW OF LITERATURE

1.0. SKELETAL MUSCLE

Skeletal muscle comprises approximately 40% of total human body mass, and contributes significantly to multiple whole-body, intracellular and molecular functions [1]. From a mechanical point of view, this organ can harness the chemical energy stored in the pyrophosphate bonds of ATP and produce mechanical energy to facilitate and maintain locomotion, respiration and posture [1-3]. Metabolically, skeletal muscle regulates whole-body energy expenditure at both basal and active states, substrate utilization, glucose homeostasis and heat production [1-3]. To sustain such functions during the onslaught of altered energy demands/stressors, skeletal muscle is capable of undergoing profound morphological, physiological and biochemical phenotypic adaptations [4]. This relates to its well-known classification of being a highly dynamic and "plastic" tissue within the human body [4]. Nonetheless, the importance of this organ in mediating such functions has driven a vast interest in the scientific community to extensively explore the physiological mechanisms responsible for its malleability in response to a plethora of deleterious conditions and external stressors. However, although it is universally acknowledged that skeletal muscle is perhaps one of the major determinants of human health and quality of life, the precise molecular mechanisms responsible for such immense adaptive capabilities have not yet been fully elucidated.

1.1. Skeletal Muscle Physiology

1.1.1. Structure

To fully appreciate and understand the molecular mechanisms that govern skeletal muscle function, its malleability, and importance in mediating physiological health, it is critical to first recognize its unique morphological constituents. At the whole tissue level, skeletal muscle is comprised of highly organized elongated and cylindrical multinucleated muscle fibers, termed 'myofibers', that are arranged in a parallel manner and encased in a layer of connective tissue [1]. Each myofiber represents a single muscle cell and consists of multiple bundles of myofibrils that

contain the basic contractile units termed sarcomeres, repeated across the length of the fiber, owing to its striated appearance [5]. Sarcomeres are composed of the overlapping myofilament proteins, actin and myosin, which interact physically to form the actin-myosin cross-bridge [6]. This complex is necessary to facilitate muscle contractions and force production in an ATP-dependent manner, which is recognized as excitation-contraction (EC) coupling [6]. Located within the periphery of the myofiber, beneath the sarcolemma, lie the myonuclei, that regulate the expression of muscle and intracellular gene products in response to various stimuli and myogenic regulatory factors [7]. A multitude of debilitating conditions that reduce the extent of energy expenditure and activation of skeletal muscle drastically attenuates the number of functional myonuclei, contributing to the enhancement of localized muscle atrophy [8-10]. In adult muscle, specialized progenitor cells known as satellite cells which are normally in a quiescent state, reside under the basal lamina and can contribute to the myonuclei population or muscle growth/regeneration once provoked by several factors [11]. Along with the muscle fiber population, skeletal muscle is also embedded with various tissues that support efficient muscle energy production and cellular homeostasis, such as α-motoneurons for muscle innervation and capillaries for oxygenation and nutrient transport [12, 13]. Coordinated activity between each of these components is essential for dictating the state of muscular health and associated motor activity [5]. Aberrations to either constituents of this organ results in the decline of muscle health and function.

1.1.2. Fiber Types

Mammalian skeletal muscle was elucidated to be heterogenous in nature from pioneering work conducted in the early 1950's-60's. Through the use of various biochemical assays and histochemical myofibrillar ATPase analyses, it was established that muscle is comprised of Type I and II fibers [14,15]. Following this, immense literature focused on further classifying these

fibers by examining the expression of the myosin heavy chain isoforms (MHC) and metabolic enzyme analyses via immunoprobing assays, which indeed confirmed and lead to the distinct classification of the four major fiber types, within the Type I and II classifications, present in mammalian muscle [16]. The standard muscle fiber type classifications are as followed: 1) slow-twitch red (STR) fibers predominantly comprised of the MHC Type 1 isoform (Type 1), 2) fast-twitch red (FTR) fiber containing mostly MHC Type IIa isoforms (Type IIa), and 3) fast-twitch white (FTW) fibers which contain mostly Type IIx or IIb MHC isoforms (Type IIx, Type IIb), where the latter is only present in rodents [16, 17]. These standard classifications based off MHC expression are used vastly in the muscle physiology realm, however, fiber type characteristics are also further reflected in the variability between the following physiological parameters: 1) calcium handling and respective twitch kinetics, 2) relative mitochondrial content, 3) expression of oxidative and glycolytic enzymes, 4) extent of vascularization and relative diffusion distances, 5) isoforms of excitation-contraction coupling proteins, and 6) properties of motor units and their rate of recruitment [18-25]. Phenotypically, Type I (STR) fibers are the most fatigue resistant, highly oxidative and thereby recruited during low intensity endurance exercises, however, their maximal force production is less than that of the Type II fiber group [16-18]. Type IIa (FTR) fibers are mixed oxidative-glycolytic and are thus fast contracting yet fatigue resistant, as well as recruited at increasing intensities of endurance exercise, thereby commonly classified as the “intermediate” fiber type between Type I and Type IIx/IIb [16-18]. On the other hand, Type IIx/b muscles (FTW), contain a high glycolytic capacity, exhibit faster contractile activity at greater forces, and are recruited at high-intensities or during phasic exercises, yet they are more fatigable than the previously discussed fiber types [16-18]. In whole muscle groups the different fiber types are normally interspersed, forming what is called a mosaic pattern, and thus the proportion of each

fiber type can vary from muscle to muscle [16]. For instance, the human soleus muscle (slow) is comprised of 64% Type I, 19% Type IIa and 17% Type IIx, whereas the gastrocnemius muscle, which is often denoted as a mixed muscle, contains 52% Type I, 31% Type IIa and 16% Type IIx [26].

Thought to be mostly static in nature, the fiber type profile in adults has been shown to exhibit contractile and metabolic plasticity. Indeed, there is overwhelming evidence stating that muscle fibers possess the capacity to adapt and convert from one type to another following periods of exercise and disuse [27]. The most common fiber type proportion alterations/conversions are seen between Type IIa and Type IIx/IIb fibers, during mechanical overload or endurance training, which enhances the pool of Type IIa fibers while reducing the proportion of Type IIx/b [28]. The conversion of Type IIa to Type IIx/b fibers is possible in cases of spinal cord injury (SCI) [29]. Lastly, Type I fiber conversions are most often seen in animal models under extremely high workloads, however this application to humans is far more extensive to observe [27].

Nonetheless, these differences in fiber types are based on the diverse protein/enzyme isoforms, which govern the phenotypic differences observed between fiber types.

1.1.3. Skeletal Muscle Mitochondria: The Powerhouses of the Cell

1.1.3.1 Mitochondrial Structure

Mitochondria, colloquially termed the powerhouses of the cell, are responsible for mediating the oxidative capacity of skeletal muscle through the provision of ATP from aerobic respiration. These organelles were hypothesized to be derived from endosymbiosis, an evolutionary based theory, in which proteobacteria populated primordial eukaryotic cells through the process of endocytosis more than 1.5 billion years ago [30, 31]. This origin was indeed further supported by the findings that mitochondria retained their own 16 kB circular genome [32]. The mitochondrial genome (mtDNA) only codes for 37 genes, of which 13 are structural genes encoding subunits of

the mitochondrial respiratory chain, 22 tRNAs, and 2 rRNAs, which gives rise to the gene expression machinery [33, 34]. Pioneering evidence from the early 1950's using Electron Microscopy (EM) first defined the distinct structural morphology of mitochondria, which is comprised of two phospholipid bilayer laden membranes termed the outer mitochondrial membrane (OMM) and the cristae dense inner mitochondrial membrane (IMM) [35]. This sub-cellularization correspondingly forms the intermembrane space, between the OMM and IMM, and the mitochondrial matrix, the innermost biochemically active space bound by the IMM [36]. Furthermore, the IMM contains extensive foldings termed cristae which increases the IMM surface area and houses the electron transport chain (ETC) complexes [36]. Thus, the relative cristae density is proportional to mitochondrial performance and bioenergetic capacity [37]. Indeed, these structural components are critical in mediating mitochondrial function and health. In particular, the OMM is porous and allows small molecules to diffuse into intermembrane space [38]. On the other hand, the IMM houses specialized protein import machinery (PIM) that is highly selective and strictly regulates protein import into the mitochondrial matrix. This regulation is necessary as the mitochondrial matrix milieu is a critical determinant of mitochondrial function and houses the mtDNA, which is highly suspectable to oxidative damage [36].

Within skeletal muscle, mitochondria exist as an interconnected reticulum which enhances the flow of ions, protein, lipids, mtDNA and sustains efficient energy generation along the network [39]. Thus, it is critical to maintain this network and be able to adapt to energetic stressors that may impose and diminish mitochondrial health. This maintenance is regulated by mitochondrial dynamic events termed fission and fusion, which remove dysfunctional mitochondrial or expand the network, respectively [40].

1.1.3.2. Mitochondrial Subfractions

It has been extensively revealed that skeletal muscle contains two subcellular mitochondrial populations, one residing beneath the sarcolemma (SS mitochondria) and the other between myofibrils (IMF mitochondria), which serve distinct physiological roles and differ in their morphological and biochemical characteristics [41-44]. SS mitochondria reside in clusters directly below the sarcolemma of the muscle fiber and lie within proximity to the myonuclei. This population of mitochondria is characterized by their distinct morphology as they present as large, punctate globules [45, 46]. Due to their locale, SS mitochondria largely provide ATP to drive membrane functions, such as the coupling of ATP-driven ion pumps, as well as support the energetic demands of myonuclear gene expression [45, 46]. Conversely, IMF mitochondria are primarily found intermingled within the myofibers, and comprise approximately 80% of mitochondrial content within muscle [45, 46]. This subpopulation exists in a more reticular network with branches that extend adjacent to sarcomeres. Thereby, IMF mitochondria support the cellular energy demand required for the interaction between actin and myosin and thus muscle contractile events [47, 48]. Over the past half-century, these subfractions have been experimentally isolated to elucidate their differing properties and their capacity to adapt following various conditions. Evidence suggests that SS mitochondria experience enhanced alterations (positive or negative) in comparison to the IMF subfraction during conditions of chronic muscle use and disuse [49-54]. This inherent difference may be attributed to their cellular location and regulation of protein import, which thus construes the differential "sensitivity" in response to common changes in the cellular environment [54]. Compared to IMF mitochondria, the SS fraction displays greater exercise-induced increases in volume and membrane potential, however, they also show more pronounced decrements of mitochondrial function in response to muscle disuse [51, 53-56]. On

the other hand, IMF mitochondria basally possess higher enzymatic activity, respiratory and protein synthesis rates, as well as elevated import rates of precursor proteins [57]. Nevertheless, these diverse properties and characteristics of the mitochondrial subfractions support the multitude of molecular mechanisms that require sufficient energy to not only support muscle homeostasis, but to also maintain optimal muscle health.

1.1.3.3. Mitochondrial Function

In 1957, Philip Siekevitz branded the mitochondria as the "powerhouses of the cell" for their efficient capacity to produce ATP via oxidative phosphorylation [58]. Since then, it has become apparent that mitochondria indeed also play a crucial role in regulating multiple cellular signaling events both basally and in response to energetic stress [59]. This is in part due to their distinct morphological properties within muscle fibers and their ability to communicate with peripheral organelles following changes in the molecular environment [48, 60]. Notably, these cellular events include calcium handling, redox homeostasis and programmed cell death (mitochondrially-mediated apoptosis). Briefly, mitochondria are capable of up-taking free cytosolic Ca^{2+} to maintain intracellular homeostatic levels of Ca^{2+} [61]. It has been identified that Ca^{2+} entry in the mitochondria promotes ATP production by stimulating the Krebs' cycle and electron transport chain activity and is thereby beneficial under normal physiological conditions [62]. However, this regulation is indeed a double-edged sword as excessive Ca^{2+} accumulation in mitochondria can initiate a cascade of deleterious signaling events, which consequently leads to mitochondrial dysfunction [63]. Moreover, it is widely accepted that redox signals to and from mitochondria are at the core of a wide variety of biological processes, including cell proliferation and differentiation, adaptation to hypoxia, autophagy, immune function, and hormone signaling [64]. The most studied and best characterized mitochondrial redox signaling molecule, acting as a second messenger, is

H_2O_2, which has a plethora of signaling targets such as PGC-1α, p53 and c-Jun N-terminal kinase, thereby initiating signaling events that contribute to cellular and phenotypic adaptations [65, 66]. Lastly, mitochondria can initiate cellular apoptosis in response to changes in mitochondrial function or physiological environment [8-10, 51]. For instance, when there is an overload of Ca^{2+} or a severe accumulation of ROS within the mitochondrial matrix that cannot be scavenged, the opening of a mitochondria permeability transition pore (mtPTP) is triggered, which consequently leads the release of mitochondrial-laden apoptotic factors, cytochrome c, AIF and EndoG [8-10, 67]. These factors induce nuclear DNA fragmentation and thus nuclear decay. Nonetheless, the process of generating ATP should not be overlooked as it is still one of the major mitochondrial functions and reason for the immense popularity of this organelle in molecular biology. In that regard, mitochondria produce ATP via a series of redox reactions by utilizing the substrates generated from Krebs' cycle. Precisely the substrates NADH and $FADH_2$ donate a pair of electrons to the Electron Transport Chain (ETC) Complex I (NADH dehydrogenase) and Complex II (Succinate dehydrogenase), respectively. The electron flow is coupled with the generation of a proton gradient across the inner membrane from the matrix into the intermembrane space (IMS) [68]. The donated electrons are then subsequentially passed through a chain of cofactors, ubiquinone (Q), downstream complex and cytochrome c to their final destination, Complex IV (cytochrome c oxidase) where molecular oxygen acts as a terminal electron acceptor and is reduced to water [69]. The movement of protons from the mitochondrial matrix into the intermembrane space creates a protonmotive force (Δp), which is the proton concentration (pH) combined with the electrochemical proton gradient, known as the mitochondrial membrane potential ($\Delta\Psi$) [68, 69]. The production of ATP from ADP is coupled to the dissipation of the protonmotive force by the pumping of H^+ back into the matrix through Complex V (F0/F1-ATP synthase). This force is

thereby transformed into kinetic energy and is utilized to join inorganic phosphate and ADP [69]. This process is dependent on the cellular levels of ADP imported into the mitochondria via the adenine nucleotide translocase, making this molecule the rate limiting factor in this process. Nonetheless, mitochondria as briefly described, play an incredible role in regulating a variety of critical cellular functions, which contribute to its importance in supporting muscle and human health.

2.0. Adaptations To Exercise

As previously discussed, skeletal muscle is highly adaptive and capable of responding to and matching the energetic demands placed upon it. The lability and metabolic flexibility of this tissue is centrally mediated by mitochondria and their bioenergetic availability. Exercise is a potent external stressor that challenges muscle homeostasis and induces a multitude of cellular adaptations to sustain ideal functioning. During the onset of exercise, intracellular concentrations of ATP are reduced, causing an energy deficit [70]. This insufficiency elicits various intracellular responses/changes to appropriately match the newly imposed energetic demand and maintain tissue function. Mitochondria, being the powerhouses of the cell and mediators of skeletal muscle plasticity, drastically respond to this exercise-induced cellular stress by undergoing a myriad of alterations, such as reticulum remodeling/dynamics (biogenesis and mitophagy), to optimize network functioning, supply the required ATP, restore cellular homeostasis, and enhance muscle performance.

Acute exercise has garnered interest in the scientific community due to its ability to initiate robust muscular signal transduction and cellular stress response pathways, which when repeated, are the basis for substantial mitochondrial adaptations, such as in exercise training [71-73]. It has been elucidated that the beneficial effects of exercise typically occur during the recovery period

(~1-48 hours), as there are transient elevations the expression of genes responsible for enhancing the mitochondrial network [72]. With repeated bouts of exercise, followed by sufficient recovery, stark changes in protein content indeed alter the skeletal muscle phenotype and improve overall exercise performance [73, 74].

Our laboratory has optimized an *in situ* model to elicit acute contractile activity/signaling. Substantial work has shown that this protocol is capable of eliciting acute muscle fatigue and can be used to evaluate intracellular signaling events as well as the kinetic properties of the muscle in question (gastrocnemius or tibalis anterior) [75-78]. Briefly, the *in situ* model evokes acute muscle contractile activity via nerve stimulation. With this, experimenters can tightly control and evaluate the stimulus parameters, maintain homeostatic conditions and analyze the mechanical response in real time. Indeed, other groups have also used a modified version of this protocol and have shown an induction of intracellular signaling pathways that are typically seen with whole body exercise paradigms, which will be discussed in a later section [79, 80].

2.1. A Drive for Mitochondrial Biogenesis

Contractile activity, as previously discussed, induces a metabolic stressor to muscle and results in the initiation of muscle plasticity, which is driven by the enhancements/modifications of the mitochondrial reticulum. Pioneering work from John Holloszy first demonstrated that endurance exercise training could induce increases in mitochondrial content, mitochondrial networking and thereby enhance endurance performance [81]. This mitochondrial remodelling event, now commonly termed mitochondrial biogenesis, is recognized as the synthesis and integration of new mitochondria into the pre-existing reticulum and has been thoroughly examined in the context of various exercise paradigms (Fig. 1) [82]. Mitochondrial biogenesis is reliant on the coordinated expression and interaction of both the mitochondrial and nuclear genomes [74].

This unique association is necessary as the majority (99%) of proteins that comprise the organelle (~1200) are derived from the nuclear genome, whereas the remaining 1% are transcribed from mtDNA [83]. The expansion of the mitochondrial network not only requires the finely tuned regulation of both genomes, but also the incorporation of nuclear derived mitochondrial proteins into their respective mitochondrial compartments, a process termed protein import, which will be described in a later section [84]. During exercise, contractile activity-induced signals are known to activate protein modifying enzymes such kinases, phosphatases, and deacetylases that alter the protein conformation and activity [74]. This enzymatic activity ultimately results in a cascade of events that leads to alterations in the expression of both mitochondrial and nuclear gene products, thereby enhancing the rate of protein integration into the expanding reticulum to form ETC complex holoenzymes and produce functional organelles [85]. Following an acute bout of exercise, this drive for biogenesis is indeed transiently observed as there are dramatic increases in the activation of the signaling kinases and their downstream effects on related transcription factors [86]. With exercise training, the cumulative effects of the signaling processes that occur acutely leads to net changes in the expression of mitochondrial proteins thereby increasing mitochondrial content, improving the capacity for oxidative phosphorylation, reducing the requirement for glycolytic activation, and lowering lactic acid production [83-86]. Therefore, the summation of such transient molecular events improves exercise capacity and produces a more oxidative muscle phenotype that is highly fatigue resistant, dictated by enhancements in mitochondrial density and enzyme activity [86].

2.1.1. Molecular Signaling During Exercise

The initiation of mitochondrial biogenesis, and thus muscle adaptations, during exercise training occurs from the early signals induced by repeated (acute) muscle contractions [85-87].

These signals are related to the rapid dynamic events evoked during sarcomere shortening, such as intracellular calcium oscillations, increases in ATP turnover, enhanced ROS production, and oxygen consumption [85, 88, 89]. The magnitude of each signal increases in a proportional manner dependent on the intensity and duration of the contractile effort [83]. The exercise-induced signaling kinases that are particularly involved in the induction of mitochondrial biogenesis include calcium/calmodulin-dependent protein kinase (CaMK), p38 mitogen-activated protein kinase (p38 MAPK), and AMP-activated protein kinase (AMPK) (Fig. 1) [90-95]. During contractile activity, Ca^{2+} is released from the sarcoplasmic reticulum (SR) via the interaction between the dihydropyridine receptor (DHPR) and the ryanodine receptor (RyR), to mediate the activity of the actin-myosin cross-bridges. Elevations in intracellular Ca^{2+} activate calcium/calmodulin-dependent protein kinases (CaMKII, CaMKIV) [96, 97]. Upon activation, the CaMKs phosphorylate the cAMP response element (CRE) binding protein (CREB), thereby stimulating its binding to the CRE element on the promoter region of PGC-1α, the "master regulator" of mitochondrial biogenesis, discussed in a later section, to enhance its transcriptional drive [91]. Furthermore, CaMKIV catalyzes specific phosphorylation events on histone deacetylase complexes (HDACs), leading to their nuclear exclusion and release of their inhibitory action on MEF2 and its transcriptional activity on the PGC-1α promoter [98-100]. Intracellular calcium also activates the phosphatase Calcineurin which dephosphorylates MEF2, further boosting its transcriptional activity [101]. Next, exercise increases ATP hydrolysis and turnover, resulting in a rise in AMP:ATP levels and subsequent activation of AMPK, where it directly phosphorylates PGC-1α post-translationally to enhance its co-transcriptional control [102-104]. Moreover, AMPK can bind to the E-box on the PGC-1α promoter region to drive its expression by interacting with the transcription factor USF-1, thereby contributing to the overall enhancement

of mitochondrial biogenesis [105]. During contractile activity, elevations in ROS production activates the kinase, p38 MAPK, which can phosphorylate the transcription factors CREB, ATF2, MEF2, and p53, enhancing their binding to the PGC-1α promoter [93, 106-108]. Moreover, p38 MAPK can directly phosphorylate PGC-1α in a post-translational manner to promote its stability and enhance its co-transcriptional activity proportionally [109]. Lastly, in this cellular state, the ratio of NAD^+ to NADH increases due to the enhanced oxidative phosphorylation of NADH that emanates from Complex I of the ETC. This change in ratio during a low energy status triggers the activation of the histone deacetylase Sirtuin 1 (SIRT1), located within the nucleus, which will activate PGC-1α by deacetylating specific amino acid residues, thus enhancing its activity [110-112]. Nonetheless, as described, during contractile activity, the regulation of mitochondrial biogenesis is mediated mostly though the enhancement of the transcriptional coactivator PGC-1α. Indeed, the myriad of signals that are evoked during contractile activity ultimately converge on PGC-1α, making this transcription factor the hallmark for mediating mitochondrial biogenesis and adaptations during exercise.

2.1.2. PGC-1α

Peroxisome proliferator activated receptor gamma (PPARγ) coactivator-1a (PGC-1α), as its name suggests, was first identified based on its interaction with the nuclear hormone receptor, PPARγ, during adaptive thermogenesis [113]. Literature has now established the importance of PGC-1α in metabolic organs such as the heart, liver, brain, adipose tissue, and skeletal muscle as it can regulate of a variety of processes ranging from gluconeogenesis, brown fat thermogenesis, muscle fiber type specialization, and oxidative phosphorylation [114, 115]. As illustrated in the former section, PGC-1α is commonly recognized as the “master regulator” of mitochondrial biogenesis (Fig. 1). The intracellular signals invoked during contractile activity converge on its

activation to enhance the expression of nuclear genes encoding mitochondrial proteins, known as NuGEMPs [82-86]. Functionally, PGC-1α is a transcriptional coactivator that is unable to directly bind with the genome but can augment gene transcription by docking with nuclear receptors/transcription factors and additional proteins on the promoter regions of NuGEMPs to induce expressional changes and initiate mitochondrial biogenesis [116-120]. In particular, PGC-1α coactivates multiple transcription factors such as, ERRs, PPARs, and both NRF-1 and -2 [121, 122]. Interactions with the aforementioned nuclear receptors result in the transactivation of a plethora of mitochondrial proteins, including cytochrome c, components of the electron transport chain complexes, mitochondrial import proteins, heme biosynthesis proteins, and transcription factors of mtDNA, such as the mitochondrial transcription factor A (Tfam), which thereby maintains/improves the mitochondrial pool and contributes to exercise induced adaptations [115, 123].

The importance of PGC-1α has been demonstrated in various human, animal and cell culture models in response to exercise and with marked alterations of its expression. For instance, a single bout of exercise in human tissue, initiates the transcription of PGC-1α and its nuclear abundance 3 hrs into recovery which corresponds to an increase in mitochondrial protein content and enzyme activity [124]. Following exercise training, there is an enhancement of the mitochondrial pool and respiratory capacity, concomitant with the repeated induction and activation of PGC-1α seen with acute exercise [84, 125-131]. In contrast, PGC-1α null animals are more exercise intolerant in comparison to wild-type (WT) controls, due to the stark reductions in mitochondrial volume and respiratory capacity, as well elevations in ROS production [132-134]. However, with endurance training, PGC-1α null mice display a similar fold-increase in mitochondrial protein levels compared to controls [132, 135-137]. This reveals possible pathway redundancies or compensatory

mechanisms that exist to improve mitochondrial health in response to exercise. On the other hand, the muscle-specific overexpression of PGC-1α is sufficient to induce a more oxidative muscle phenotype basally, as there are increases in mitochondrial content and a shift towards a greater proportion of oxidative Type 1 fibers (slow-twitch phenotype), improving overall fatigue resistance and exercise performance [114, 138]. Therefore, as highlighted, PGC-1α is a critical transcriptional co-activator that maintains basal mitochondrial content, as well as has a role in mediating exercise adaptations, which thereby emphasizes the importance of understanding it's the regulation not only during exercise but in regard to mitochondrial diseases or myopathies.

2.1.3. Protein Handling Machinery and Import

Since a large proportion of the mitochondrial proteome is derived from nuclear-encoded genes, mitochondrial biogenesis is thus dependent on the efficient import and coordination of nuclear derived mitochondrial precursor proteins into the organelle [82]. In this regard, mitochondria contain a unique and elaborate import system to transport these nuclear-encoded proteins into the mitochondrion to thereby be incorporated into their distinct mitochondrial destination. This import process is highly regulated and occurs via the multi-subunit complexes termed the mitochondrial protein import machinery (PIM), which comprises the translocases of the outer and inner membrane (TOM and TIM, respectively) (Fig. 1) [139, 140]. The specific allocation of the nuclear derived precursor proteins into the mitochondrial sub-compartments is dictated by the mitochondrial targeting sequence (MTS) that is often either located at the N-terminus or as an internal sequence [141]. Nascent precursor proteins, once recognized, are maintained in a recognizable unfolded confirmation and transported to the organelle import site via cytosolic chaperones, such as HSP70 and HSP90, where the import process is initiated by the TOM complex [142]. Mitochondrial matrix destined precursors transit through the OM via the

Tom40 channel and then sequence to the TIM complex, where the precursor passes through the IMs major protein channel, Tim23 [143]. The translocation process through the IM and into the mitochondrial matrix is dependent on the negative membrane potential ($\Delta\Psi$) and the ATP-dependent function of the presequence translocase-associated motor (PAM), which is comprised of mtHSP70 and other associated proteins [144]. Following IM translocation, the transiting precursor proteins are actively pulled into the matrix by mtHSP70 (of the PAM) in an ATP-dependent manner [144]. Once in the matrix, the MTS on the precursor protein is cleaved by mitochondrial processing peptidase (MPP) where it will be refolded by resident chaperones such as HSP60 and chaperonin10 (cpn10) into their mature conformation to thereby be released into the matrix or be incorporated into functional holoenzyme complexes [144]. On the other hand, OM destined proteins are sorted and inserted via a separate group of multi-subunit proteins, termed the SAM complex, once interacted with TOM [145]. Nonetheless, mitochondrial protein import is a highly responsive and dynamic process as its functional rate can be adjusted to match the needs of the cell and thus reflect the drive for mitochondrial biogenesis. For instance, during exercise training, the protein expression of the PIM components are increased, such as Tom20, Tim23 and other constituents, and this coincides with increased rates of protein translocation into the mitochondrion [146, 147]. As well, the cytosolic and mitochondrial chaperones that mediate this import process, HSP70, HSP90, MSF, cpn10, HSP60 and mtHSP70, are also substantially elevated in their expression and content following training [148]. These adaptations and thereby alterations of the PIM following contractile activity (acute and training) are vital to support the augmented drive of mitochondrial biogenesis that occurs with various exercise paradigms, ultimately to support the expansion of mitochondrial reticulum and contribute to improvements in muscle functionality.

It should be noted that stark increases in the rate of protein import, which can occur during the onset of acute unaccustomed exercise-induced stress, can lead to the activation of stress response pathways, notably the Integrated Stress Response (ISR) and the mitochondrial Unfolded Protein Response (UPR^{mt}), described in a later section (Fig. 1). The protein import pathway therefore plays a pivotal role in the maintenance of cellular homeostasis, acting as a sensor of mitochondrial dysfunction and triggering adaptive stress responses. In that regard, during such acute cellular stress, the rate of protein import exceeds the intrinsic capacity of the PIM and chaperones to fold incoming precursor proteins into their mature configuration, which leads to the accumulation of unfolded proteins within the organelle. This accumulation is indeed detrimental as it disrupts the mitochondrial proteostatic status and leads to acute organelle dysfunction, such as enhanced ROS production and impaired functioning. However, the activation of such stress responses contributes to combating such dysfunction via transcriptional regulation in an attempt to return the cell to its homeostatic condition [149, 150].

2.2. A Drive for Selective Mitochondrial Degradation (Mitophagy)

Although contractile activity and exercise training elicits mitochondrial biogenesis to match the energetic demands placed upon the cell, it is also vital to eliminate any segments of the mitochondrial network that are defective and unable to support the metabolic demands which thereby perturb normal muscle physiology and function [52, 151, 152]. This process of elimination is termed mitophagy, a selective form of autophagy specified for degrading dysfunctional mitochondria, to thus improve and maintain the quality of the mitochondrial pool during instances of exercise-induced stress (Fig.1) [153]. When mitochondria produce excessive amounts of ROS in the absence of ATP production and/or exhibit a decrease in their membrane potential, they are thereby classified as dysfunctional and contribute to reductions in the quality of the mitochondrial

pool [154, 155]. Once deemed dysfunctional, the process of selective autophagy ensues, initiated by the flagging of the organelle and degradation via the lysosome. The lysosome contains a highly acidic lumen and a multitude of catalytic enzymes that facilitate the degradation of the damaged organelles into their basic constituents, amino acids, which are released and recycled in the cytosol to support future protein synthesis [155, 156]. The main mitophagy pathway that has been elucidated in skeletal muscle homeostasis and exercise involves the PINK1 and Parkin proteins [151-155]. In functional mitochondria, PINK1 is imported into the mitochondria where it is degraded by resident proteases [157, 158]. However, when mitochondria become dysfunctional, such as during severe exercise-induced cellular stress, PINK1 can no longer be imported due to a loss of PIM functionality [157, 158]. Instead, PINK1 accumulates on the outer membrane of the mitochondria to subsequently facilitate the recruitment of the E3-ubiquitin ligase Parkin to this mitochondrial site [157, 159]. Upon recruitment, Parkin mediates the ubiquitination of the outer membrane proteins for lysosomal degradation. This tagging process initiates a signal for the lipidation of LC3-1 into its active form, LC3-II, mediating the nucleation and growth of the phagophore [160]. Once this basis has begun, the adapter protein p62/SQSTM1 protein anchors the ubiquitinated mitochondria and the LC3-II laden double-membraned phagophore, facilitating the formation of the mature double-membraned autophagosome, encapsulating the dysfunction organelle entirely [161]. Finally, the autophagosome will travel via microtubules in the cell and fuse with the lysosome to degrade the organelle into its basic constituents [162].

In response to the energetic imbalance brought about by acute exercise, similar to biogenesis, mitophagy is also initiated, and this is primarily mediated by the change in the AMP/ATP ratio, leading to the activation of AMPK [162, 163]. Once induced, AMPK, will phosphorylate a downstream target, Unc-51 like autophagy activating kinase 1 (ULK1), at specific residues,

inducing its activation, whilst concurrently inhibiting the known suppressor of the mitophagic pathway, mTORC1 [164, 165]. Following acute exercise, various signaling pathways induce this mitophagic process and thereby enhance the flux/rate of mitochondrial degradation in response to cellular changes in the environment [163, 166, 167]. As well, the intracellular signals that are increased with acute exercise also leads to the enhanced expression of the proteins that mediate the formation of the autophagosome and lysosome, as well as their interaction [163, 166, 167]. However, in response to endurance exercise training, multiple studies have indeed identified that the exercise-induced increase in mitophagy flux was blunted, whist observing increases in the basal expression of mitophagy and lysosomal markers [151, 167]. Such evidence indeed suggests that in response to an acute bout of exercise, mitophagy signaling is elicited to enhance the mitochondrial pool. However, with exercise training, the improvements in mitochondrial function and optimization of mitochondrial pool evident with this mode of exercise reduces the necessity for in mitophagy signaling/drive in comparison to untrained controls.

3.0. Mitochondrial Stress Response Pathways

Mitochondria, given their distinct cellular roles, must maintain homeostatic conditions to sustain an optimal organelle network within skeletal muscle in response to energetically demanding conditions. This regulation and thus adaptative capacity is largely mediated by the distinct processes of mitochondrial biogenesis and mitophagy. However, organisms have evolved multiple mechanisms to recognize and resolve stress and/or dysfunction within the mitochondrial network. This concept of a mitochondrial stress response was first established in pioneering work from Vandana Parikh and colleagues [168], who showed that mitochondrial dysfunction alters nuclear gene expression in yeast. In this regard, it has now been elucidated that mitochondria possess robust intermediary mechanisms to help maintain cellular functioning and thereby enhance

their adaptative capability to various stressors [169]. Such organelles can elicit appropriate stress responses in the face of acute organelle perturbations/stress. This is accomplished via the generation of a "retrograde response", a form of communication with the nucleus, that initiates the enhancement of the expression of specific/protective NuGEMPs to resolve the original organellar perturbations and contribute to the improvement of mitochondrial function/adaptations [169-171]. Collectively, these responses are generally considered a mechanism of mitochondrial repair, rather than remodeling, and are thought to be the first line of "defense" to quickly restore homeostasis and avoid substantial harm to the cell that could trigger the induction of more drastic outcomes, such as mitophagy and cell death through apoptosis [170]. Mitochondrial stress response pathways can be activated during exercise-induced energetic stress as exercise triggers mitochondrial remodeling in an attempt to satisfy the newly elevated energy requirements [172-174]. In this regard, exercise has been shown to potentially induce acute mitochondrial stress in the form of enhanced protein misfolding (proteotoxicity), due to the enhanced transcription of mitochondrial genes and their respective organelle protein import and exacerbate the presence of damaging reactive oxygen species (ROS), thereby negatively impacting mitochondrial function [175, 176].

Two prominent stress response pathways, as previously mentioned, the ISR and UPR^{mt}, have garnered recent interest in the scientific community due to their wide ability to incorporate and sense mitochondrial stress in response to extenuating conditions (Fig. 1). Although their role in maintaining mitochondrial stress has been partially explored, their direct link to exercise-induced mitochondrial stress has not been fully elucidated.

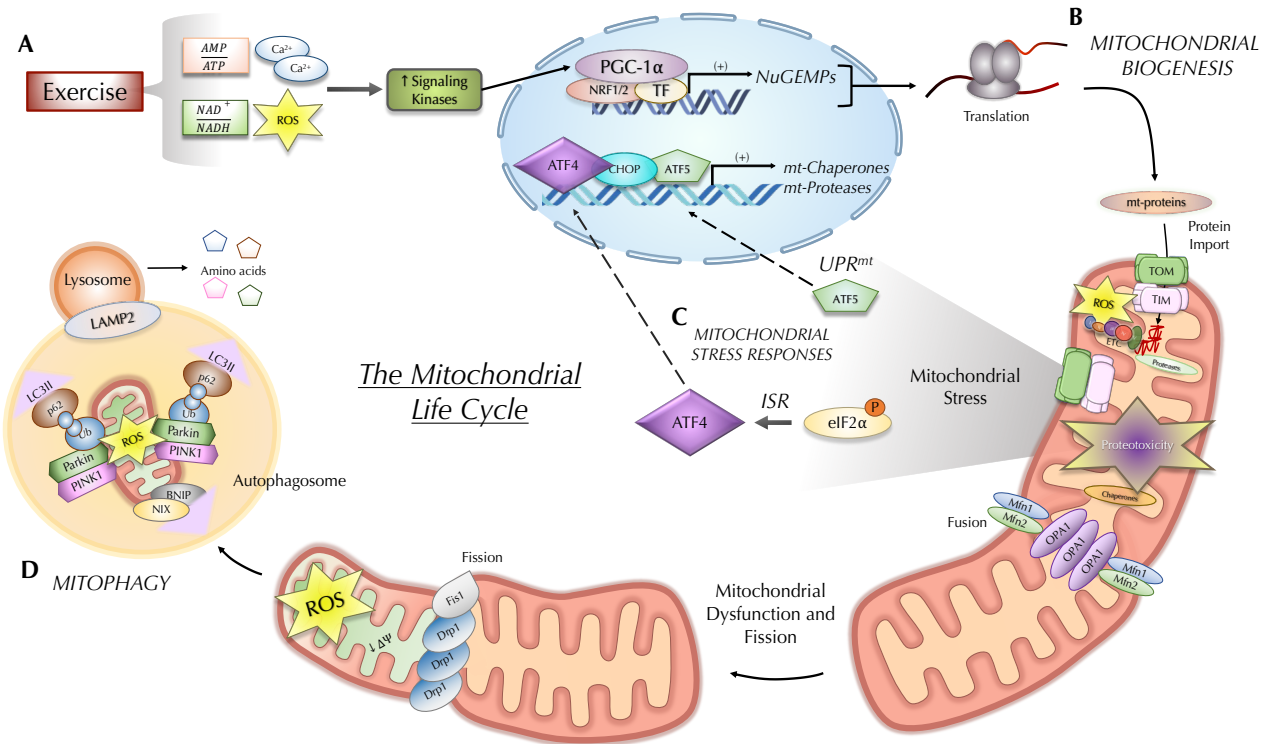

Figure 1. The Mitochondrial Life Cycle During Exercise: Mitochondrial Quality Control Processes. A) Contractile activity of muscle during exercise induces various metabolic and cellular alterations, including increases in ROS production, cytosolic Ca^{2+} concentrations, NAD+/NADH, and AMP/ATP, which all activate specific signaling kinases. Upon activation, such kinases will converge on the activation and induce the nuclear translocation of the master regulator of mitochondrial biogenesis, PGC-1α. Acting as a co-transcriptional activator, PGC-1α will bind other transcription factors, such as NRF-1/2 to enhance the transcription of NuGEMPs. Once transcribed and translated, these pre-proteins, which contain a cleavable mitochondrial presequence on their N-terminals, will be imported into the mitochondria via the TIM and TOM complexes (PIM). **B)** The newly imported proteins will be cleaved and processed into their mature conformations to be incorporated into the mitochondria, thereby contributing to the expansion of the mitochondrial reticulum, known as mitochondrial biogenesis, via fusion events. **C)** During unaccustomed exercise, however, the rate of protein import into the mitochondria exceeds the intrinsic folding capacity of the mitochondrial chaperones and degradation via proteases thereby leading to an accumulation of misfolded proteins, causing temporary mitochondrial proteotoxicity and stress in various forms, such as reductions in membrane potential and enhanced ROS production. This mitochondrial stress is sensed by the stress responses, the ISR and UPR^{mt}, which orchestrate a transcriptional regulation to combat such stressor(s) by upregulating cytoprotective genes, such as chaperone and proteases, to thus restore mitochondrial functioning. **D)** However, if such mitochondrial stress cannot be alleviated, signaling towards mitochondrial degradation occurs. This is mediated by the separation of the dysfunctional organelle via fission from the reticulum, and subsequent degradation via the lysosome following tagging and autophagosome formation.

3.1. The Integrated Stress Response (ISR): Activation and Regulation

The integrated stress response (ISR) is an evolutionally conserved adaptive translation program that is responsive to a variety of different environmental and pathological stressors [177]. Such stressors include, protein homeostasis (proteostasis) defects, nutrient deprivation, viral infection, oxidative stress and most recently, mitochondrial dysfunction/perturbations [178]. The ISR ultimately serves to maintain cellular health and overcome stressors by reprogramming gene expression [179]. With regards to mitochondria, the ISR serves as a hallmark response to mitochondrial stress that ultimately maintains overall mitochondrial quality in the face of organellar disturbances. However, this stress response program can also execute cell death mechanisms, such as apoptosis, if cellular health cannot be restored [177, 178]. The ISR is activated via distinct stress signals that are transmitted and sensed in various cellular compartments through the induction of four serine/threonine upstream kinases, protein kinase RNA-like endoplasmic reticulum kinase (PERK), general control nonderepressible 2 (GCN2), RNA-activated protein kinase (PKR), and heme-regulated inhibitor kinase (HRI) [179]. The four kinases share extensive homology in their kinase catalytic domains but possess distinct regulatory domains, reflective of their unique response to stressors [180]. Upon sensing stress, these kinases will undergo full activation via autophosphorylation and homodimerization events, where they will then converge on a common target, the eukaryotic translation initiation factor eIF2, a heterotrimer consisting of an α, β, and γ subunit [181]. Specific to the ISR, the α subunit is phosphorylated at serine 51 by one or more of the four kinases, leading to reduced global translation as well as selective synthesis of important regulators of homeostatic control [182-184]. This distinct regulation ultimately alleviates the pressure of continued translation, which can be

damaging to cellular constituents that are already facing stress, and primarily focus on restoring cellular homeostasis and thus overall survival.

The prominent feature of ISR signaling lies in the alterations of the ternary complex (TC) which is instrumental in initiating the translation of cap-dependant translation, commonly identified as AUG-initiated upstream open reading frames (uORFs) in the cell's transcriptome [185]. The TC is composed of the heterotrimeric eukaryotic translation initiation factor eIF2 bound with guanosine 5′-triphosphate (GTP), and a charged methionyl-initiator tRNA (Met-tRNA$_i$) [178]. Under basal conditions, the TC will dock onto the 40S ribosomal subunit, creating the 43S preinitiation complex (PIC) [186]. The recognition of the start codon AUG on mRNA triggers GTP hydrolysis of eIF2 and its release, followed by the recruitment and binding of the 60S ribosomal subunit, thus allowing the elongation phase of protein synthesis to commence [186]. The GDP bound to eIF2 is then exchanged for GTP, recycling eIF2 to its active state, allowing for another round of translation initiation [178]. This recycling is catalyzed by the interaction with the guanine exchange factor (GEF) eIF2B [187]. Briefly, eIF2B is composed of two copies of five different subunits (α, β, δ, γ, and ε) that assemble into a large two-fold symmetric heterodecamer; however, eIF2B's catalytic nucleotide exchange activity resides in eIF2Bε subunit [188]. In order to exchange GDP for GTP, eIF2B must form a complex with its substrate eIF2. Phosphorylation of eIF2α induces a profound structural rearrangement, which alters its binding to eIF2B, thereby restricting the nucleotide-binding domain and preventing access to the catalytic GEF domain [187, 188]. This inhibition subsequently blocks the eIF2B-mediated exchange of GDP for GTP and reduces the formation and availability of the 43S PIC, rendering the cell unable to re-initiate protein translation and thus attenuating global translation of 5' cap-dependant mRNAs [186-188]. Simultaneously, the translation of mRNAs that contain short "inhibitory" upstream open reading

frames (uORFs) in their 5' untranslated region (5'UTR) are enhanced [189]. Under basal/normal conditions, these "inhibitory" uORFs prevent the translation of downstream coding DNA sequences (CDS) by causing the translation machinery to "skip" the start codon of the sequence, however, the reduced availability of the TC when eIF2α is phosphorylated allows for the inhibitory uORF to be skipped enabling the downstream coding sequence to be expressed [177, 178]. As a result of this, selective transcripts which contain inhibitory uORFs in their mRNA, such as ATF4, the main effector of the ISR, can be expressed in response to stressful conditions [178].

The ISR is terminated by the dephosphorylation of the central signaling molecule, eIF2α. This event typically occurs when the initial stressor has been relieved, thus warranting normal protein synthesis and cell functioning to be resumed. The dephosphorylation of eIF2α is mediated by a protein phosphatase 1 (PP1) complex that recruits a catalytic subunit (PP1c) and a regulatory subunit [190]. In mammals, the most prevalent regulatory subunits of the phosphatase activity are GADD34, known as growth arrest and DNA damage-inducible protein, and CReP, the constitutive repressor of eIF2α phosphorylation [191, 192]. In a complex with PP1c, CReP, in unstressed conditions, is ubiquitously responsible for monitoring the basal levels of eIF2α phosphorylation [192]. Conversely, GADD34, which is a downstream target of the ISR and ATF4, specifically during the later stages of response activation, forms a complex with PP1c to significantly increase eIF2α dephosphorylation, acting as an important negative feedback loop to restore protein synthesis [191].

3.1.1. ATF4: Main Effector of the ISR

The activating transcription factor 4 (ATF4), also known as cAMP-response element binding protein 2 (CREB-2), has recently been established as the best characterized effector of the ISR in response to a multitude of organellar stressors, such as with mitochondrial insults [193, 194]. Its

structure is a critical facet in terms of its functional capabilities and overall means of gene regulation (Fig. 2). ATF4 is categorized as a basic leucine zipper (bZIP) transcription factor, since it contains a bZIP domain, which consists of a basic region and a leucine zipper, in the C-terminus of its peptide sequence, allowing it to bind to DNA and either a nonidentical bZIP protein (heterodimers) which includes three major subfamilies: cJun/cFos, ATF/CREB and CCAAT enhancer binding protein (C/EBP) or to itself (homodimer) [195-197]. This bZIP domain in ATF4 makes up a small proportion of the overall protein (~18%), with the remaining portion of the peptide sequence being variable between bZIP family members [193, 198]. The basic region mediates DNA binding and dictates which genetic regulatory elements within the promoters of various genes can be targeted by the bZIP homo-and heterodimers [177, 193, 194]. Conversely, the leucine zipper is an amphipathic helix that forms a coiled structure and is essential to mediate the dimerization between two bZIP proteins [194]. A majority of bZIP proteins are structurally suitable to homodimerize and remain functional/stable, however, it has been well noted that ATF4 cannot [199]. Conversely, the ATF4 leucine zipper has a high affinity to bind to the bZIP domains of other proteins (~30), forming stable and highly functional heterodimers, thereby illustrating its breadth of gene regulation [199]. The stable ATF4 heterodimers can bind to a wide array of response elements (REs) on a plethora of genes, including including amino acid (AARE), C/EBP-ATF (CARE), cAMP (CRE), antioxidant (ARE), and mitochondrial (MURE) response elements [200, 201]. This further highlights the classical biological phenomenon of combinatorial control, due to the variety of ATF4 heterodimers and their distinct regulatory mechanisms capable of generating a unique set of downstream effects. On the other hand, the N-terminal of the ATF4 peptide sequence contains a transactivation domain (TAD), comprised of various sites for post-translational modifications, including phosphorylation, acetylation, ubiquitination, hydroxylation,

and interactions with non-bZIP family proteins, which regulates the protein stability of ATF4 [177, 193, 194]. Specifically, in the TAD, a β-transducin repeat-containing protein (βTrCP) recognition motif (DSG*XX(X)*S) is present in this domain where βTrCP, an F-box protein and the receptor component of the SCF E3 ubiquitin ligase, can bind to upon stimulation [202]. When the serine residues of this motif are phosphorylated, it results in the interaction with βTrCP and the subsequent degradation by the proteasome, thereby reducing the protein stability of ATF4 [202]. Further, the histone acetyltransferase p300 can bind to the TAD and induce the stability of ATF4, independently of its catalytic activity, by inhibiting the phosphorylated driven proteasomal degradation [203]. Lastly, binding of the prolyl-4-hydroxylase domain (PHD) 3 protein (PHD3) on the oxygen-dependent degradation region (ODDD), can also reduce the stability of ATF4 [204].

Although heavily regulated at the translational level, the transcriptional expression of ATF4 is also altered in response to various cellular stressors. For example, ATF4 mRNA levels are lowered 3-fold in response to UV stress, whereas ATF4 transcript levels are significantly increased during ER stress, thereby contributing to the extent of the stress response activation [205]. The precise transcription factor(s) that induce such expressional regulation have not yet been elucidated in the literature, however, evidence points to the activity of c-jun N-terminal kinase 2 (JNK2), which has been proposed to induce the binding of the transcription factor c-Jun to the ATF4 promotor region [206]. As well, the regulatory kinase mTORC1 has also been suggested to be associated with upregulating the transcription of ATF4 in response to mitochondrial dysfunction, as such regulation was impaired with the mTORC1 inhibitor rapamycin [207]. Indeed, further work elucidating the transcriptional regulation of ATF4 must be conducted in response to stress conditions, such as with mitochondrial dysfunction and exercise.

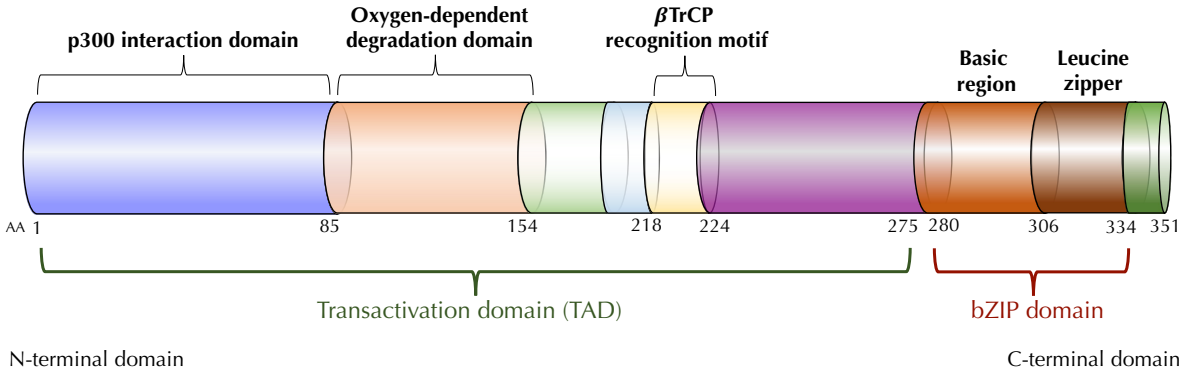

Figure 2. Structure of the ATF4 protein. A schematic illustration of the 351 amino acid (AA) structure of ATF4. The N-terminal consists of the transactivation domain (TAD), which contains various interaction domains and sites for post-translational modifications, including phosphorylation, acetylation, ubiquitination, and hydroxylation, which alters the protein stabilization or degradation of ATF4. The C-terminal consists of the bZIP domain, comprised of the basic region and the leucine zipper, which mediates DNA binding and dimerization (protein-protein interactions) with other family transcription factors (bZIP).

3.1.1.1. ATF4: A Regulator of Gene Expression

During the onslaught of mitochondrial stress, the ISR induces the activation of ATF4, which is subsequently capable of alleviating organelle perturbations by upregulating a myriad of nuclear encoded protective genes [179, 193, 194, 208, 209]. Mitochondrial stress, such as with reductions in mitochondrial membrane potential, inhibition of OXPHOS functioning, attenuations in mitochondrial translation, hinderance in protein import, and protein misfolding/proteotoxicity, lead to an ATF4 mediated regulation of transcriptomic, proteomic, and mitochondrial metabolic adaptations [210]. In various tissues, ATF4 is responsible for upregulating necessary mitochondrial genes related to serine biosynthesis, one carbon metabolism, amino acid synthesis and transport, protein folding and handling, and antioxidant capacity [211-214]. Additionally, ATF4, along with its notable downstream targets, the transcription factors ATF5 and CHOP, which also play a role in further enhancing the mitochondrial stress response via the UPR^{mt}, discussed in a later section, upregulate the expression of mitochondrial chaperones, proteases and enzymes

required for proper organelle function and homeostatic maintenance [177, 215-218]. When examining the importance of ATF4 in maintaining mitochondrial health, it was found that the absence of ATF4 in HeLa cells lead to severe decrements in the expression of several mitochondrial enzymes and ATP-dependent respiration [210]. In a muscle-specific context, recent work from our laboratory in C2C12 myotubes has shown that ATF4 is an early responder to contractile activity and is a critical factor in enhancing mitochondrial networking, protein handling, and capacity for the clearance of dysfunctional organelles under acute contractile activity stress [219]. Furthermore, ATF4 was shown to be induced in the early stages of mitochondrial adaptations following repeated bouts of contractile activity in myotubes and was capable of regulating genes associated with both mitochondrial biogenesis and autophagy, such as PGC-1α, p62 and LC3, respectively [149, 220, 221]. The overexpression of ATF4 in myotubes basally improves mitochondrial oxygen consumption rates, are better equipped to match the new energy demand during contractile activity and display lower reactive oxygen species production [219]. Conversely, the knockdown of ATF4 severely blunts basal mitochondrial respiration rates, and concomitantly increases the production of ROS [219]. Altogether, these findings demonstrate that ATF4, induced via the ISR following mitochondrial insults, serves to maintain overall mitochondrial health, network quality and beneficial/necessary adaptations required in the face of organellar stress. However, these mechanisms of mitochondrial regulation have not yet been fully elucidated *in vivo*, basally, and with respect to exercise-induced mitochondrial stress. Indeed, research on this transcription factor is on the rise in hopes of characterizing the precise mechanism of its activity in maintaining skeletal muscle mitochondrial quality during organelle stress, such as with exercise and disuse.

It should be noted that ATF4 is also capable of regulating a plethora of additional genes dependant on the type, intensity and duration of stressors related to cell survival and apoptosis in other cellular compartments, as well as muscle atrophy [197]. For example, ATF4 can induce the expression of genes that are important for cell survival in the context of ER misfolded proteins, such as the chaperone BiP, as well as the stress-induced genes ChaC1 and CTH, by heterodimerizing with C/EBPγ [222, 223]. On the other hand, if the stressor chronically persists and ATF4 is over-activated, the expression of pro-apoptotic genes, such as PUMA and NOXA, as well as autophagy-related genes, are enhanced [224]. Furthermore, in skeletal muscle, over a decade of research has elucidated that ATF4 plays a role in mediating age-related and disuse-induced muscle atrophy [193, 225]. This muscle specific outcome is mediated by the heterodimer, consisting of ATF4 and C/EBPβ, which enhances the expression of growth arrest and DNA damage inducible α (Gadd45a) and p21, known proteins responsible for inducing muscle atrophy [226, 227]. With chronic muscle disuse, ATF4 expression was observed to be increased, suggesting its contribution to the changing muscle phenotype [228]. When ATF4 is knocked down in either aged animals or those subjected to prolonged muscle disuse, muscle atrophy is attenuated, however, when overexpressed, the progression of atrophy is enhanced [229, 230]. Nonetheless, such evidence and regulatory effects on a wide array of genes further illustrates how different stress signals can generate unique expressional responses, thereby suggesting that the effect of ATF4 and downstream consequences are highly context dependent.

3.1.2. ISR Activation in Response to Mitochondrial Stress

As alluded to in the previous section, evidence has shown that the ISR is activated following a wide range of mitochondrial stressors to maintain mitochondrial quality and functioning,

however the major open question that remains to be fully explored is how this stress is sensed and translated into an ATF4 mediated cytoprotective response [179, 210].

Multiple mechanisms have partially established that mitochondrial stress activates the ISR kinases, GCN2, HRI, and PKR, but not PERK, which can evidently trigger a mitochondrial-specific response to alleviate that initial perturbation [179, 210, 231] (Fig. 3). In particular, GCN2 is known to respond to amino acid deprivation and increases in reactive oxygen species (ROS) which are insults that are generated by oxidative phosphorylation (OXPHOS) complexes under stress [231-236]. However, the precise mechanism of GCN2 activation is still uncharacterized. Conversely, HRI is responsive to mitochondrial stress through a newly explored pathway, which involves the mitochondrial stress responsive protease OMA1, and the mitochondrial protein DELE1 [237, 238]. Mechanistically, the OMA1 protease is dormant under physiological conditions but is rapidly activated upon mitochondrial stress, such as with a loss of membrane potential or excessive reactive oxygen species [239, 240]. Upon mitochondrial stress, OMA1 will interact with DELE1 and cleave it into short peptide fragments, identified as S-DELE1 [241]. These fragments will then be exported out of the mitochondria in an unknown mechanism where they will accumulate in the cytosol [237, 238]. This accumulation will ultimately lead to the interaction between S-DELE1 and HRI via the N-terminal tetranucleotide repeats present in S-DELE1, which mediates protein–protein interactions and thus the autophosphorylation and homodimerization of HRI [242]. Lastly, PKR has been associated with responding to mitochondrial proteotoxicity/protein misfolding, however such a relationship requires further substantial evidence [243]. Activated PKR not only phosphorylates eIF2α, but also JNK2, resulting in the activation of the transcription factor c-Jun, which mediates the expression of further cytoprotective genes [243]. Nonetheless, once the three kinases have undergone activation in

response to mitochondrial stress, they will thereby induce eIF2α phosphorylation, which leads to a subsequent upregulation in ATF4 expression. This trigger will ultimately dictate the nuclear translocation of ATF4 to enhance the expression of genes associated with restoring mitochondrial function and homeostasis.

3.2. The Mammalian Mitochondrial Unfolded Protein Response (UPR^{mt})

The second mitochondrial stress response pathway that has been identified as a critical mediator of mitochondrial quality control is the UPR^{mt}, which is an adaptive transcriptional program that aims to maintain mitochondrial homeostasis during dysfunction or instances of cellular stress [244]. The UPR^{mt} was initially characterized in mammalian cells, however, advances in the mechanism of this response pathway were greatly explored and elucidated in *C. elegans* [245]. This response pathway, as its name suggests, has evolved over time to maintain optimal mitochondrial functioning since mitochondria greatly rely on the import of nuclear-derived mitochondrial proteins [246, 247]. Thus, this pathway regulates the folding, and quality control of the mitochondrial proteome. Evidence has now indicated that the UPR^{mt} protects cells from stressors including OXPHOS dysfunction, ATP depletion, and reductions in the mitochondrial inner membrane potential [248]. The UPR^{mt} is thereby suggested to be an intermediary mechanism in maintaining mitochondrial quality and a first responder to mitochondrial insults. Similar to the ISR, if mitochondrial stress cannot be alleviated, in instances of chronic dysfunction, mitophagy is activated to eliminate the dysfunctional organelles, and in severe cases, apoptosis/cell death occurs [249]. With this being said, it is still apparent that the precise mechanisms of the mitochondrial UPR^{mt} activation and downstream consequences in mammalian cells are largely unknown, however a handful of studies have attempted to reveal these responses during a wide array of stressors. In early work, depleting cells of mtDNA and inducing

heat shock enhanced the expression of the stress-responsive chaperones HSP60/10 and proteases ClpP, YME1L1 and LonP, which are now known markers of the mammalian UPR^{mt} [245]. In terms of the main regulator of the UPR^{mt}, initially, work in *C. elegans* identified the stress activated transcription factor (ATFS-1) as the main mediator of such response, however, in mammals the transcription factor ATF5 was established to be the mammalian homolog to ATFS-1 [217]. This identification was based off the restoration of mitochondrial function in ATFS-1 KO *C. elegans* upon the exogenous expression of ATF5 [217]. It has since been acknowledged that ATF5, like ATFS-1, contains both a bZIP domain and a mitochondrial targeting sequence, allowing both its nuclear and mitochondrial localization, dictated by the presence of mitochondrial stress [217, 246]. However, more recent work has demonstrated that ATF5 alone is not sufficient to induce the UPR^{mt} and upregulate the necessary cytoprotective genes to relieve mitochondrial stress. Consequently, ATF5 requires the cooperation with ATF4 and CHOP to induce a mitochondrial-specific response, thereby deeming all three factors as plausible "master regulators" of the UPR^{mt} (Fig. 3) [247]. This regulation was elucidated through global transcriptomic analyses which identified that all three transcription factors contain binding motifs in the promotor regions of numerous UPR^{mt} responsive genes that are induced by mitochondrial dysfunction [250]. These findings were further confirmed with gene expression analysis in both human and mouse tissues [250]. Although each of these transcription factors have been implicated in promoting transcription of genes required to overcome mitochondrial dysfunction, it is unclear how they function in concert. It has been revealed that under stressful conditions, ATF4 operates upstream of CHOP and ATF5 [251, 252]. However, the exact mechanism and relationship of how these transcription factors impart their transcriptional control remains to be fully elucidated.

3.3. Interconnecting the UPR^{mt} and the ISR During Mitochondrial Stress

Research of the mammalian UPR^{mt} has recently highlighted the importance of the ISR and its subsequent activation during mitochondrial stress. Numerous reports have demonstrated that the increased phosphorylation of eIF2α and thereby induction of the ISR during mitochondrial stress enables the preferential translation the newly appointed master regulators of the UPR^{mt}, ATF4, CHOP, and ATF5 (Fig. 3) [251-253]. Such regulation is necessary as all three transcription factors contain inhibitory uORFs upstream of their coding sequence, thus their expression is reliant on the alternative translation that occurs following TC inhibition [252, 254]. These findings make it clear that the UPR^{mt} in mammals is possibly dependent on the ISR and requires such translational regulation to enhance the availability of the master regulators. On the other hand, notably in *C. elegans*, the ISR has been shown to be dispensable for UPR^{mt} induction [232]. Evidence has also shown that activation of the UPR^{mt} can also lead to a mild increase in eIF2α phosphorylation, however the precise mechanism or inductee responsible for such regulation is still unknown [250, 255]. Thus, there seems to be a plausible crosstalk or overlap between these two stress response pathways following mitochondrial perturbations, however, major questions remain unsolved: 1) which stress response pathway is activated first? 2) does one response enhance the activation of the other, as previously alluded to, 3) how does the cross talk between these stress response pathways contribute to maintaining organellar health, and 4) is there an overlap with the protective genes being expressed? Nonetheless, it will be interesting to understand how these responses coordinate to promote mitochondrial health and beneficial adaptations in muscle.

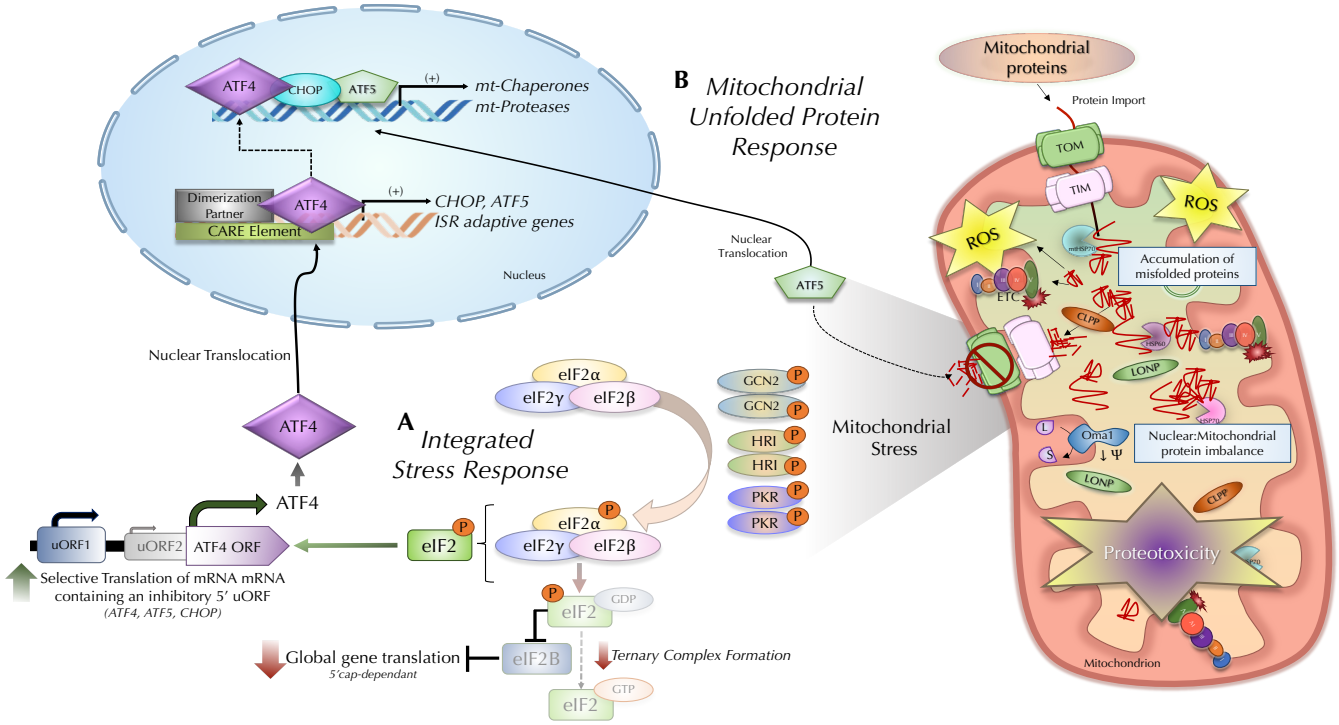

Figure 3. Interconnecting the Integrated Stress Response and the UPR^{mt} during mitochondrial stress. A) Mitochondrial proteotoxicity, ROS accumulation and transient reductions in mitochondrial membrane potential activate the upstream ISR kinases, GCN2, HRI, and PKR, but not PERK, which converge on the α-subunit of the eIF2 complex and induce its phosphorylation. Once eIF2α is phosphorylated, it undergoes profound structural changes leading to the inhibition of eIF2B and its nucleotide-exchange of GDP for GTP, thereby preventing the formation of the ternary complex (TC) and thus global 5'cap-dependent translation. Under basal conditions, the TC begins scanning at the upstream open reading frames (uORFs) 1 and 2 of the ATF4 mRNA. In particular, the uORF2 is the inhibiting uORF as it prevents the re-initiation of the ribosome at the ATF4 coding DNA sequence (CDS) and thus its translation. When the TC is inhibited or unable to form, it allows for longer ribosomal scanning along the ATF4 mRNA, skipping the uORF2 and allowing for re-initiation at the ATF4 CDS, increasing the translation of ATF4. Once ATF4 is translated, it will translocate to the nucleus where it can form heterodimers to induce the expression of CHOP, ATF5 and ISR adaptive genes to combat the initial mitochondrial stressor and restore mitochondrial function/homeostasis. **B)** In addition to the Integrated Stress Response, the UPR^{mt} is activated in conjunction to enhance the protection of mitochondrial function. In response to the protein overload seen with proteotoxicity, as described previously, mitochondrial chaperones and proteases can block the import of mitochondrial proteins, such as ATF5, thus promoting the translocation of ATF5 to the nucleus instead of the mitochondrial matrix. The ISR mediated activation of ATF4 also promotes the expression of downstream targets ATF5 and CHOP, in which all three factors cooperate together and are thus capable of regulating and enhancing the expression of cytoprotective genes to combat the initial stressor and restore mitochondrial function.

RESEARCH OBJECTIVES:

Based on the literature cited above, the objectives of my thesis were to:

1. Assess the effect of brief, acute contractile activity on the activation of the ISR through observing the protein expression of early signaling events and eIF2α phosphorylation;
2. Elucidate the mechanism of ATF4 activation in response to mitochondrial stress after an acute bout of contractile and following recovery;
3. Determine if the activation of ATF4 coincides with the upregulation of downstream cytoprotective genes, CHOP and ATF5;
4. Identify whether ATF4 translocates to the nucleus upon acute exercise-induced stress.

HYPOTHESES:

We hypothesized that:

1. The acute contractile activity will induce mitochondrial stress and elicit the early stages of ISR activation;
2. ATF4 will be responsive to the acute contractile activity-induced stress at both the mRNA and protein level, which will be enhanced following recovery;
3. Both the expression of CHOP and ATF5 will consequently be upregulated following the activation of ATF4;
4. Contractile activity will stimulate the nuclear translocation of ATF4.

REFERENCES

1. Frontera, W. R., & Ochala, J. (2015). Skeletal muscle: a brief review of structure and function. *Calcified tissue international*, *96*(3), 183–195. https://doi.org/10.1007/s00223-014-9915-y
2. Tieland, M., Trouwborst, I., & Clark, B. C. (2018). Skeletal muscle performance and ageing. *Journal of cachexia, sarcopenia and muscle*, *9*(1), 3–19. https://doi.org/10.1002/jcsm.12238
3. McLeod, M., Breen, L., Hamilton, D. L., & Philp, A. (2016). Live strong and prosper: the importance of skeletal muscle strength for healthy ageing. *Biogerontology*, *17*(3), 497–510. https://doi.org/10.1007/s10522-015-9631-7
4. Hood, D. A., Irrcher, I., Ljubicic, V., & Joseph, A. M. (2006). Coordination of metabolic plasticity in skeletal muscle. *The Journal of experimental biology*, *209*(Pt 12), 2265–2275. https://doi.org/10.1242/jeb.02182
5. Mukund, K., & Subramaniam, S. (2020). Skeletal muscle: A review of molecular structure and function, in health and disease. *Wiley interdisciplinary reviews. Systems biology and medicine*, *12*(1), e1462. https://doi.org/10.1002/wsbm.1462
6. Rebbeck, R. T., Karunasekara, Y., Board, P. G., Beard, N. A., Casarotto, M. G., & Dulhunty, A. F. (2014). Skeletal muscle excitation-contraction coupling: who are the dancing partners?. *The international journal of biochemistry & cell biology*, *48*, 28–38. https://doi.org/10.1016/j.biocel.2013.12.001
7. Shenkman BS, Turtikova OV, Nemirovskaya TL, Grigoriev AI. Skeletal muscle activity and the fate of myonuclei. Acta Naturae. (2010). Jul;2(2):59-66. PMID: 22649641; PMCID: PMC3347558.
8. Dupont-Versteegden EE. (2006). Apoptosis in skeletal muscle and its relevance to atrophy. *World J Gastroenterol*. 12(46):7463-6. doi: 10.3748/wjg.v12.i46.7463.
9. Dupont-Versteegden, E. E., Strotman, B. A., Gurley, C. M., Gaddy, D., Knox, M., Fluckey, J. D., & Peterson, C. A. (2006). Nuclear translocation of EndoG at the initiation of disuse muscle atrophy and apoptosis is specific to myonuclei. *American journal of physiology. Regulatory, integrative and comparative physiology*, *291*(6), R1730–R1740. https://doi.org/10.1152/ajpregu.00176.2006
10. Adhihetty, P.J. & Hood, David. (2003). Mechanisms of apoptosis in skeletal muscle. *Basic Appl Myol*. 13. 171-179.
11. Dumont, N. A., Bentzinger, C. F., Sincennes, M. C., & Rudnicki, M. A. (2015). Satellite Cells and Skeletal Muscle Regeneration. *Comprehensive Physiology*, *5*(3), 1027–1059. https://doi.org/10.1002/cphy.c140068
12. Segal SS, Kurjiaka DT. (1995). Coordination of blood flow control in the resistance vasculature of skeletal muscle. Medicine and Science in Sports and Exercise. 27(8):1158-1164. PMID: 7476060.
13. Powis, R. A., & Gillingwater, T. H. (2016). Selective loss of alpha motor neurons with sparing of gamma motor neurons and spinal cord cholinergic neurons in a mouse model of spinal muscular atrophy. *Journal of anatomy*, *228*(3), 443–451. https://doi.org/10.1111/joa.12419
14. Padykula, H. A., & Herman, E. (1955). Factors affecting the activity of adenosine triphosphatase and other phosphatases as measured by histochemical techniques. *The journal*

of histochemistry and cytochemistry: official journal of the Histochemistry Society, *3*(3), 161–169. https://doi.org/10.1177/3.3.161
15. Engel W. K. (1962). The essentiality of histo- and cytochemical studies of skeletal muscle in the investigation of neuromuscular disease. *Neurology*, *12*(11). https://doi.org/10.1212/WNL.12.11.778
16. Schiaffino, S., & Reggiani, C. (2011). Fiber types in mammalian skeletal muscles. *Physiological reviews*, *91*(4), 1447–1531. https://doi.org/10.1152/physrev.00031.2010
17. Bottinelli, R., & Reggiani, C. (2000). Human skeletal muscle fibres: molecular and functional diversity. *Progress in biophysics and molecular biology*, *73*(2-4), 195–262. https://doi.org/10.1016/s0079-6107(00)00006-7
18. Scott, W., Stevens, J., Binder–Macleod, S.A. (2001) Human Skeletal Muscle Fiber Type Classifications, *Physical Therapy*, 81 (11), 1810–1816, https://doi.org/10.1093/ptj/81.11.1810
19. Zierath JR, Hawley JA. Skeletal muscle fiber type: influence on contractile and metabolic properties. (2004) *PLoS Biol.* 2(10):e348. doi: 10.1371/journal.pbio.0020348. Epub 2004 Oct 12. PMID: 15486583; PMCID: PMC521732.
20. Larsson L, Moss RL. (1993). Maximum velocity of shortening in relation to myosin isoform composition in single fibres from human skeletal muscles. *J Physiol.* 472:595-614. doi: 10.1113/jphysiol.1993.sp019964. PMID: 8145163; PMCID: PMC1160504.
21. Liu, G., Mac Gabhann, F., & Popel, A. S. (2012). Effects of fiber type and size on the heterogeneity of oxygen distribution in exercising skeletal muscle. *PloS one*, *7*(9), e44375. https://doi.org/10.1371/journal.pone.0044375
22. Locke, M., Noble, E. G., & Atkinson, B. G. (1991). Inducible isoform of HSP70 is constitutively expressed in a muscle fiber type specific pattern. *The American journal of physiology*, *261*(5 Pt 1), C774–C779. https://doi.org/10.1152/ajpcell.1991.261.5.C774
23. Lamboley CR, Murphy RM, McKenna MJ, Lamb GD. Sarcoplasmic reticulum Ca2+ uptake and leak properties, and SERCA isoform expression, in type I and type II fibres of human skeletal muscle. J Physiol. 2014 Mar 15;592(6):1381-95. doi: 10.1113/jphysiol.2013.269373. Epub 2014 Jan 27. PMID: 24469076; PMCID: PMC3961094.
24. Summermatter, S., Thurnheer, R., Santos, G., Mosca, B., Baum, O., Treves, S., Hoppeler, H., Zorzato, F., & Handschin, C. (2012). Remodeling of calcium handling in skeletal muscle through PGC-1α: impact on force, fatigability, and fiber type. *American journal of physiology. Cell physiology*, *302*(1), C88–C99. https://doi.org/10.1152/ajpcell.00190.2011
25. Ogata, T., & Yamasaki, Y. (1985). Scanning electron-microscopic studies on the three-dimensional structure of mitochondria in the mammalian red, white and intermediate muscle fibers. *Cell and tissue research*, *241*(2), 251–256. https://doi.org/10.1007/BF00217168
26. Edgerton, V. R., Smith, J. L., & Simpson, D. R. (1975). Muscle fibre type populations of human leg muscles. *The Histochemical journal*, *7*(3), 259–266. https://doi.org/10.1007/BF01003594
27. Baldwin, K. M., & Haddad, F. (2002). Skeletal muscle plasticity: cellular and molecular responses to altered physical activity paradigms. *American journal of physical medicine & rehabilitation*, *81*(11 Suppl), S40–S51. https://doi.org/10.1097/01.PHM.0000029723.36419.0D

28. Andersen, J. L., & Aagaard, P. (2000). Myosin heavy chain IIX overshoot in human skeletal muscle. *Muscle & nerve*, *23*(7), 1095–1104. https://doi.org/10.1002/1097-4598(200007)23:7<1095::aid-mus13>3.0.co;2-o
29. Plotkin DL, Roberts MD, Haun CT, Schoenfeld BJ. Muscle Fiber Type Transitions with Exercise Training: Shifting Perspectives. Sports (Basel). 2021 Sep 10;9(9):127. doi: 10.3390/sports9090127. PMID: 34564332; PMCID: PMC8473039.
30. Martin, W. F., Garg, S., & Zimorski, V. (2015). Endosymbiotic theories for eukaryote origin. *Philosophical transactions of the Royal Society of London. Series B, Biological sciences*, *370*(1678), 20140330. https://doi.org/10.1098/rstb.2014.0330
31. Roger, A. J., Muñoz-Gómez, S. A., & Kamikawa, R. (2017). The Origin and Diversification of Mitochondria. *Current biology: CB*, *27*(21), R1177–R1192. https://doi.org/10.1016/j.cub.2017.09.015
32. Gray, M. W., Burger, G., & Lang, B. F. (2001). The origin and early evolution of mitochondria. *Genome biology*, *2*(6), REVIEWS1018. https://doi.org/10.1186/gb-2001-2-6-reviews1018
33. Ernster, L., & Schatz, G. (1981). Mitochondria: a historical review. *The Journal of cell biology*, *91*(3 Pt 2), 227s–255s. https://doi.org/10.1083/jcb.91.3.227s
34. Greaves, L. C., Reeve, A. K., Taylor, R. W., & Turnbull, D. M. (2012). Mitochondrial DNA and disease. *The Journal of pathology*, *226*(2), 274–286. https://doi.org/10.1002/path.3028
35. Palade G. E. (1953). An electron microscope study of the mitochondrial structure. *The journal of histochemistry and cytochemistry: official journal of the Histochemistry Society*, *1*(4), 188–211. https://doi.org/10.1177/1.4.188
36. Frey, T. G., & Mannella, C. A. (2000). The internal structure of mitochondria. *Trends in biochemical sciences*, *25*(7), 319–324. https://doi.org/10.1016/s0968-0004(00)01609-1
37. Leveille CF, Mikhaeil JS, Turner KD, Silvera S, Wilkinson J, Fajardo VA. (2017). Mitochondrial cristae density: a dynamic entity that is critical for energy production and metabolic power in skeletal muscle. *J Physiol*. 2017 May 1;595(9):2779-2780. doi: 10.1113/JP274158.
38. L.S. Zalman, H. Nikaido, Y. Kagawa. (1980). Mitochondrial outer membrane contains a protein producing nonspecific diffusion channels. *Journal of Biological Chemistry*, 255, (5), 1771-1774. https://doi.org/10.1016/S0021-9258(19)85942-2.
39. Kirkwood, S. P., Munn, E. A., & Brooks, G. A. (1986). Mitochondrial reticulum in limb skeletal muscle. *The American journal of physiology*, *251*(3 Pt 1), C395–C402. https://doi.org/10.1152/ajpcell.1986.251.3.C395
40. Sheridan, C., & Martin, S. J. (2010). Mitochondrial fission/fusion dynamics and apoptosis. *Mitochondrion*, *10*(6), 640–648. https://doi.org/10.1016/j.mito.2010.08.005
41. Picard M, White K, Turnbull DM. (2013). Mitochondrial morphology, topology, and membrane interactions in skeletal muscle: a quantitative three-dimensional electron microscopy study. *J Appl Physiol*, 114(2):161-71. doi: 10.1152/japplphysiol.01096.2012.
42. Laird, A. K., Nygaard, O., Ris, H., & Barton, A. D. (1953). Separation of mitochondria into two morphologically and biochemically distinct types. *Experimental cell research*, *5*(1), 147–160. https://doi.org/10.1016/0014-4827(53)90100-1
43. Palmer, J. W., Tandler, B., & Hoppel, C. L. (1977). Biochemical properties of subsarcolemmal and interfibrillar mitochondria isolated from rat cardiac muscle. *The Journal of biological chemistry*, *252*(23), 8731–8739.

44. Koves, T. R., Noland, R. C., Bates, A. L., Henes, S. T., Muoio, D. M., & Cortright, R. N. (2005). Subsarcolemmal and intermyofibrillar mitochondria play distinct roles in regulating skeletal muscle fatty acid metabolism. *American journal of physiology. Cell physiology*, *288*(5), C1074–C1082. https://doi.org/10.1152/ajpcell.00391.2004
45. Heine, K. B., & Hood, W. R. (2020). Mitochondrial behaviour, morphology, and animal performance. *Biological reviews of the Cambridge Philosophical Society*, *95*(3), 730–737. https://doi.org/10.1111/brv.12584
46. Willingham, T. B., Ajayi, P. T., & Glancy, B. (2021). Subcellular Specialization of Mitochondrial Form and Function in Skeletal Muscle Cells. *Frontiers in cell and developmental biology*, *9*, 757305. https://doi.org/10.3389/fcell.2021.757305
47. Kuznetsov AV, Margreiter R. Heterogeneity of mitochondria and mitochondrial function within cells as another level of mitochondrial complexity. Int J Mol Sci. 2009 Apr 24;10(4):1911-1929. doi: 10.3390/ijms10041911. PMID: 19468346; PMCID: PMC2680654.
48. Glancy, B., Hartnell, L. M., Malide, D., Yu, Z. X., Combs, C. A., Connelly, P. S., Subramaniam, S., & Balaban, R. S. (2015). Mitochondrial reticulum for cellular energy distribution in muscle. *Nature*, *523*(7562), 617–620. https://doi.org/10.1038/nature14614
49. Adhihetty, P. J., O'Leary, M. F., & Hood, D. A. (2008). Mitochondria in skeletal muscle: adaptable rheostats of apoptotic susceptibility. *Exercise and sport sciences reviews*, *36*(3), 116–121. https://doi.org/10.1097/JES.0b013e31817be7b7
50. Adhihetty, P. J., Ljubicic, V., & Hood, D. A. (2007). Effect of chronic contractile activity on SS and IMF mitochondrial apoptotic susceptibility in skeletal muscle. *American journal of physiology. Endocrinology and metabolism*, *292*(3), E748–E755. https://doi.org/10.1152/ajpendo.00311.2006
51. Adhihetty, P. J., Ljubicic, V., Menzies, K. J., & Hood, D. A. (2005). Differential susceptibility of subsarcolemmal and intermyofibrillar mitochondria to apoptotic stimuli. *American journal of physiology. Cell physiology*, *289*(4), C994–C1001. https://doi.org/10.1152/ajpcell.00031.2005
52. Adhihetty, P. J., Irrcher, I., Joseph, A. M., Ljubicic, V., & Hood, D. A. (2003). Plasticity of skeletal muscle mitochondria in response to contractile activity. *Experimental physiology*, *88*(1), 99–107.https://doi.org/10.1113/eph8802505
53. Adhihetty, P. J., O'Leary, M. F., Chabi, B., Wicks, K. L., & Hood, D. A. (2007). Effect of denervation on mitochondrially mediated apoptosis in skeletal muscle. *Journal of applied physiology (Bethesda, Md.: 1985)*, *102*(3), 1143–1151. https://doi.org/10.1152/japplphysiol.00768.2006
54. Ljubicic, V., Joseph, A. M., Adhihetty, P. J., Huang, J. H., Saleem, A., Uguccioni, G., & Hood, D. A. (2009). Molecular basis for an attenuated mitochondrial adaptive plasticity in aged skeletal muscle. *Aging*, *1*(9), 818–830. https://doi.org/10.18632/aging.100083
55. Takahashi, M., & Hood, D. A. (1996). Protein import into subsarcolemmal and intermyofibrillar skeletal muscle mitochondria. Differential import regulation in distinct subcellular regions. *The Journal of biological chemistry*, *271*(44), 27285–27291. https://doi.org/10.1074/jbc.271.44.27285
56. Connor, M. K., Bezborodova, O., Escobar, C. P., & Hood, D. A. (2000). Effect of contractile activity on protein turnover in skeletal muscle mitochondrial subfractions. *Journal of applied physiology (Bethesda, Md. : 1985)*, *88*(5), 1601–1606. https://doi.org/10.1152/jappl.2000.88.5.1601

57. Cogswell, A. M., Stevens, R. J., & Hood, D. A. (1993). Properties of skeletal muscle mitochondria isolated from subsarcolemmal and intermyofibrillar regions. *The American journal of physiology*, *264*(2 Pt 1), C383–C389. https://doi.org/10.1152/ajpcell.1993.264.2.C383
58. Siekevitz, P. (1957). Powerhouse of the cell. Scientific American. 197(1), 131-144
59. Osellame LD, Blacker TS, Duchen MR. Cellular and molecular mechanisms of mitochondrial function. (2012). *Best Pract Res Clin Endocrinol Metab*. 26(6):711-23. doi: 10.1016/j.beem.2012.05.003.
60. Kotiadis, V. N., Duchen, M. R., & Osellame, L. D. (2014). Mitochondrial quality control and communications with the nucleus are important in maintaining mitochondrial function and cell health. *Biochimica et biophysica acta*, *1840*(4), 1254–1265. https://doi.org/10.1016/j.bbagen.2013.10.041
61. Zhou J, Dhakal K, Yi J. Mitochondrial Ca(2+) uptake in skeletal muscle health and disease. (2016). *Sci China Life Sci.* 59(8):770-6. doi: 10.1007/s11427-016-5089-3.
62. Nicholls D. G. (2005). Mitochondria and calcium signaling. *Cell calcium*, *38*(3-4), 311–317. https://doi.org/10.1016/j.ceca.2005.06.011
63. Wang, X., Weisleder, N., Collet, C., Zhou, J., Chu, Y., Hirata, Y., Zhao, X., Pan, Z., Brotto, M., Cheng, H., & Ma, J. (2005). Uncontrolled calcium sparks act as a dystrophic signal for mammalian skeletal muscle. *Nature cell biology*, *7*(5), 525–530. https://doi.org/10.1038/ncb1254
64. Ježek P, Holendová B, Plecitá-Hlavatá L. Redox Signaling from Mitochondria: Signal Propagation and Its Targets. (2020). *Biomolecules.* 10(1):93. doi: 10.3390/biom10010093. PMID: 31935965; PMCID: PMC7023504.
65. Kuksal, N., Chalker, J., & Mailloux, R. J. (2017). Progress in understanding the molecular oxygen paradox - function of mitochondrial reactive oxygen species in cell signaling. *Biological chemistry*, *398*(11), 1209–1227. https://doi.org/10.1515/hsz-2017-0160
66. Lee, S., Tak, E., Lee, J., Rashid, M. A., Murphy, M. P., Ha, J., & Kim, S. S. (2011). Mitochondrial H2O2 generated from electron transport chain complex I stimulates muscle differentiation. *Cell research*, *21*(5), 817–834. https://doi.org/10.1038/cr.2011.55
67. Singh, K., & Hood, D. A. (2011). Effect of denervation-induced muscle disuse on mitochondrial protein import. *American journal of physiology. Cell physiology*, *300*(1), C138–C145. https://doi.org/10.1152/ajpcell.00181.2010
68. Zhao, R. Z., Jiang, S., Zhang, L., & Yu, Z. B. (2019). Mitochondrial electron transport chain, ROS generation and uncoupling (Review). *International journal of molecular medicine*, *44*(1), 3–15. https://doi.org/10.3892/ijmm.2019.4188
69. Nolfi-Donegan, D., Braganza, A., & Shiva, S. (2020). Mitochondrial electron transport chain: Oxidative phosphorylation, oxidant production, and methods of measurement. *Redox biology*, *37*, 101674. https://doi.org/10.1016/j.redox.2020.101674
70. Bo, H., Zhang, Y., & Ji, L. L. (2010). Redefining the role of mitochondria in exercise: a dynamic remodeling. Annals of the New York Academy of Sciences, 1201, 121–128. https://doi.org/10.1111/j.1749-6632.2010.05618.x
71. Drake, J. C., Wilson, R. J., & Yan, Z. (2016). Molecular mechanisms for mitochondrial adaptation to exercise training in skeletal muscle. FASEB journal: official publication of the Federation of American Societies for Experimental Biology, 30(1), 13–22. https://doi.org/10.1096/fj.15-276337

72. Little, J. P., Safdar, A., Bishop, D., Tarnopolsky, M. A., & Gibala, M. J. (2011). An acute bout of high-intensity interval training increases the nuclear abundance of PGC-1α and activates mitochondrial biogenesis in human skeletal muscle. *American journal of physiology. Regulatory, integrative and comparative physiology*, *300*(6), R1303–R1310. https://doi.org/10.1152/ajpregu.00538.2010
73. Egan, B., & Sharples, A. P. (2022). Molecular Responses to Acute Exercise and Their Relevance for Adaptations in Skeletal Muscle to Exercise Training. *Physiological reviews*, 10.1152/physrev.00054.2021. Advance online publication. https://doi.org/10.1152/physrev.00054.2021
74. Hood D. A. (2009). Mechanisms of exercise-induced mitochondrial biogenesis in skeletal muscle. *Applied physiology, nutrition, and metabolism = Physiologie appliquee, nutrition et metabolisme*, *34*(3), 465–472. https://doi.org/10.1139/H09-045
75. Saleem, A., Adhihetty, P. J., & Hood, D. A. (2009). Role of p53 in mitochondrial biogenesis and apoptosis in skeletal muscle. *Physiological genomics*, *37*(1), 58–66. https://doi.org/10.1152/physiolgenomics.90346.2008
76. Crilly, M. J., Tryon, L. D., Erlich, A. T., & Hood, D. A. (2016). The role of Nrf2 in skeletal muscle contractile and mitochondrial function. *Journal of applied physiology (Bethesda, Md.: 1985)*, *121*(3), 730–740. https://doi.org/10.1152/japplphysiol.00042.2016
77. Carter, H. N., Pauly, M., Tryon, L. D., & Hood, D. A. (2018). Effect of contractile activity on PGC-1α transcription in young and aged skeletal muscle. *Journal of applied physiology (Bethesda, Md.: 1985)*, *124*(6), 1605–1615. https://doi.org/10.1152/japplphysiol.01110.2017
78. Slavin, M. B., Kumari, R., & Hood, D. A. (2022). ATF5 is a regulator of exercise-induced mitochondrial quality control in skeletal muscle. *Molecular metabolism*, *66*, 101623. https://doi.org/10.1016/j.molmet.2022.101623
79. Nader, G. A., & Esser, K. A. (2001). Intracellular signaling specificity in skeletal muscle in response to different modes of exercise. *Journal of applied physiology (Bethesda, Md.: 1985)*, *90*(5), 1936–1942. https://doi.org/10.1152/jappl.2001.90.5.1936
80. Ato, S., Makanae, Y., Kido, K., & Fujita, S. (2016). Contraction mode itself does not determine the level of mTORC1 activity in rat skeletal muscle. *Physiological reports*, *4*(19), e12976. https://doi.org/10.14814/phy2.12976
81. Holloszy J. O. (1967). Biochemical adaptations in muscle. Effects of exercise on mitochondrial oxygen uptake and respiratory enzyme activity in skeletal muscle. *The Journal of biological chemistry*, *242*(9), 2278–2282.
82. Hood, D. A., Adhihetty, P. J., Colavecchia, M., Gordon, J. W., Irrcher, I., Joseph, A. M., Lowe, S. T., & Rungi, A. A. (2003). Mitochondrial biogenesis and the role of the protein import pathway. *Medicine and science in sports and exercise*, *35*(1), 86–94. https://doi.org/10.1097/00005768-200301000-00015
83. Hood D. A. (2001). Invited Review: contractile activity-induced mitochondrial biogenesis in skeletal muscle. *Journal of applied physiology (Bethesda, Md. : 1985)*, *90*(3), 1137–1157. https://doi.org/10.1152/jappl.2001.90.3.1137
84. Irrcher, I., Adhihetty, P. J., Joseph, A. M., Ljubicic, V., & Hood, D. A. (2003). Regulation of mitochondrial biogenesis in muscle by endurance exercise. *Sports medicine (Auckland, N.Z.)*, *33*(11), 783–793. https://doi.org/10.2165/00007256-200333110-00001
85. Ljubicic, V., Joseph, A. M., Saleem, A., Uguccioni, G., Collu-Marchese, M., Lai, R. Y., Nguyen, L. M., & Hood, D. A. (2010). Transcriptional and post-transcriptional regulation of

mitochondrial biogenesis in skeletal muscle: effects of exercise and aging. *Biochimica et biophysica acta*, *1800*(3), 223–234. https://doi.org/10.1016/j.bbagen.2009.07.031
86. Hood, D. A., Uguccioni, G., Vainshtein, A., & D'souza, D. (2011). Mechanisms of exercise-induced mitochondrial biogenesis in skeletal muscle: implications for health and disease. *Comprehensive Physiology*, *1*(3), 1119–1134. https://doi.org/10.1002/cphy.c100074
87. Gottlieb R. A. (2000). Mitochondria: execution central. *FEBS letters*, *482*(1-2), 6–12. https://doi.org/10.1016/s0014-5793(00)02010-x
88. Sakamoto, K., & Goodyear, L. J. (2002). Invited review: intracellular signaling in contracting skeletal muscle. *Journal of applied physiology (Bethesda, Md. : 1985)*, *93*(1), 369–383. https://doi.org/10.1152/japplphysiol.00167.2002
89. Hood D. A. (2009). Mechanisms of exercise-induced mitochondrial biogenesis in skeletal muscle. *Applied physiology, nutrition, and metabolism = Physiologie appliquee, nutrition et metabolisme*, *34*(3), 465–472. https://doi.org/10.1139/H09-045
90. Ljubicic, V., & Hood, D. A. (2008). Kinase-specific responsiveness to incremental contractile activity in skeletal muscle with low and high mitochondrial content. *American journal of physiology. Endocrinology and metabolism*, *295*(1), E195–E204. https://doi.org/10.1152/ajpendo.90276.2008
91. Ojuka, E. O., Jones, T. E., Han, D. H., Chen, M., & Holloszy, J. O. (2003). Raising Ca2+ in L6 myotubes mimics effects of exercise on mitochondrial biogenesis in muscle. *FASEB journal : official publication of the Federation of American Societies for Experimental Biology*, *17*(6), 675–681. https://doi.org/10.1096/fj.02-0951com
92. Puigserver, P., Rhee, J., Lin, J., Wu, Z., Yoon, J. C., Zhang, C. Y., Krauss, S., Mootha, V. K., Lowell, B. B., & Spiegelman, B. M. (2001). Cytokine stimulation of energy expenditure through p38 MAP kinase activation of PPARgamma coactivator-1. *Molecular cell*, *8*(5), 971–982. https://doi.org/10.1016/s1097-2765(01)00390-2
93. Akimoto, T., Pohnert, S. C., Li, P., Zhang, M., Gumbs, C., Rosenberg, P. B., Williams, R. S., & Yan, Z. (2005). Exercise stimulates Pgc-1alpha transcription in skeletal muscle through activation of the p38 MAPK pathway. *The Journal of biological chemistry*, *280*(20), 19587–19593. https://doi.org/10.1074/jbc.M408862200
94. Irrcher, I., Ljubicic, V., & Hood, D. A. (2009). Interactions between ROS and AMP kinase activity in the regulation of PGC-1alpha transcription in skeletal muscle cells. *American journal of physiology. Cell physiology*, *296*(1), C116–C123. https://doi.org/10.1152/ajpcell.00267.2007
95. Ristow, M., Zarse, K., Oberbach, A., Klöting, N., Birringer, M., Kiehntopf, M., Stumvoll, M., Kahn, C. R., & Blüher, M. (2009). Antioxidants prevent health-promoting effects of physical exercise in humans. *Proceedings of the National Academy of Sciences of the United States of America*, *106*(21), 8665–8670. https://doi.org/10.1073/pnas.0903485106
96. Wu, H., Kanatous, S. B., Thurmond, F. A., Gallardo, T., Isotani, E., Bassel-Duby, R., & Williams, R. S. (2002). Regulation of mitochondrial biogenesis in skeletal muscle by CaMK. *Science (New York, N.Y.)*, *296*(5566), 349–352. https://doi.org/10.1126/science.1071163
97. Chin E. R. (2004). The role of calcium and calcium/calmodulin-dependent kinases in skeletal muscle plasticity and mitochondrial biogenesis. *The Proceedings of the Nutrition Society*, *63*(2), 279–286. https://doi.org/10.1079/PNS2004335

98. Youn HD, Chatila TA, Liu JO. Integration of calcineurin and MEF2 signals by the coactivator p300 during T-cell apoptosis. EMBO J. 2000 Aug 15;19(16):4323-31. doi: 10.1093/emboj/19.16.4323. PMID: 10944115; PMCID: PMC302027.
99. Wu H, Naya FJ, McKinsey TA, Mercer B, Shelton JM, Chin ER, Simard AR, Michel RN, Bassel-Duby R, Olson EN, Williams RS. (2000). MEF2 responds to multiple calcium-regulated signals in the control of skeletal muscle fiber type. EMBO J. 19(9):1963-73. doi: 10.1093/emboj/19.9.1963
100. He, T., Huang, J., Chen, L., Han, G., Stanmore, D., Krebs-Haupenthal, J., Avkiran, M., Hagenmüller, M., & Backs, J. (2020). Cyclic AMP represses pathological MEF2 activation by myocyte-specific hypo-phosphorylation of HDAC5. *Journal of molecular and cellular cardiology*, *145*, 88–98. https://doi.org/10.1016/j.yjmcc.2020.05.018
101. Li, J., Vargas, M. A., Kapiloff, M. S., & Dodge-Kafka, K. L. (2013). Regulation of MEF2 transcriptional activity by calcineurin/mAKAP complexes. *Experimental cell research*, *319*(4), 447–454. https://doi.org/10.1016/j.yexcr.2012.12.016
102. Wu S, Zou MH. (2020). AMPK, Mitochondrial Function, and Cardiovascular Disease. Int J Mol Sci. 21(14):4987. doi: 10.3390/ijms21144987. PMID: 32679729; PMCID: PMC7404275.
103. Jäger, S., Handschin, C., St-Pierre, J., & Spiegelman, B. M. (2007). AMP-activated protein kinase (AMPK) action in skeletal muscle via direct phosphorylation of PGC-1alpha. *Proceedings of the National Academy of Sciences of the United States of America*, *104*(29), 12017–12022. https://doi.org/10.1073/pnas.0705070104
104. Cantó C, Auwerx J. (2009). PGC-1alpha, SIRT1 and AMPK, an energy sensing network that controls energy expenditure. Curr Opin Lipidol. 20(2):98-105. doi: 10.1097/MOL.0b013e328328d0a4. PMID: 19276888; PMCID: PMC3627054.
105. Irrcher, I., Ljubicic, V., Kirwan, A. F., & Hood, D. A. (2008). AMP-activated protein kinase-regulated activation of the PGC-1alpha promoter in skeletal muscle cells. *PloS one*, *3*(10), e3614. https://doi.org/10.1371/journal.pone.0003614
106. Handschin, C., Rhee, J., Lin, J., Tarr, P. T., & Spiegelman, B. M. (2003). An autoregulatory loop controls peroxisome proliferator-activated receptor gamma coactivator 1alpha expression in muscle. *Proceedings of the National Academy of Sciences of the United States of America*, *100*(12), 7111–7116. https://doi.org/10.1073/pnas.1232352100
107. Goodyear, L. J., Chang, P. Y., Sherwood, D. J., Dufresne, S. D., & Moller, D. E. (1996). Effects of exercise and insulin on mitogen-activated protein kinase signaling pathways in rat skeletal muscle. *The American journal of physiology*, *271*(2 Pt 1), E403–E408. https://doi.org/10.1152/ajpendo.1996.271.2.E403
108. Zhao, M., New, L., Kravchenko, V. V., Kato, Y., Gram, H., di Padova, F., Olson, E. N., Ulevitch, R. J., & Han, J. (1999). Regulation of the MEF2 family of transcription factors by p38. *Molecular and cellular biology*, *19*(1), 21–30. https://doi.org/10.1128/MCB.19.1.21
109. Puigserver, P., Rhee, J., Lin, J., Wu, Z., Yoon, J. C., Zhang, C. Y., Krauss, S., Mootha, V. K., Lowell, B. B., & Spiegelman, B. M. (2001). Cytokine stimulation of energy expenditure through p38 MAP kinase activation of PPARgamma coactivator-1. *Molecular cell*, *8*(5), 971–982. https://doi.org/10.1016/s1097-2765(01)00390-2
110. Amat, R., Planavila, A., Chen, S. L., Iglesias, R., Giralt, M., & Villarroya, F. (2009). SIRT1 controls the transcription of the peroxisome proliferator-activated receptor-gamma Co-activator-1alpha (PGC-1alpha) gene in skeletal muscle through the PGC-1alpha

autoregulatory loop and interaction with MyoD. *The Journal of biological chemistry*, *284*(33), 21872–21880. https://doi.org/10.1074/jbc.M109.022749
111. Suwa, M., Nakano, H., Radak, Z., & Kumagai, S. (2008). Endurance exercise increases the SIRT1 and peroxisome proliferator-activated receptor gamma coactivator-1alpha protein expressions in rat skeletal muscle. *Metabolism: clinical and experimental*, *57*(7), 986–998. https://doi.org/10.1016/j.metabol.2008.02.017
112. Gurd B. J. (2011). Deacetylation of PGC-1α by SIRT1: importance for skeletal muscle function and exercise-induced mitochondrial biogenesis. *Applied physiology, nutrition, and metabolism = Physiologie appliquee, nutrition et metabolisme*, *36*(5), 589–597. https://doi.org/10.1139/h11-070
113. Puigserver, P., Wu, Z., Park, C. W., Graves, R., Wright, M., & Spiegelman, B. M. (1998). A cold-inducible coactivator of nuclear receptors linked to adaptive thermogenesis. *Cell*, *92*(6), 829–839. https://doi.org/10.1016/s0092-8674(00)81410-5
114. Lin, J., Wu, H., Tarr, P. T., Zhang, C. Y., Wu, Z., Boss, O., Michael, L. F., Puigserver, P., Isotani, E., Olson, E. N., Lowell, B. B., Bassel-Duby, R., & Spiegelman, B. M. (2002). Transcriptional co-activator PGC-1 alpha drives the formation of slow-twitch muscle fibres. *Nature*, *418*(6899), 797–801. https://doi.org/10.1038/nature00904
115. Wu, Z., Puigserver, P., Andersson, U., Zhang, C., Adelmant, G., Mootha, V., Troy, A., Cinti, S., Lowell, B., Scarpulla, R. C., & Spiegelman, B. M. (1999). Mechanisms controlling mitochondrial biogenesis and respiration through the thermogenic coactivator PGC-1. *Cell*, *98*(1), 115–124. https://doi.org/10.1016/S0092-8674(00)80611-X
116. Handschin, C., & Spiegelman, B. M. (2006). Peroxisome proliferator-activated receptor gamma coactivator 1 coactivators, energy homeostasis, and metabolism. *Endocrine reviews*, *27*(7), 728–735. https://doi.org/10.1210/er.2006-0037
117. Puigserver, P., Adelmant, G., Wu, Z., Fan, M., Xu, J., O'Malley, B., & Spiegelman, B. M. (1999). Activation of PPARgamma coactivator-1 through transcription factor docking. *Science (New York, N.Y.)*, *286*(5443), 1368–1371. https://doi.org/10.1126/science.286.5443.1368
118. Wallberg, A. E., Yamamura, S., Malik, S., Spiegelman, B. M., & Roeder, R. G. (2003). Coordination of p300-mediated chromatin remodeling and TRAP/mediator function through coactivator PGC-1alpha. *Molecular cell*, *12*(5), 1137–1149. https://doi.org/10.1016/s1097-2765(03)00391-5
119. Scarpulla R. C. (2011). Metabolic control of mitochondrial biogenesis through the PGC-1 family regulatory network. *Biochimica et biophysica acta*, *1813*(7), 1269–1278. https://doi.org/10.1016/j.bbamcr.2010.09.019
120. Scarpulla, R. C., Vega, R. B., & Kelly, D. P. (2012). Transcriptional integration of mitochondrial biogenesis. *Trends in endocrinology and metabolism: TEM*, *23*(9), 459–466. https://doi.org/10.1016/j.tem.2012.06.006
121. Gleyzer, N., Vercauteren, K., & Scarpulla, R. C. (2005). Control of mitochondrial transcription specificity factors (TFB1M and TFB2M) by nuclear respiratory factors (NRF-1 and NRF-2) and PGC-1 family coactivators. *Molecular and cellular biology*, *25*(4), 1354–1366. https://doi.org/10.1128/MCB.25.4.1354-1366.2005
122. Scarpulla R. C. (2006). Nuclear control of respiratory gene expression in mammalian cells. *Journal of cellular biochemistry*, *97*(4), 673–683. https://doi.org/10.1002/jcb.20743

123. Scarpulla R. C. (2008). Transcriptional paradigms in mammalian mitochondrial biogenesis and function. *Physiological reviews*, *88*(2), 611–638. https://doi.org/10.1152/physrev.00025.2007
124. Little, J. P., Safdar, A., Bishop, D., Tarnopolsky, M. A., & Gibala, M. J. (2011). An acute bout of high-intensity interval training increases the nuclear abundance of PGC-1α and activates mitochondrial biogenesis in human skeletal muscle. *American journal of physiology. Regulatory, integrative and comparative physiology*, *300*(6), R1303–R1310. https://doi.org/10.1152/ajpregu.00538.2010
125. Baar, K., Wende, A. R., Jones, T. E., Marison, M., Nolte, L. A., Chen, M., Kelly, D. P., & Holloszy, J. O. (2002). Adaptations of skeletal muscle to exercise: rapid increase in the transcriptional coactivator PGC-1. *FASEB journal : official publication of the Federation of American Societies for Experimental Biology*, *16*(14), 1879–1886. https://doi.org/10.1096/fj.02-0367com
126. Pilegaard, H., Saltin, B., & Neufer, P. D. (2003). Exercise induces transient transcriptional activation of the PGC-1alpha gene in human skeletal muscle. *The Journal of physiology*, *546*(Pt 3), 851–858. https://doi.org/10.1113/jphysiol.2002.034850
127. Irrcher, I., Adhihetty, P. J., Sheehan, T., Joseph, A. M., & Hood, D. A. (2003). PPARgamma coactivator-1alpha expression during thyroid hormone- and contractile activity-induced mitochondrial adaptations. *American journal of physiology. Cell physiology*, *284*(6), C1669–C1677. https://doi.org/10.1152/ajpcell.00409.2002
128. Joseph, A. M., Pilegaard, H., Litvintsev, A., Leick, L., & Hood, D. A. (2006). Control of gene expression and mitochondrial biogenesis in the muscular adaptation to endurance exercise. *Essays in biochemistry*, *42*, 13–29. https://doi.org/10.1042/bse0420013
129. Carter, H. N., & Hood, D. A. (2012). Contractile activity-induced mitochondrial biogenesis and mTORC1. *American journal of physiology. Cell physiology*, *303*(5), C540–C547. https://doi.org/10.1152/ajpcell.00156.2012
130. Uguccioni, G., & Hood, D. A. (2011). The importance of PGC-1α in contractile activity-induced mitochondrial adaptations. *American journal of physiology. Endocrinology and metabolism*, *300*(2), E361–E371. https://doi.org/10.1152/ajpendo.00292.2010
131. Baldwin, K. M., Klinkerfuss, G. H., Terjung, R. L., Molé, P. A., & Holloszy, J. O. (1972). Respiratory capacity of white, red, and intermediate muscle: adaptative response to exercise. *The American journal of physiology*, *222*(2), 373–378. https://doi.org/10.1152/ajplegacy.1972.222.2.373
132. Adhihetty, P. J., Uguccioni, G., Leick, L., Hidalgo, J., Pilegaard, H., & Hood, D. A. (2009). The role of PGC-1alpha on mitochondrial function and apoptotic susceptibility in muscle. *American journal of physiology. Cell physiology*, *297*(1), C217–C225. https://doi.org/10.1152/ajpcell.00070.2009
133. Handschin, C., Chin, S., Li, P., Liu, F., Maratos-Flier, E., Lebrasseur, N. K., Yan, Z., & Spiegelman, B. M. (2007). Skeletal muscle fiber-type switching, exercise intolerance, and myopathy in PGC-1alpha muscle-specific knock-out animals. *The Journal of biological chemistry*, *282*(41), 30014–30021. https://doi.org/10.1074/jbc.M704817200
134. Leone, T. C., Lehman, J. J., Finck, B. N., Schaeffer, P. J., Wende, A. R., Boudina, S., Courtois, M., Wozniak, D. F., Sambandam, N., Bernal-Mizrachi, C., Chen, Z., Holloszy, J. O., Medeiros, D. M., Schmidt, R. E., Saffitz, J. E., Abel, E. D., Semenkovich, C. F., & Kelly, D. P. (2005). PGC-1alpha deficiency causes multi-system energy metabolic derangements:

muscle dysfunction, abnormal weight control and hepatic steatosis. *PLoS biology*, *3*(4), e101. https://doi.org/10.1371/journal.pbio.0030101

135. Leick, L., Wojtaszewski, J. F., Johansen, S. T., Kiilerich, K., Comes, G., Hellsten, Y., Hidalgo, J., & Pilegaard, H. (2008). PGC-1alpha is not mandatory for exercise- and training-induced adaptive gene responses in mouse skeletal muscle. *American journal of physiology. Endocrinology and metabolism*, *294*(2), E463–E474. https://doi.org/10.1152/ajpendo.00666.2007
136. Rowe, G. C., El-Khoury, R., Patten, I. S., Rustin, P., & Arany, Z. (2012). PGC-1α is dispensable for exercise-induced mitochondrial biogenesis in skeletal muscle. *PloS one*, *7*(7), e41817. https://doi.org/10.1371/journal.pone.0041817
137. Leick, L., Wojtaszewski, J. F., Johansen, S. T., Kiilerich, K., Comes, G., Hellsten, Y., Hidalgo, J., & Pilegaard, H. (2008). PGC-1alpha is not mandatory for exercise- and training-induced adaptive gene responses in mouse skeletal muscle. *American journal of physiology. Endocrinology and metabolism*, *294*(2), E463–E474. https://doi.org/10.1152/ajpendo.00666.2007
138. Calvo, J. A., Daniels, T. G., Wang, X., Paul, A., Lin, J., Spiegelman, B. M., Stevenson, S. C., & Rangwala, S. M. (2008). Muscle-specific expression of PPARgamma coactivator-1alpha improves exercise performance and increases peak oxygen uptake. *Journal of applied physiology (Bethesda, Md.: 1985)*, *104*(5), 1304–1312. https://doi.org/10.1152/japplphysiol.01231.2007
139. Bolender N, Sickmann A, Wagner R, Meisinger C, Pfanner N. (2008). Multiple pathways for sorting mitochondrial precursor proteins. EMBO Rep. 9(1):42-9. doi: 10.1038/sj.embor.7401126. PMID: 18174896; PMCID: PMC2246611.
140. Chacinska, A., Koehler, C. M., Milenkovic, D., Lithgow, T., & Pfanner, N. (2009). Importing mitochondrial proteins: machineries and mechanisms. *Cell*, *138*(4), 628–644. https://doi.org/10.1016/j.cell.2009.08.005
141. Koehler C. M. (2000). Protein translocation pathways of the mitochondrion. *FEBS letters*, *476*(1-2), 27–31. https://doi.org/10.1016/s0014-5793(00)01664-1
142. Wiedemann, N., & Pfanner, N. (2017). Mitochondrial Machineries for Protein Import and Assembly. *Annual review of biochemistry*, *86*, 685–714. https://doi.org/10.1146/annurev-biochem-060815-014352
143. Hood, D. A., Memme, J. M., Oliveira, A. N., & Triolo, M. (2019). Maintenance of Skeletal Muscle Mitochondria in Health, Exercise, and Aging. *Annual review of physiology*, *81*, 19–41. https://doi.org/10.1146/annurev-physiol-020518-114310
144. Matouschek, A., Pfanner, N., & Voos, W. (2000). Protein unfolding by mitochondria. The Hsp70 import motor. *EMBO reports*, *1*(5), 404–410. https://doi.org/10.1093/embo-reports/kvd093
145. Kutik, S., Stojanovski, D., Becker, L., Becker, T., Meinecke, M., Krüger, V., Prinz, C., Meisinger, C., Guiard, B., Wagner, R., Pfanner, N., & Wiedemann, N. (2008). Dissecting membrane insertion of mitochondrial beta-barrel proteins. *Cell*, *132*(6), 1011–1024. https://doi.org/10.1016/j.cell.2008.01.028
146. Takahashi, M., & Hood, D. A. (1993). Chronic stimulation-induced changes in mitochondria and performance in rat skeletal muscle. *Journal of applied physiology (Bethesda, Md.: 1985)*, *74*(2), 934–941. https://doi.org/10.1152/jappl.1993.74.2.934

147. Ornatsky, O. I., Connor, M. K., & Hood, D. A. (1995). Expression of stress proteins and mitochondrial chaperonins in chronically stimulated skeletal muscle. *The Biochemical journal*, *311 (Pt 1)*(Pt 1), 119–123. https://doi.org/10.1042/bj3110119
148. Takahashi, M., Chesley, A., Freyssenet, D., & Hood, D. A. (1998). Contractile activity-induced adaptations in the mitochondrial protein import system. *The American journal of physiology*, *274*(5), C1380–C1387. https://doi.org/10.1152/ajpcell.1998.274.5.C1380
149. Mesbah Moosavi, Z. S., & Hood, D. A. (2017). The unfolded protein response in relation to mitochondrial biogenesis in skeletal muscle cells. *American journal of physiology. Cell physiology*, *312*(5), C583–C594. https://doi.org/10.1152/ajpcell.00320.2016
150. Mottis, A., Jovaisaite, V., & Auwerx, J. (2014). The mitochondrial unfolded protein response in mammalian physiology. *Mammalian genome: official journal of the International Mammalian Genome Society*, *25*(9-10), 424–433. https://doi.org/10.1007/s00335-014-9525-z
151. Lira, V. A., Okutsu, M., Zhang, M., Greene, N. P., Laker, R. C., Breen, D. S., Hoehn, K. L., & Yan, Z. (2013). Autophagy is required for exercise training-induced skeletal muscle adaptation and improvement of physical performance. *FASEB journal : official publication of the Federation of American Societies for Experimental Biology*, *27*(10), 4184–4193. https://doi.org/10.1096/fj.13-228486
152. Kim, Y., Triolo, M., Erlich, A. T., & Hood, D. A. (2019). Regulation of autophagic and mitophagic flux during chronic contractile activity-induced muscle adaptations. *Pflugers Archiv : European journal of physiology*, *471*(3), 431–440. https://doi.org/10.1007/s00424-018-2225-x
153. Pickles, S., Vigié, P., & Youle, R. J. (2018). Mitophagy and Quality Control Mechanisms in Mitochondrial Maintenance. *Current biology : CB*, *28*(4), R170–R185. https://doi.org/10.1016/j.cub.2018.01.004
154. Wei, H., Liu, L., & Chen, Q. (2015). Selective removal of mitochondria via mitophagy: distinct pathways for different mitochondrial stresses. *Biochimica et biophysica acta*, *1853*(10 Pt B), 2784–2790. https://doi.org/10.1016/j.bbamcr.2015.03.013
155. Kim, Y., & Hood, D. A. (2017). Regulation of the autophagy system during chronic contractile activity-induced muscle adaptations. *Physiological reports*, *5*(14), e13307. https://doi.org/10.14814/phy2.13307
156. Zeng J, Shirihai OS, Grinstaff MW. (2020). Modulating lysosomal pH: a molecular and nanoscale materials design perspective. J Life Sci (Westlake Village). (4):25-37. doi: 10.36069/jols/20201204. PMID: 33403369; PMCID: PMC7781074.
157. Geisler, S., Holmström, K. M., Skujat, D., Fiesel, F. C., Rothfuss, O. C., Kahle, P. J., & Springer, W. (2010). PINK1/Parkin-mediated mitophagy is dependent on VDAC1 and p62/SQSTM1. *Nature cell biology*, *12*(2), 119–131. https://doi.org/10.1038/ncb2012
158. Jin, S. M., Lazarou, M., Wang, C., Kane, L. A., Narendra, D. P., & Youle, R. J. (2010). Mitochondrial membrane potential regulates PINK1 import and proteolytic destabilization by PARL. *The Journal of cell biology*, *191*(5), 933–942. https://doi.org/10.1083/jcb.201008084
159. Narendra, D. P., Jin, S. M., Tanaka, A., Suen, D. F., Gautier, C. A., Shen, J., Cookson, M. R., & Youle, R. J. (2010). PINK1 is selectively stabilized on impaired mitochondria to activate Parkin. *PLoS biology*, *8*(1), e1000298. https://doi.org/10.1371/journal.pbio.1000298

160. Tanida, I., Ueno, T., & Kominami, E. (2004). LC3 conjugation system in mammalian autophagy. *The international journal of biochemistry & cell biology*, *36*(12), 2503–2518. https://doi.org/10.1016/j.biocel.2004.05.009
161. Mizushima, N., Yoshimori, T., & Ohsumi, Y. (2011). The role of Atg proteins in autophagosome formation. *Annual review of cell and developmental biology*, *27*, 107–132. https://doi.org/10.1146/annurev-cellbio-092910-154005
162. Vainshtein, A., & Hood, D. A. (2016). The regulation of autophagy during exercise in skeletal muscle. *Journal of applied physiology (Bethesda, Md.: 1985)*, *120*(6), 664–673. https://doi.org/10.1152/japplphysiol.00550.2015
163. Chen, C. C. W., Erlich, A. T., & Hood, D. A. (2018). Role of Parkin and endurance training on mitochondrial turnover in skeletal muscle. *Skeletal muscle*, *8*(1), 10. https://doi.org/10.1186/s13395-018-0157-y
164. Tian, W., Li, W., Chen, Y., Yan, Z., Huang, X., Zhuang, H., Zhong, W., Chen, Y., Wu, W., Lin, C., Chen, H., Hou, X., Zhang, L., Sui, S., Zhao, B., Hu, Z., Li, L., & Feng, D. (2015). Phosphorylation of ULK1 by AMPK regulates translocation of ULK1 to mitochondria and mitophagy. *FEBS letters*, *589*(15), 1847–1854. https://doi.org/10.1016/j.febslet.2015.05.020
165. Laker, R. C., Drake, J. C., Wilson, R. J., Lira, V. A., Lewellen, B. M., Ryall, K. A., Fisher, C. C., Zhang, M., Saucerman, J. J., Goodyear, L. J., Kundu, M., & Yan, Z. (2017). Ampk phosphorylation of Ulk1 is required for targeting of mitochondria to lysosomes in exercise-induced mitophagy. *Nature communications*, *8*(1), 548. https://doi.org/10.1038/s41467-017-00520-9
166. Vainshtein, A., Tryon, L. D., Pauly, M., & Hood, D. A. (2015). Role of PGC-1α during acute exercise-induced autophagy and mitophagy in skeletal muscle. *American journal of physiology. Cell physiology*, *308*(9), C710–C719. https://doi.org/10.1152/ajpcell.00380.2014
167. Chen, C. C. W., Erlich, A. T., Crilly, M. J., & Hood, D. A. (2018). Parkin is required for exercise-induced mitophagy in muscle: impact of aging. *American journal of physiology. Endocrinology and metabolism*, *315*(3), E404–E415. https://doi.org/10.1152/ajpendo.00391.2017
168. Parikh, V. S., Morgan, M. M., Scott, R., Clements, L. S., & Butow, R. A. (1987). The mitochondrial genotype can influence nuclear gene expression in yeast. *Science (New York, N.Y.)*, *235*(4788), 576–580. https://doi.org/10.1126/science.3027892
169. Quirós, P. M., Mottis, A., & Auwerx, J. (2016). Mitonuclear communication in homeostasis and stress. *Nature reviews. Molecular cell biology*, *17*(4), 213–226. https://doi.org/10.1038/nrm.2016.23
170. Eckl, E. M., Ziegemann, O., Krumwiede, L., Fessler, E., & Jae, L. T. (2021). Sensing, signaling and surviving mitochondrial stress. *Cellular and molecular life sciences : CMLS*, *78*(16), 5925–5951. https://doi.org/10.1007/s00018-021-03887-7
171. Roca-Portoles, A., & Tait, S. W. G. (2021). Mitochondrial quality control: from molecule to organelle. *Cellular and molecular life sciences : CMLS*, *78*(8), 3853–3866. https://doi.org/10.1007/s00018-021-03775-0
172. Huertas, J. R., Casuso, R. A., Agustín, P. H., & Cogliati, S. (2019). Stay Fit, Stay Young: Mitochondria in Movement: The Role of Exercise in the New Mitochondrial Paradigm. *Oxidative medicine and cellular longevity*, *2019*, 7058350. https://doi.org/10.1155/2019/7058350
173. Merry, T. L., & Ristow, M. (2016). Mitohormesis in exercise training. *Free radical biology & medicine*, *98*, 123–130. https://doi.org/10.1016/j.freeradbiomed.2015.11.032

174. Philp, A. M., Saner, N. J., Lazarou, M., Ganley, I. G., & Philp, A. (2021). The influence of aerobic exercise on mitochondrial quality control in skeletal muscle. *The Journal of physiology*, *599*(14), 3463–3476. https://doi.org/10.1113/JP279411
175. Vargas-Mendoza, N., Angeles-Valencia, M., Morales-González, Á., Madrigal-Santillán, E. O., Morales-Martínez, M., Madrigal-Bujaidar, E., Álvarez-González, I., Gutiérrez-Salinas, J., Esquivel-Chirino, C., Chamorro-Cevallos, G., Cristóbal-Luna, J. M., & Morales-González, J. A. (2021). Oxidative Stress, Mitochondrial Function and Adaptation to Exercise: New Perspectives in Nutrition. *Life (Basel, Switzerland)*, *11*(11), 1269. https://doi.org/10.3390/life11111269
176. Musci, R. V., Hamilton, K. L., & Linden, M. A. (2019). Exercise-Induced Mitohormesis for the Maintenance of Skeletal Muscle and Healthspan Extension. *Sports (Basel, Switzerland)*, *7*(7), 170. https://doi.org/10.3390/sports7070170
177. Pakos-Zebrucka, K., Koryga, I., Mnich, K., Ljujic, M., Samali, A., & Gorman, A. M. (2016). The integrated stress response. *EMBO reports*, *17*(10), 1374–1395. https://doi.org/10.15252/embr.201642195
178. Costa-Mattioli, M., & Walter, P. (2020). The integrated stress response: From mechanism to disease. *Science (New York, N.Y.)*, *368*(6489), eaat5314. https://doi.org/10.1126/science.aat5314
179. Mick, E., Titov, D. V., Skinner, O. S., Sharma, R., Jourdain, A. A., & Mootha, V. K. (2020). Distinct mitochondrial defects trigger the integrated stress response depending on the metabolic state of the cell. *eLife*, *9*, e49178. https://doi.org/10.7554/eLife.49178
180. Donnelly, N., Gorman, A. M., Gupta, S., & Samali, A. (2013). The eIF2α kinases: their structures and functions. *Cellular and molecular life sciences : CMLS*, *70*(19), 3493–3511. https://doi.org/10.1007/s00018-012-1252-6
181. Kimball S. R. (1999). Eukaryotic initiation factor eIF2. *The international journal of biochemistry & cell biology*, *31*(1), 25–29. https://doi.org/10.1016/s1357-2725(98)00128-9
182. Dever T. E. (2002). Gene-specific regulation by general translation factors. *Cell*, *108*(4), 545–556. https://doi.org/10.1016/s0092-8674(02)00642-6
183. Wek R. C. (2018). Role of eIF2α Kinases in Translational Control and Adaptation to Cellular Stress. *Cold Spring Harbor perspectives in biology*, *10*(7), a032870. https://doi.org/10.1101/cshperspect.a032870
184. Harding, H. P., Novoa, I., Zhang, Y., Zeng, H., Wek, R., Schapira, M., & Ron, D. (2000). Regulated translation initiation controls stress-induced gene expression in mammalian cells. *Molecular cell*, *6*(5), 1099–1108. https://doi.org/10.1016/s1097-2765(00)00108-8
185. Algire, M. A., Maag, D., & Lorsch, J. R. (2005). Pi release from eIF2, not GTP hydrolysis, is the step controlled by start-site selection during eukaryotic translation initiation. *Molecular cell*, *20*(2), 251–262. https://doi.org/10.1016/j.molcel.2005.09.008
186. Jackson, R. J., Hellen, C. U., & Pestova, T. V. (2010). The mechanism of eukaryotic translation initiation and principles of its regulation. *Nature reviews. Molecular cell biology*, *11*(2), 113–127. https://doi.org/10.1038/nrm2838
187. Sonenberg, N., & Hinnebusch, A. G. (2009). Regulation of translation initiation in eukaryotes: mechanisms and biological targets. *Cell*, *136*(4), 731–745. https://doi.org/10.1016/j.cell.2009.01.042
188. Pavitt G. D. (2018). Regulation of translation initiation factor eIF2B at the hub of the integrated stress response. *Wiley interdisciplinary reviews. RNA*, *9*(6), e1491. https://doi.org/10.1002/wrna.1491

189. Sidrauski, C., Tsai, J. C., Kampmann, M., Hearn, B. R., Vedantham, P., Jaishankar, P., Sokabe, M., Mendez, A. S., Newton, B. W., Tang, E. L., Verschueren, E., Johnson, J. R., Krogan, N. J., Fraser, C. S., Weissman, J. S., Renslo, A. R., & Walter, P. (2015). Pharmacological dimerization and activation of the exchange factor eIF2B antagonizes the integrated stress response. *eLife*, *4*, e07314. https://doi.org/10.7554/eLife.07314
190. Cohen P. T. (2002). Protein phosphatase 1--targeted in many directions. *Journal of cell science*, *115*(Pt 2), 241–256. https://doi.org/10.1242/jcs.115.2.241
191. Novoa, I., Zeng, H., Harding, H. P., & Ron, D. (2001). Feedback inhibition of the unfolded protein response by GADD34-mediated dephosphorylation of eIF2alpha. *The Journal of cell biology*, *153*(5), 1011–1022. https://doi.org/10.1083/jcb.153.5.1011
192. Jousse, C., Oyadomari, S., Novoa, I., Lu, P., Zhang, Y., Harding, H. P., & Ron, D. (2003). Inhibition of a constitutive translation initiation factor 2alpha phosphatase, CReP, promotes survival of stressed cells. *The Journal of cell biology*, *163*(4), 767–775. https://doi.org/10.1083/jcb.200308075
193. Ebert, S. M., Rasmussen, B. B., Judge, A. R., Judge, S. M., Larsson, L., Wek, R. C., Anthony, T. G., Marcotte, G. R., Miller, M. J., Yorek, M. A., Vella, A., Volpi, E., Stern, J. I., Strub, M. D., Ryan, Z., Talley, J. J., & Adams, C. M. (2022). Biology of Activating Transcription Factor 4 (ATF4) and Its Role in Skeletal Muscle Atrophy. *The Journal of nutrition*, *152*(4), 926–938. https://doi.org/10.1093/jn/nxab440
194. Ameri, K., & Harris, A. L. (2008). Activating transcription factor 4. *The international journal of biochemistry & cell biology*, *40*(1), 14–21. https://doi.org/10.1016/j.biocel.2007.01.020
195. Vallejo, M., Ron, D., Miller, C. P., & Habener, J. F. (1993). C/ATF, a member of the activating transcription factor family of DNA-binding proteins, dimerizes with CAAT/enhancer-binding proteins and directs their binding to cAMP response elements. *Proceedings of the National Academy of Sciences of the United States of America*, *90*(10), 4679–4683. https://doi.org/10.1073/pnas.90.10.4679
196. Karpinski, B. A., Morle, G. D., Huggenvik, J., Uhler, M. D., & Leiden, J. M. (1992). Molecular cloning of human CREB-2: an ATF/CREB transcription factor that can negatively regulate transcription from the cAMP response element. *Proceedings of the National Academy of Sciences of the United States of America*, *89*(11), 4820–4824. https://doi.org/10.1073/pnas.89.11.4820
197. Wortel, I. M. N., van der Meer, L. T., Kilberg, M. S., & van Leeuwen, F. N. (2017). Surviving Stress: Modulation of ATF4-Mediated Stress Responses in Normal and Malignant Cells. *Trends in endocrinology and metabolism: TEM*, *28*(11), 794–806. https://doi.org/10.1016/j.tem.2017.07.003
198. Pons, J., Evrard-Todeschi, N., Bertho, G., Gharbi-Benarous, J., Benarous, R., & Girault, J. P. (2007). Phosphorylation-dependent structure of ATF4 peptides derived from a human ATF4 protein, a member of the family of transcription factors. *Peptides*, *28*(12), 2253–2267. https://doi.org/10.1016/j.peptides.2007.09.016
199. Podust, L. M., Krezel, A. M., & Kim, Y. (2001). Crystal structure of the CCAAT box/enhancer-binding protein beta activating transcription factor-4 basic leucine zipper heterodimer in the absence of DNA. *The Journal of biological chemistry*, *276*(1), 505–513. https://doi.org/10.1074/jbc.M005594200
200. Keerthiga, R., Pei, D. S., & Fu, A. (2021). Mitochondrial dysfunction, UPR^{mt} signaling, and targeted therapy in metastasis tumor. *Cell & bioscience*, *11*(1), 186. https://doi.org/10.1186/s13578-021-00696-0

201. B'chir, W., Maurin, A. C., Carraro, V., Averous, J., Jousse, C., Muranishi, Y., Parry, L., Stepien, G., Fafournoux, P., & Bruhat, A. (2013). The eIF2α/ATF4 pathway is essential for stress-induced autophagy gene expression. *Nucleic acids research*, *41*(16), 7683–7699. https://doi.org/10.1093/nar/gkt563
202. Lassot, I., Ségéral, E., Berlioz-Torrent, C., Durand, H., Groussin, L., Hai, T., Benarous, R., & Margottin-Goguet, F. (2001). ATF4 degradation relies on a phosphorylation-dependent interaction with the SCF(betaTrCP) ubiquitin ligase. *Molecular and cellular biology*, *21*(6), 2192–2202. https://doi.org/10.1128/MCB.21.6.2192-2202.2001
203. Lassot, I., Estrabaud, E., Emiliani, S., Benkirane, M., Benarous, R., & Margottin-Goguet, F. (2005). p300 modulates ATF4 stability and transcriptional activity independently of its acetyltransferase domain. *The Journal of biological chemistry*, *280*(50), 41537–41545. https://doi.org/10.1074/jbc.M505294200
204. Köditz, J., Nesper, J., Wottawa, M., Stiehl, D. P., Camenisch, G., Franke, C., Myllyharju, J., Wenger, R. H., & Katschinski, D. M. (2007). Oxygen-dependent ATF-4 stability is mediated by the PHD3 oxygen sensor. *Blood*, *110*(10), 3610–3617. https://doi.org/10.1182/blood-2007-06-094441
205. Dey S, Baird TD, Zhou D, Palam LR, Spandau DF, Wek RC. Both transcriptional regulation and translational control of ATF4 are central to the integrated stress response. J Biol Chem. 2010 Oct 22;285(43):33165-33174. doi: 10.1074/jbc.M110.167213.
206. Matsuguchi, T., Chiba, N., Bandow, K., Kakimoto, K., Masuda, A., & Ohnishi, T. (2009). JNK activity is essential for Atf4 expression and late-stage osteoblast differentiation. *Journal of bone and mineral research : the official journal of the American Society for Bone and Mineral Research*, *24*(3), 398–410. https://doi.org/10.1359/jbmr.081107
207. Khan, N. A., Nikkanen, J., Yatsuga, S., Jackson, C., Wang, L., Pradhan, S., Kivelä, R., Pessia, A., Velagapudi, V., & Suomalainen, A. (2017). mTORC1 Regulates Mitochondrial Integrated Stress Response and Mitochondrial Myopathy Progression. *Cell metabolism*, *26*(2), 419–428.e5. https://doi.org/10.1016/j.cmet.2017.07.007
208. Bilen, M.; Benhammouda, S.; Slack, R.S.; Germain, M. The integrated stress response as a key pathway downstream of mitochondrial dysfunction. *Curr. Opin. Physiol.* **2022**, *27*, 100555.
209. Baird TD, Wek RC. Eukaryotic initiation factor 2 phosphorylation and translational control in metabolism. Adv Nutr. 2012 May 1;3(3):307-21. doi: 10.3945/an.112.002113.
210. Quirós, P. M., Prado, M. A., Zamboni, N., D'Amico, D., Williams, R. W., Finley, D., Gygi, S. P., & Auwerx, J. (2017). Multi-omics analysis identifies ATF4 as a key regulator of the mitochondrial stress response in mammals. *The Journal of cell biology*, *216*(7), 2027–2045. https://doi.org/10.1083/jcb.201702058
211. Sasaki, K., Uchiumi, T., Toshima, T., Yagi, M., Do, Y., Hirai, H., Igami, K., Gotoh, K., & Kang, D. (2020). Mitochondrial translation inhibition triggers ATF4 activation, leading to integrated stress response but not to mitochondrial unfolded protein response. *Bioscience reports*, *40*(11), BSR20201289. https://doi.org/10.1042/BSR20201289
212. Mahor, D., Pandey, R., & Bulusu, V. (2022). TCA cycle off, ATF4 on for metabolic homeostasis. *Trends in biochemical sciences*, *47*(7), 558–560. https://doi.org/10.1016/j.tibs.2022.03.006
213. Kasai S, Yamazaki H, Tanji K, Engler MJ, Matsumiya T, Itoh K. (2019). Role of the ISR-ATF4 pathway and its cross talk with Nrf2 in mitochondrial quality control. J Clin Biochem Nutr. 64(1):1-12. doi: 10.3164/jcbn.18-37

214. Harding, H. P., Zhang, Y., Zeng, H., Novoa, I., Lu, P. D., Calfon, M., Sadri, N., Yun, C., Popko, B., Paules, R., Stojdl, D. F., Bell, J. C., Hettmann, T., Leiden, J. M., & Ron, D. (2003). An integrated stress response regulates amino acid metabolism and resistance to oxidative stress. *Molecular cell*, *11*(3), 619–633. https://doi.org/10.1016/s1097-2765(03)00105-9
215. Fusakio ME, Willy JA, Wang Y, Mirek ET, Al Baghdadi RJ, Adams CM, Anthony TG, Wek RC. Transcription factor ATF4 directs basal and stress-induced gene expression in the unfolded protein response and cholesterol metabolism in the liver. Mol Biol Cell. 2016 May 1;27(9):1536-51. doi: 10.1091/mbc.E16-01-0039.
216. Teske BF, Fusakio ME, Zhou D, Shan J, McClintick JN, Kilberg MS, Wek RC. CHOP induces activating transcription factor 5 (ATF5) to trigger apoptosis in response to perturbations in protein homeostasis. Mol Biol Cell. 2013 Aug;24(15):2477-90. doi: 10.1091/mbc.E13-01-0067..
217. Fiorese, C. J., Schulz, A. M., Lin, Y. F., Rosin, N., Pellegrino, M. W., & Haynes, C. M. (2016). The Transcription Factor ATF5 Mediates a Mammalian Mitochondrial UPR. *Current biology : CB*, *26*(15), 2037–2043. https://doi.org/10.1016/j.cub.2016.06.002
218. Zhao, Q., Wang, J., Levichkin, I. V., Stasinopoulos, S., Ryan, M. T., & Hoogenraad, N. J. (2002). A mitochondrial specific stress response in mammalian cells. *The EMBO journal*, *21*(17), 4411–4419. https://doi.org/10.1093/emboj/cdf445
219. Memme, J.M., Sanfrancesco, V. C., & Hood, D. A. (2023). ATF4 regulates mitochondrial content, morphology, and function in skeletal muscle cells. *American Journal of Physiology, Cell Physiology.* (In Press).
220. Memme, J. M., Oliveira, A. N., & Hood, D. A. (2016). Chronology of UPR activation in skeletal muscle adaptations to chronic contractile activity. *American journal of physiology. Cell physiology*, *310*(11), C1024–C1036. https://doi.org/10.1152/ajpcell.00009.2016
221. Montori-Grau, M., Aguilar-Recarte, D., Zarei, M., Pizarro-Delgado, J., Palomer, X., & Vázquez-Carrera, M. (2022). Endoplasmic reticulum stress downregulates PGC-1α in skeletal muscle through ATF4 and an mTOR-mediated reduction of CRTC2. *Cell communication and signaling : CCS*, *20*(1), 53. https://doi.org/10.1186/s12964-022-00865-9
222. Luo, S., Baumeister, P., Yang, S., Abcouwer, S. F., & Lee, A. S. (2003). Induction of Grp78/BiP by translational block: activation of the Grp78 promoter by ATF4 through and upstream ATF/CRE site independent of the endoplasmic reticulum stress elements. *The Journal of biological chemistry*, *278*(39), 37375–37385. https://doi.org/10.1074/jbc.M303619200
223. Huggins, C. J., Mayekar, M. K., Martin, N., Saylor, K. L., Gonit, M., Jailwala, P., Kasoji, M., Haines, D. C., Quiñones, O. A., & Johnson, P. F. (2015). C/EBPγ Is a Critical Regulator of Cellular Stress Response Networks through Heterodimerization with ATF4. *Molecular and cellular biology*, *36*(5), 693–713. https://doi.org/10.1128/MCB.00911-15
224. Roufayel, R., Younes, K., Al-Sabi, A., & Murshid, N. (2022). BH3-Only Proteins Noxa and Puma Are Key Regulators of Induced Apoptosis. *Life (Basel, Switzerland)*, *12*(2), 256. https://doi.org/10.3390/life12020256
225. Adams, C. M., Ebert, S. M., & Dyle, M. C. (2017). Role of ATF4 in skeletal muscle atrophy. *Current opinion in clinical nutrition and metabolic care*, *20*(3), 164–168. https://doi.org/10.1097/MCO.0000000000000362
226. Ebert, S. M., Bullard, S. A., Basisty, N., Marcotte, G. R., Skopec, Z. P., Dierdorff, J. M., Al-Zougbi, A., Tomcheck, K. C., DeLau, A. D., Rathmacher, J. A., Bodine, S. C., Schilling, B., & Adams, C. M. (2020). Activating transcription factor 4 (ATF4) promotes skeletal muscle

atrophy by forming a heterodimer with the transcriptional regulator C/EBPβ. *The Journal of biological chemistry*, *295*(9), 2787–2803. https://doi.org/10.1074/jbc.RA119.012095
227. Llano-Diez, M., Fury, W., Okamoto, H., Bai, Y., Gromada, J., & Larsson, L. (2019). RNA-sequencing reveals altered skeletal muscle contraction, E3 ligases, autophagy, apoptosis, and chaperone expression in patients with critical illness myopathy. *Skeletal muscle*, *9*(1), 9. https://doi.org/10.1186/s13395-019-0194-1
228. Ebert, S. M., Monteys, A. M., Fox, D. K., Bongers, K. S., Shields, B. E., Malmberg, S. E., Davidson, B. L., Suneja, M., & Adams, C. M. (2010). The transcription factor ATF4 promotes skeletal myofiber atrophy during fasting. *Molecular endocrinology (Baltimore, Md.)*, *24*(4), 790–799. https://doi.org/10.1210/me.2009-0345
229. Ebert, S. M., Dyle, M. C., Bullard, S. A., Dierdorff, J. M., Murry, D. J., Fox, D. K., Bongers, K. S., Lira, V. A., Meyerholz, D. K., Talley, J. J., & Adams, C. M. (2015). Identification and Small Molecule Inhibition of an Activating Transcription Factor 4 (ATF4)-dependent Pathway to Age-related Skeletal Muscle Weakness and Atrophy. *The Journal of biological chemistry*, *290*(42), 25497–25511. https://doi.org/10.1074/jbc.M115.681445
230. Fox, D. K., Ebert, S. M., Bongers, K. S., Dyle, M. C., Bullard, S. A., Dierdorff, J. M., Kunkel, S. D., & Adams, C. M. (2014). p53 and ATF4 mediate distinct and additive pathways to skeletal muscle atrophy during limb immobilization. *American journal of physiology. Endocrinology and metabolism*, *307*(3), E245–E261. https://doi.org/10.1152/ajpendo.00010.2014
231. Koncha, R. R., Ramachandran, G., Sepuri, N. B. V., & Ramaiah, K. V. A. (2021). CCCP-induced mitochondrial dysfunction - characterization and analysis of integrated stress response to cellular signaling and homeostasis. *The FEBS journal*, *288*(19), 5737–5754. https://doi.org/10.1111/febs.15868
232. Baker, B. M., Nargund, A. M., Sun, T., & Haynes, C. M. (2012). Protective coupling of mitochondrial function and protein synthesis via the eIF2α kinase GCN-2. *PLoS genetics*, *8*(6), e1002760. https://doi.org/10.1371/journal.pgen.1002760
233. Falcón, P., Escandón, M., Brito, Á., & Matus, S. (2019). Nutrient Sensing and Redox Balance: GCN2 as a New Integrator in Aging. *Oxidative medicine and cellular longevity*, *2019*, 5730532. https://doi.org/10.1155/2019/5730532
234. Castilho, B. A., Shanmugam, R., Silva, R. C., Ramesh, R., Himme, B. M., & Sattlegger, E. (2014). Keeping the eIF2 alpha kinase Gcn2 in check. *Biochimica et biophysica acta*, *1843*(9), 1948–1968. https://doi.org/10.1016/j.bbamcr.2014.04.006
235. Masson GR. Towards a model of GCN2 activation. Biochem Soc Trans. 2019 Oct 31;47(5):1481-1488. doi: 10.1042/BST20190331. PMID: 31647517; PMCID: PMC6824675.
236. Chaveroux, C., Lambert-Langlais, S., Parry, L., Carraro, V., Jousse, C., Maurin, A. C., Bruhat, A., Marceau, G., Sapin, V., Averous, J., & Fafournoux, P. (2011). Identification of GCN2 as new redox regulator for oxidative stress prevention in vivo. *Biochemical and biophysical research communications*, *415*(1), 120–124. https://doi.org/10.1016/j.bbrc.2011.10.027
237. Guo, X., Aviles, G., Liu, Y., Tian, R., Unger, B. A., Lin, Y. T., Wiita, A. P., Xu, K., Correia, M. A., & Kampmann, M. (2020). Mitochondrial stress is relayed to the cytosol by an OMA1-DELE1-HRI pathway. *Nature*, *579*(7799), 427–432. https://doi.org/10.1038/s41586-020-2078-2

238. Fessler, E., Eckl, E. M., Schmitt, S., Mancilla, I. A., Meyer-Bender, M. F., Hanf, M., Philippou-Massier, J., Krebs, S., Zischka, H., & Jae, L. T. (2020). A pathway coordinated by DELE1 relays mitochondrial stress to the cytosol. *Nature*, *579*(7799), 433–437. https://doi.org/10.1038/s41586-020-2076-4
239. Alavi MV. OMA1-An integral membrane protease? Biochim Biophys Acta Proteins Proteom. 2021 Feb;1869(2):140558. doi: 10.1016/j.bbapap.2020.140558.
240. Baker, M. J., Lampe, P. A., Stojanovski, D., Korwitz, A., Anand, R., Tatsuta, T., & Langer, T. (2014). Stress-induced OMA1 activation and autocatalytic turnover regulate OPA1-dependent mitochondrial dynamics. *The EMBO journal*, *33*(6), 578–593. https://doi.org/10.1002/embj.201386474
241. Fessler, E., Krumwiede, L., & Jae, L. T. (2022). DELE1 tracks perturbed protein import and processing in human mitochondria. *Nature communications*, *13*(1), 1853. https://doi.org/10.1038/s41467-022-29479-y
242. Guo, X., Aviles, G., Liu, Y., Tian, R., Unger, B. A., Lin, Y. T., Wiita, A. P., Xu, K., Correia, M. A., & Kampmann, M. (2020). Mitochondrial stress is relayed to the cytosol by an OMA1-DELE1-HRI pathway. *Nature*, *579*(7799), 427–432. https://doi.org/10.1038/s41586-020-2078-2
243. Rath, E., Berger, E., Messlik, A., Nunes, T., Liu, B., Kim, S. C., Hoogenraad, N., Sans, M., Sartor, R. B., & Haller, D. (2012). Induction of dsRNA-activated protein kinase links mitochondrial unfolded protein response to the pathogenesis of intestinal inflammation. *Gut*, *61*(9), 1269–1278. https://doi.org/10.1136/gutjnl-2011-300767
244. Naresh, N. U., & Haynes, C. M. (2019). Signaling and Regulation of the Mitochondrial Unfolded Protein Response. *Cold Spring Harbor perspectives in biology*, *11*(6), a033944. https://doi.org/10.1101/cshperspect.a033944
245. Martinus, R. D., Garth, G. P., Webster, T. L., Cartwright, P., Naylor, D. J., Høj, P. B., & Hoogenraad, N. J. (1996). Selective induction of mitochondrial chaperones in response to loss of the mitochondrial genome. *European journal of biochemistry*, *240*(1), 98–103. https://doi.org/10.1111/j.1432-1033.1996.0098h.x
246. Lu, H., Wang, X., Li, M., Ji, D., Liang, D., Liang, C., Liu, Y., Zhang, Z., Cao, Y., & Zou, W. (2022). Mitochondrial Unfolded Protein Response and Integrated Stress Response as Promising Therapeutic Targets for Mitochondrial Diseases. *Cells*, *12*(1), 20. https://doi.org/10.3390/cells12010020
247. Shpilka, T., & Haynes, C. M. (2018). The mitochondrial UPR: mechanisms, physiological functions and implications in ageing. *Nature reviews. Molecular cell biology*, *19*(2), 109–120. https://doi.org/10.1038/nrm.2017.110
248. Nargund, A. M., Pellegrino, M. W., Fiorese, C. J., Baker, B. M., & Haynes, C. M. (2012). Mitochondrial import efficiency of ATFS-1 regulates mitochondrial UPR activation. *Science (New York, N.Y.)*, *337*(6094), 587–590. https://doi.org/10.1126/science.1223560
249. Nicolas, E., Tricarico, R., Savage, M., Golemis, E. A., & Hall, M. J. (2019). Disease-Associated Genetic Variation in Human Mitochondrial Protein Import. *American journal of human genetics*, *104*(5), 784–801. https://doi.org/10.1016/j.ajhg.2019.03.019
250. Münch, C., & Harper, J. W. (2016). Mitochondrial unfolded protein response controls matrix pre-RNA processing and translation. *Nature*, *534*(7609), 710–713. https://doi.org/10.1038/nature18302
251. Zhou, D., Palam, L. R., Jiang, L., Narasimhan, J., Staschke, K. A., & Wek, R. C. (2008). Phosphorylation of eIF2 directs ATF5 translational control in response to diverse stress

conditions. *The Journal of biological chemistry*, *283*(11), 7064–7073. https://doi.org/10.1074/jbc.M708530200

252. Teske, B. F., Fusakio, M. E., Zhou, D., Shan, J., McClintick, J. N., Kilberg, M. S., & Wek, R. C. (2013). CHOP induces activating transcription factor 5 (ATF5) to trigger apoptosis in response to perturbations in protein homeostasis. *Molecular biology of the cell*, *24*(15), 2477–2490. https://doi.org/10.1091/mbc.E13-01-0067
253. Hinnebusch, A. G., Ivanov, I. P., & Sonenberg, N. (2016). Translational control by 5' untranslated regions of eukaryotic mRNAs. *Science (New York, N.Y.)*, *352*(6292), 1413–1416. https://doi.org/10.1126/science.aad9868
254. Watatani, Y., Ichikawa, K., Nakanishi, N., Fujimoto, M., Takeda, H., Kimura, N., Hirose, H., Takahashi, S., & Takahashi, Y. (2008). Stress-induced translation of ATF5 mRNA is regulated by the 5'-untranslated region. *The Journal of biological chemistry*, *283*(5), 2543–2553. https://doi.org/10.1074/jbc.M707781200
255. Samluk, L., Urbanska, M., Kisielewska, K., Mohanraj, K., Kim, M. J., Machnicka, K., Liszewska, E., Jaworski, J., & Chacinska, A. (2019). Cytosolic translational responses differ under conditions of severe short-term and long-term mitochondrial stress. *Molecular biology of the cell*, *30*(15), 1864–1877. https://doi.org/10.1091/mbc.E18-10-0628

CHAPTER 2:

MANUSCRIPT

MANUSCRIPT AUTHOR CONTRIBUTIONS:

Victoria C. Sanfrancesco: Performed all *in situ* surgeries and tissue collection for experimental and control animals; subcellular isolations; plasmid amplification; electroporation; Luciferase assay; qPCR; mRNA stability assay; western blotting experiments; RNA-Seq analysis, data analysis and interpretation; wrote the manuscript.

Dr. David A. Hood: Supervised this project and is the principal investigator.

The Role Of ATF4 In Mediating Skeletal Muscle Function In Response To Acute Contractile Activity

Victoria C. Sanfrancesco and David A. Hood

Muscle Health Research Centre, School of Kinesiology and Health Science, York University, Toronto, Ontario, M3J 1P3, Canada

To whom correspondence should be addressed: David A. Hood, PhD. (dhood@yorku.ca)
Muscle Health Research Centre
School of Kinesiology and Health Science
York University, Toronto, ON M3J 1P3, Canada

ABSTRACT

Skeletal muscle relies on mitochondria to produce energy and support its metabolic flexibility. The mitochondrial pool is regulated by the quality control (MQC) processes biogenesis and mitophagy. In the face of stress, mitochondria can initiate a transient retrograde signal termed the integrated stress response (ISR) to the nucleus, inducing a cytoprotective transcriptional program to maintain organellar homeostasis. The transcription factor ATF4, the main effector of the ISR, ameliorates cellular stress by upregulating cytoprotective genes, such as CHOP and ATF5. It is not yet established whether the ISR is activated by acute contractile activity. To investigate this, a mouse *in situ* hindlimb muscle protocol was utilized to stimulate muscles at 0.25-1 tetani/per second for 9 mins, followed by a 1-hour recovery period. We observed robust 2-fold increases in the mRNA expression of ATF4 and CHOP. These increases were further enhanced following the recovery period, independent of transcriptional activation, as assessed using an ATF4 promoter-reporter plasmid. An *in vitro* assessment of ATF4 RNA decay revealed that acute contractile activity enhanced ATF4 transcript stability by reducing its rate of decay by 3-fold. Contractile activity also increased ATF4 localization to the nucleus by 2.5-fold, while total ATF4 protein content remained unchanged. The initial stages of ISR activation, assessed via eIF2α phosphorylation, were increased by 2-fold during the recovery phase following contractile activity. Our data indicate that acute contractile activity initiates processes that promote ISR activation at an early stage during exercise-induced mitochondrial stress and leads to the activation of ATF4.

INTRODUCTION

Skeletal muscle, which accounts for approximately 40% of human body mass, has a critical role in facilitating locomotion, energy expenditure and metabolic homeostasis [1]. To maintain tissue function and health in response to altered external stressors, skeletal muscle must adapt and modify its cellular, metabolic, and phenotypic attributes accordingly [2, 3]. This plasticity is a consequence of the highly adaptable mitochondrial reticulum and its capacity to optimize network functioning, whilst maintaining optimal health in response to demanding requirements, such as with exercise [4]. It has been well established that exercise elicits various beneficial physiological adaptations, such as mitochondrial reticulum remodeling, a process mediated largely by biogenesis (synthesis) and mitophagy (breakdown), to enhance overall muscle health and function [5-7].

Mitochondria are notorious for their ability to generate energy-rich ATP through aerobic respiration [8]. However, it is now acknowledged that these organelles are also major signaling hubs that are capable of continuously communicating with the nucleus to initiate “retrograde” signals and maintain optimal functioning [9-11]. This coordination is critical as a majority of the mitochondrial proteome (~99%), and thus OXPHOS complex components, are encoded with the nuclear genome, whereas the remainder (~1%) are mitochondrially-derived [12]. The expression of both genomes and their protein products must be tightly regulated, most predominantly during instances of reticulum remodelling, such as with biogenesis, to ensure proper protein homeostasis (proteostasis), complex assembly and mitochondrial functioning [4, 13]. Consequently, mitochondria possess a robust intrinsic protein quality control system, mediated by resident proteases and chaperones, to maintain this dual-genomic balance [14]. In the face of mitochondrial stress, distinct mito-nuclear signals induce a biphasic response to activate transcriptional nuclear cytoprotective adaptations and restore organelle network homeostasis and functioning [10, 14].

This mitohormesis cross-talk is thus a crucial facet of the mitochondrial quality control (MQC) system that acts as an intermediary "defense" mechanism to help maintain organellar health.

During the onset of contractile activity, early cellular signaling events are initiated in response to metabolite and reactive oxygen species (ROS) accumulation [8, 15-17]. These signaling cascades converge on the coactivator PGC-1α to promote mitochondrial biogenesis and increase the nuclear transcription of genes encoding mitochondrial proteins (NuGEMPs), which require directed import into the organelle through the protein import machinery (PIM) [18-20]. However, unaccustomed exercise may elicit mitochondrial stress via accelerations in the rate of biogenesis, mitochondrial protein import and transient mito-nuclear proteome imbalances, which consequently overwhelms the intrinsic protein quality system, enhances protein misfolding/proteotoxicity, elevates the production of ROS, and thus leads to reductions in the functional capacity of the mitochondrial network [21-23]. Such exercise-induced mitochondrial stress has been theorized to acutely activate retrograde signaling responses in an attempt to resolve organelle perturbations and enhance mitochondrial network functioning.

In mammals, it has been recently elucidated that the Integrated Stress Response (ISR), an elaborate signaling pathway that is activated during a wide range of physiological changes and pathological conditions, is highly responsive to a broad range of mitochondrial stressors and is thus a primary component of the mitohormetic response [24-31]. In the context of mitochondrial stress, the ISR is initiated by the phosphorylation of Serine-51 on the ribosomal eIF2α subunit, [24-31]. This phosphorylation event is catalyzed by the eIF2α kinases, General Control Non-derepressible 2 (GCN2), Heme-Regulated Inhibitor (HRI), and Protein Kinase RNA activated (PKR) in response to excessive mitochondrial ROS production and misfolded/unfolded protein aggregates [31-33]. In this regard, the ISR thereby serves as a hallmark response to mitochondrial

stress by attenuating global protein synthesis, whilst simultaneously selectively upregulating the translation of mRNAs containing upstream inhibitory open reading frames (uORFs), such as its main effector, the transcription factor ATF4 (Activating transcription factor 4/CREB2), to induce a robust mito-nuclear response [24-33].

ATF4, a basic leucine zipper (bZIP) transcription factor, is highly responsive to mitochondrial insults, and is capable of regulating gene expression due to its high DNA binding affinity and heterodimerization compatibility [34, 35]. Generally, ATF4 is constitutively expressed in all tissues, and is known to be implicated in regulating a plethora of cellular events such as one-carbon metabolism [36], tumorigenesis [37], apoptosis [38], and muscle atrophy [39]. In a mitochondrial specific context, ATF4 is capable of alleviating organelle perturbations by upregulating a myriad of mitochondrial protective genes related to amino acid synthesis and transport, protein folding and handling, and antioxidant capacity [40-43]. Multiomics data has also suggested that ATF4 can upregulate the transcription factors ATF5 and CHOP, in which all three factors work in concert to further enhance the mitochondrial cytoprotective stress response [44].

Early work from our laboratory has demonstrated that ATF4 is a potent responder to contractile activity and is a critical factor in enhancing mitochondrial adaptations under acute contractile activity induced stress [45-47]. Although evidence has suggested the role of ATF4 in maintaining mitochondrial health and function in response to exercise-induced stress, no work has focused on elucidating the precise signaling events that induce the activation of the ISR, ATF4, and the plausible downstream consequences following acute contractile activity. Therefore, our objectives were to: 1) evaluate the effect of acute contractile activity on the activation of the ISR, and 2) elucidate the mechanism of ATF4 activation and response to mitochondrial stress after an acute bout of exercise and following recovery.

METHODS

Animals. Wild-Type male mice on a C57BL6/N background, were housed in a 12:12-hr light–dark cycle and given food and water ad libitum. Experiments were conducted after approval by the York University Animal Care Committee in accordance with Canadian Council of Animal Care guidelines. Experimental animals were used at 4-8 months of age and separated into either Control (Con), stimulated/acute contractile activity (Stim), or stimulated with recovery (Stim+Rec) (n=6–39/group).

Acute in-situ muscle contractile activity protocol. Animals were anesthetized under isoflurane inhalation with oxygen, and the right hind limb gastrocnemius muscle and innervating sciatic nerve was exposed, isolated, and doused in 0.9% saline. The Achilles tendon was tied to a hooked pin and attached to a force transducer (Grass FT 10; Grass Instruments, Quincy, MA). The right leg was fastened in a stabilizing clamp, at resting length, below the gastrocnemius. Stimulating electrode prongs were placed near the insertion of the gastrocnemius and the isolated sciatic nerve was placed on the prong electrodes securely. A thermistor was utilized and inserted in the body of the gastrocnemius to monitor muscle temperature which was maintained at ~37°C with an adjustable heat lamp. Warmed saline was used to douse the sciatic nerve and gastrocnemius periodically, and plastic wrap was placed over the working muscle and nerve to maintain constant temperature and moisture. Data were recorded using PowerLab/4SP and visualized in real time on Chart5 software (ADInstruments, Colorado Springs, CO). A length-tension curve was performed to determine optimal resting muscle length to elicit maximal contraction. Briefly, resting tension was initially pre-set to ~40-50g at the start of the protocol, followed by 3 successive maximal tetanic contractions to determine the optimal resting muscle length. Immediately after, submaximal (twitch) force production was determined by stimulating the sciatic nerve using three single shocks

(0.1 ms, 10V). This was followed by a contractile activity stimulation period of 9 mins where the muscle was stimulated via the sciatic nerve at 0.25, 0.5 and 1 tetanic contractions per second (TPS, 100ms, duration at 100Hz) consecutively for 3 mins each to induce moderate and more severe muscle fatigue, respectively. The gastrocnemius, TA, EDL, and soleus muscles of the stimulated limb were harvested and weighed, to be used immediately in subcellular fractionation or to be flash frozen in liquid nitrogen and stored at -80°C for subsequent use in further experiments. The animals separated into the recovery group were maintained under anesthesia following the contractile activity protocol to allow for 1 hour of quiet muscle recovery. During the recovery period, muscle temperature and hydration were also maintained continually. This was followed by muscle harvest, as previously described. The gastrocnemius, TA, EDL, and soleus muscles from the contralateral control (non-stimulated) limb were excised at the same time as the stimulated/recovery muscle groups. All animals were sacrificed by cervical dislocation immediately after tissue harvest.

RNA isolation and reverse transcription (cDNA). The gastrocnemius muscle was used for RNA isolations. Approximately 30-60 mg of lysed muscle tissue was combined with TRIzol® reagent (15596018, Life Technologies, Carlsbad, CA, USA) and mixed with chloroform vigorously. Samples were centrifuged at 16,000g for 15 minutes at 4°C. The resultant upper aqueous phase was transferred into a new sterile Eppendorf, mixed with isopropanol, and placed overnight at -20°C to allow for precipitation. After the precipitation process, samples were once again centrifuged at 16,000g for 10 minutes at 4°C. The resulting supernate was discarded, the pellet was lightly washed in 700µl of 75% Ethanol, and centrifugated once more at 16,000g for 10 minutes (4°C). The supernate was discarded, and the pellet was resuspended in 30-50µl in sterile H_2O. The purity and concentration of RNA for each sample were accessed using the NanoDrop

2000 (Thermo Fisher Scientific, Waltham, MA, USA). cDNA was synthesized from 1-1.5µg of total RNA into a final volume of 20µl of workable cDNA via the use of Superscript III reverse transcriptase and Oligo(dt)20 (Invitrogen, 18,418,020).

Quantitative Real-time PCR to measure mRNA expression. Primers for the target genes ATF4, CHOP, ATF5 and PGC-1α, were used to measure mRNA expression via the 7500 Real-Time PCR system (Applied Biosystems Inc., Foster City, CA, USA). The master mix for each target gene consisted of SYBR Green qPCR Master Mix (04913850001, Millipore-Sigma; Roche), forward and reverse primers specific to the gene of interest (GOI), and sterile H_2O. For each respective primer, 23µl of MasterMix was incubated with 2µl of cDNA, to obtain a final reaction volume of 25µl per well of the 96-well plate. The housekeeping genes used were GAPDH and β-2 microglobulin which were used to normalize gene expression. All samples were run in duplicate. Primer optimizations were run prior to experimental plates to control for primer dimers and nonspecific amplification via the analysis of the melt curves generated by the instrument.

Real-time PCR mRNA quantifications. Transcript expression (mRNA levels) was quantified using the $2^{-\Delta Ct}$ method. Briefly, ΔCt values for each gene were obtained by determining the average cycle threshold (Ct) value of both housekeeping genes subtracted from the Ct value of the gene of interest (GOI) for each sample. Results are reported as the fold-change in each experimental and control group using the ΔCt method, calculated as $2^{-\Delta Ct}$.

Whole muscle protein extracts. A portion of the gastrocnemius muscle was snap frozen in liquid nitrogen following excision from the animal and stored at -80°C. The tissue (~10-20mg) was diluted 10-fold and homogenized in Sakamoto buffer (20mM HEPES, 2mM EGTA, 1% Triton X-100, 50% Glycerol, 50 mM B-Glycerophosphate) containing both phosphatase (Millipore-Sigma) and protease (Roche Mississauga, ON, Canada) inhibitors using the Qiagen Tissue Lyser

II. Samples were centrifuged (14,000g) for 15 minutes at 4°C. The supernatant fraction was collected and stored at -80°C until further analysis.

Nuclear and cytosolic fractionation. Nuclear and cytosolic fractions were prepared from ~40mg of freshly harvested gastrocnemius from control and experimental groups using NE-PER Extraction Reagents (38835, Thermo Fisher Scientific) supplemented with phosphatase and protease inhibitors. Following extraction, the tissue was placed in ice cold PBS, with the corresponding phosphatase and protease inhibitors, for 20-30 minutes. The tissue was then minced on ice and homogenized in CER-I using a Dounce homogenizer. Homogenates were then left to stand on ice for 10 minutes. Following the addition of the appropriate proportion of CER-II, samples were briefly vortexed and centrifuged at 16,000g for 10 minutes at 4°C. The cytosolic fraction (supernatant) was immediately collected. The remaining pellets, containing nuclei and cellular debris, were washed 3 times in ice-cold 1x PBS and subsequently resuspended in NER. The pellets were sonicated 3 times for 3 seconds and incubated on ice for 40 minutes. During the incubation period, the samples were briefly vortexed every 10 minutes. Following incubation, the samples then underwent centrifugation at 16,000g for 10 minutes. The resulting supernatants (nuclear fractions) were collected. Both cytosolic and nuclear subfractions were stored in -80°C until further analysis.

Protein concentration. The Bradford protein assay was used to determine the protein concentration of whole muscle (Gastrocnemius) and subcellular fractionation samples. Briefly, a standard curve to determine protein concentrations was created using bovine serum albumin (2mg/ml) in combination with double distilled water. Protein extracts from each sample were mixed with double-distilled water and analyzed in comparison with the standard curve using a Bio-Tek Citation 5 micro plate reader.

In vitro mRNA decay assay. Total RNA (35 μg), derived from the gastrocnemius muscle of control mice was combined with 20 μg of S15 cytosolic extracts from the control or the acutely stimulated (with no recovery) gastrocnemius muscle. Briefly, the S15 extracts were derived from the cytosolic fractions previously isolated using the NE-PER Kit and were subjected to centrifugation for 15 minutes at 15,000g (4°C). The resulting supernate (post-mitochondrial S15 extract) was transferred into a sterile 1.5ml Eppendorf. To allow for assessment of the degradation of RNA within the incubated tubes as a percentage of the original RNA content, in the absence of cytosolic proteins, a tube containing 35 μg of RNA and 5 μl of sterile homogenization buffer (CERI) in a 100-μl reaction volume served as a baseline measure at *time 0*. Reaction volumes were set at 100 μl, and samples were incubated at 37°C for 30, 60 and 90 minutes. At the completion of each incubation time point, TRIzol® was added to each sample and shaken vigorously to halt mRNA degradation. Total RNA was then reisolated using the extraction procedure as previously described. The reisolated RNA was pelleted overnight at -20°C, washed, dried, and resuspended in sterile water, as described previously. The purity and concentration of RNA for each sample were accessed using the NanoDrop 2000 (Thermo Fisher Scientific, Waltham, MA, USA). cDNA was generated and real-time PCR was conducted, as previously described, to examine the rate of mRNA decay, presented as the percentage of ATF4 mRNA at *t=0,* normalized to GAPDH.

Immunoblotting. Whole muscle protein extracts prepared from a portion of the gastrocnemius and isolated subfractions were loaded (30-35μg of protein) on 8-15% SDS-PAGE gels for separation and subsequently transferred onto nitrocellulose membranes (Bio-Rad, Mississauga, ON, Canada). After the transfer process, the membranes were stained with Ponceau Red, and agitated for ~3 minutes. The membranes were imaged with Ponceau briefly using the Invitrogen iBright 1500 imager, and then were cut at the appropriate molecular weights. After the

membranes were briefly washed with TBS-T solution (Tris-buffered saline–Tween-20: 25 mM Tris–HCl, pH 7.5, 1 mM NaCl and 0.1% Tween-20), they were blocked at room temperature in 5% skim milk or 5% BSA for phosphorylated proteins (in TBS-T solution) for one hour to prevent non-specific protein binding. The membranes were then incubated overnight at 4°C in blocking solution with the appropriate antibodies. Subsequently, membranes were then washed 3x for 5 minutes with TBS-T, followed by incubation of the appropriate secondary antibody conjugated to horseradish peroxidase at room temperature (1 hr), and washed again 3x for 5 minutes each with TBS-T. Membranes were imaged using an ECL kit (170-5061; Bio-Rad) on the Invitrogen iBright 1500 imager and revealed using the enhanced chemiluminescence method. Quantifications were performed with ImageJ software (the National Institutes of Health, Bethesda, MD), and values were normalized to Ponceau. The approximate molecular weights in kDa (kilodaltons) of proteins are indicated on each blot.

ATF4 promoter plasmid amplification and isolation. A custom ATF4 promoter-reporter lentiviral vector expressing Firefly Luciferase (C449) was purchased from Applied Biological Materials Inc. (ABM, Richmond, Canada), which contained 1.5-Kb of the mouse ATF4 promoter region. The plasmid vector (1μl) was transformed using competent *E.coli* cells, which were heat-shocked at 42°C for 30 seconds and subsequently placed on ice for 5 minutes to facilitate plasmid uptake. Following, outgrowth media was supplemented into the *E.coli* and plasmid mixture, which was then incubated at 30°C for 1 hour on a shaker plate (250rpm). The mixture was then subsequently inoculated on agar plates with the appropriate antibiotic (Kanamycin-KAN201.10; BioShop) to undergo amplification and isolation via a HiSpeed Plasmid Maxi Prep Kit (12663; Qiagen) for electrotransfection experiments. The ATF4 vector was cotransfected with pRL-CMV to serve as a loading control and to correct for transfection efficiency.

Intramuscular DNA plasmid injection and electroporation. The lower hindlimbs of experimental mice were shaved and sterilized prior to the plasmid injection. Approximately 30 µl of the plasmid solution (containing 50µg of the ATF4-pGL3 and 1µg of pRL-CMV to normalize for electrotransfection efficiency in 0.9% sterile saline solution) was injected into the gastrocnemius muscle of both hindlimbs using a short 29-gauge insulin syringe (BD Ultra-Fine). Immediately after the DNA injection, twenty transcutaneous electrical pulses (100 V/cm^2) were applied to the muscle with forcep-style electrodes (Tweezertrodes) using an ECM 380 BTX electroporation system (Harvard Apparatus, Saint-Laurent, QC, Canada) to facilitate uptake of the construct into the muscle. Anode and cathode electrode orientation were reversed after 10 pulses (100 V/cm, 20 ms, 1 Hz per pulse). Conductive gel was applied to the electrodes to assist with transfection. The animals were given 7 days for gene amplification before the *in situ* contractile activity protocol. All muscles were then powdered at the temperature of liquid nitrogen until used in the luciferase reporter assay.

Luciferase reporter assay. Approximately 30 mg of powdered gastrocnemius muscle was diluted in 1× Passive Lysis Buffer (Promega) fivefold on ice. The sample was sonicated on ice for 3 × 3 seconds, vortexed briefly, subsequently spun in a microfuge at 4°C for 10 min at 16,100*g*, and the supernatant was collected. Using a 96-well plate, 20µl of 1x passive lysis buffer and the experimental samples were plated accordingly (in triplicate) and readings of firefly and renilla luciferase were measured using the Dual-Luciferase Reporter Assay System (E1910; Promega). Briefly, 100 µl of luciferase substrate was dispensed into each well, followed by the lysis buffer or sample to read the appropriate firefly luciferase activity. This was followed by the addition of 100µl of renilla substrate into each well to measure renillia activity, thereby producing a Dual-

Glow value. Both firefly and renllia luciferase values were averaged, and firefly luciferase values were corrected for renilla to control for transfection efficiency.

Statistics. Data were analyzed using the GraphPad Prism 9.0 software and values are reported as means ± SD. Student's paired *t*-test was employed to assess differences between conditions (Con vs. Stim) for the Luciferase experimentation. A One-Way ANOVA was performed to evaluate the differences between Control, Stimulated and Stimulated+Recovery groups. A Two-Way ANOVA was performed to evaluate the nuclear and cytosolic distribution of ATF4 in response to stimulation. A Tukey's post-hoc test was used where applicable. Non-Linear Regression Analysis was used for the mRNA decay assay. Statistical significance was achieved at $P \leq 0.05$.

Table 1. List of antibodies used for immunoblotting.

Antibody	Manufacturer	Catalog No.	Molecular Weight (kDa)
ATF4 (CREB-2)	Santa Cruz Biotechnology	sc-390063	50
ATF5	Abcam	Ab60126	31
α-Tubulin	Millipore-Sigma	CP06-100UG	60
CHOP	Cell Signaling	2895S	27
T-eIF2α	Cell Signaling	9722S	37
P-eIF2α (S51)	Invitrogen	44728G	37
P/T-HRI	Santa Cruz Biotechnology	sc-365239	71-100
H2B	Cell Signaling	2934S	15
T-SAPK/JNK	Cell Signaling	9252T	37-54
P-SAPK/JNK (Thr183, Tyr185)	Cell Signaling	4668S	37-54
T-CaMKII-α	Cell Signaling	3362S	50
P-CaMKII-α (Thr286)	Cell Signaling	3361S	50
T-p38 MAPK	Cell Signaling	9212S	40
P-p38 MAPK (Thr180/Tyr182)	Cell Signaling	9211S	43
T-AMPK	Cell Signaling	2532S	62
P-AMPK (Thr172)	Cell Signaling	2535S	62

Anti-Mouse HRP-linked 2°	Cell Signaling	7076S	-
Anti-Rabbit HRP-linked 2°	Cell Signaling	7074S	-

Table 2. List of primer oligonucleotide sequences used in real-time quantitative PCR analysis for *Mus musculus.*

Gene	Organism	Forward Primer (5' to 3')	Reverse Primer (5' to 3')
Atf4 (Creb-2)	*Mus musculus*	GCCGGTTTAAGTTGTGTGCT	CTGGATTCGAGGAATGTGCT
Atf5	*Mus musculus*	TGGAGCGGGAGATCCAGTA	GACGCTGGAGACAGACGTACA
CHOP (ddit3)	*Mus musculus*	CACCACACCTGAAAGCAGAA	AGGTGAAAGGCAGGGACTCA
PGC-1α (Ppargc1α)	*Mus musculus*	TTCCACCAAGAGCAAGTAT	CGCTGTCCCATGAGGTATT
Gapdh	*Mus musculus*	AACACTGAGCATCTCCCTCA	GTGGGTGCAGCGAACTTTAT
B2m	*Mus musculus*	GGTCTTTCTGGTGCTTGTCT	TATGTTCGGCTTCCCATTCT

RESULTS

Acute in situ contractile activity elicits muscle fatigue. To examine the molecular signaling events that govern the transient activation of the ISR and thus ATF4 in response to acute contractile activity, we utilized a 9-minute (acute) stimulation protocol (Figure 1A, 1B) to induce moderate/severe muscle fatigue and cellular stress. We evaluated the force produced as a percent of initial force production (% of initial force), at three different time points, corresponding to the changes in TPS during the 9-minute protocol. We observed a main effect of stimulation ($P<0.0001$) in the overall muscle force production at 3, 6 and 9 minute timepoints, which displayed progressive and more severe reductions in force generation (i.e., fatigue) throughout the protocol (Figure 1C). These results confirm that our protocol is sufficient to elicit potential changes in molecular signaling pathways that are responsive to such a stressor.

ATF4 and downstream targets are responsive to the acute in situ contractile activity protocol. To assess whether the acute contractile activity protocol induces the transcription of ATF4 and downstream target genes, we performed quantitative real-time PCR comparing control and stimulated samples. We first examined ATF4 mRNA expression as it lies upstream of CHOP and ATF5 and is suggested to be highly responsive to cellular stress. Correspondingly, there was a significant main effect of stimulation in ATF4 mRNA expression (Figure 2A, $P<0.0001$), with a 2-fold increase following the contractile activity protocol ($P<0.001$), and a further 3.5-fold enhancement post-recovery ($P<0.0001$) relative to controls (Figure 2A). We then evaluated the mRNA expression of ATF4 downstream targets, CHOP and ATF5, to determine whether this activation of ATF4 coincides with the transcriptional induction of target genes. Interestingly, we only observed changes in the mRNA expression of CHOP and not ATF5 (Figure 2B,C). There was a similar main effect of stimulation ($P<0.0001$) on CHOP mRNA expression, with a 2-fold increase immediately following the contractile activity protocol ($P<0.01$). This response was further elevated 3-fold post-recovery ($P<0.0001$). Thus, both ATF4 and CHOP are responsive to acute contractile activity. Lastly, we investigated the mRNA expression of PGC-1α, the master regulator of biogenesis, to examine the drive for mitochondrial remodeling. Surprisingly, however, there were no changes in PGC-1α mRNA (Figure 2D). Thus, our 9-minute contractile activity protocol is a potent stimulus that can induce changes at the mRNA level during the cellular stress imposed by contractile activity.

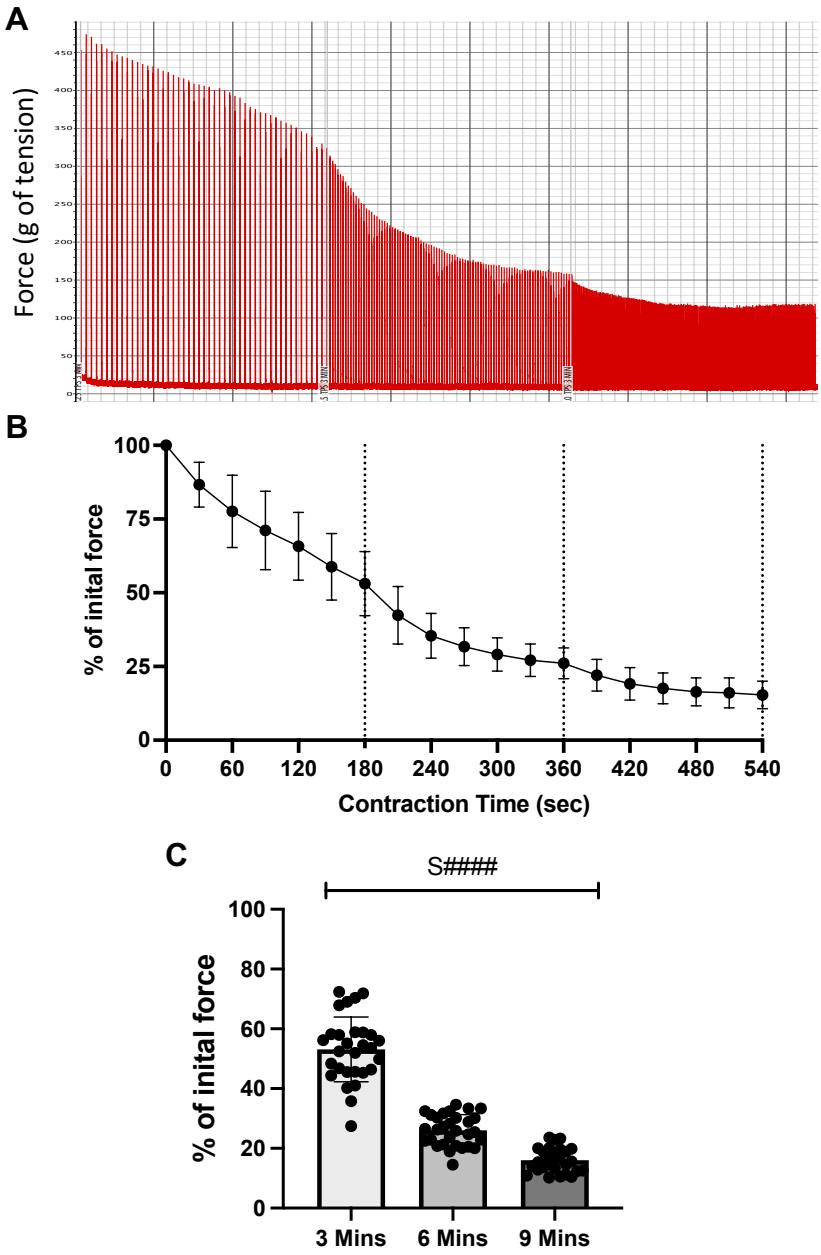

Figure 1: Muscle performance and force production during the acute *in situ* contractile activity protocol. **A)** Representative tracing of the acute *in situ* contractile stimulation protocol and progressive fatigue. Briefly, the gastrocnemius muscle was stimulated at 0.25, 0.5 and 1 tetanic contractions per second (TPS). A subset of mice underwent a 60-minute recovery period following the *in situ* protocol where the exposed muscle was maintained at a homeostatic internal temperature of 37℃. **B)** The percentage of initial force production used as a measure of muscle fatigue in response to acute exercise and thus confirmed the acute muscle activation over the course of the 9-minute protocol. **C)** Force production at **3, 6** and **9 minutes** of the acute *in situ* protocol, as a percentage of initial force production (t=0). S#### P<0.0001, main effect of stimulation, One-way ANOVA (n=29). Data are means ± SD.

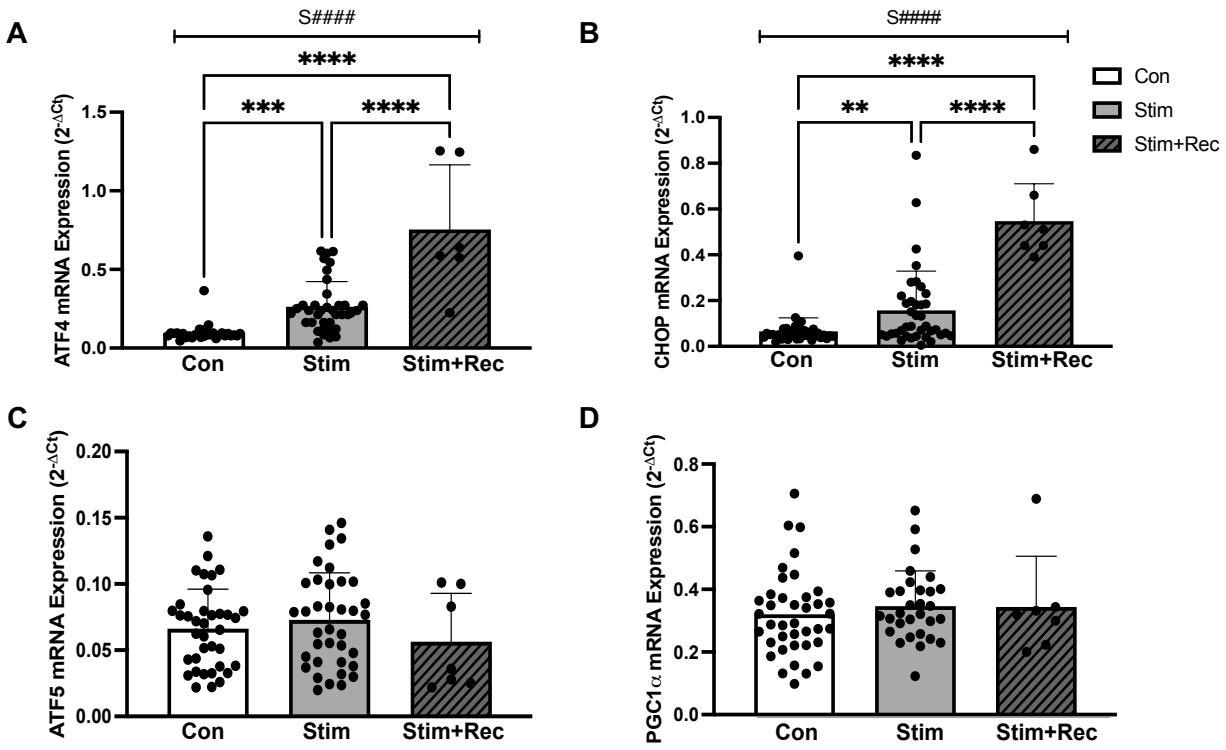

Figure 2: qPCR analysis of ATF4 and downstream targets in response to acute contractile stimulation and following recovery. Changes in the gene expression of **A)** ATF4, **B)** CHOP, and **C)** ATF5. Signaling towards mitochondrial biogenesis with acute exercise was assessed by measuring mRNA levels of **D)** PGC-1α. Con: n=30-39; Stim: n=30-39, Stim+Rec: n=6-7. S####P<0.0001, main effect of the stimulation conditions (including recovery), One-way ANOVA; Tukey's post-hoc analyses, Con vs. Stim, Stim vs. Stim+Rec, Con vs. Stim+Rec. Tukey's post-hoc: **P<0.01, ***P<0.001, ****P<0.0001. mRNA levels are indicated as fold changes using the $2^{-\Delta Ct}$. Con, Control; Stim, acute *in situ* stimulation; Stim+Rec, acute *in situ* stimulation followed by a 60-minute recovery period. Data are means ± SD.

The ISR is induced by contractile activity. We sought to evaluate the efficiency of acute contractile activity, followed by recovery, in inducing the ISR. As mentioned previously, cellular stress elicits the activation of the ISR through the phosphorylation of eIF2α, an event mediated by the four ISR kinases [24, 31]. To investigate this in our model, we first evaluated the activation of the ISR kinase, HRI, which is highly responsive to mitochondrial stress [31]. We then examined the downstream pivotal event and extent of eIF2α phosphorylation in our control and experimental samples (Figure 3A). We observed no significant changes in the protein expression of both total and phosphorylated HRI across conditions (Figure 3B,C), however, we detected a trending increase directly following contractile activity ($P=0.0619$) when expressed as ratio of phosphorylated to total HRI (Figure 3D). Downstream of this kinase activity, total eIF2α protein content remained unchanged across all groups (Figure 3E), however, there was a main effect of stimulation (including recovery) on the level of phosphorylated eIF2α with a ~1.5-fold increase following recovery ($P<0.01$). The ratio of phosphorylated to total eIF2α protein expression (Figure 3G) was increased by 2-fold following recovery ($P<0.0001$), compared to control and stimulated samples ($P<0.0001$, $P<0.001$). Thus, these data suggest that acute contractile activity is capable of inducing the ISR, an effect that becomes evident during the recovery phase.

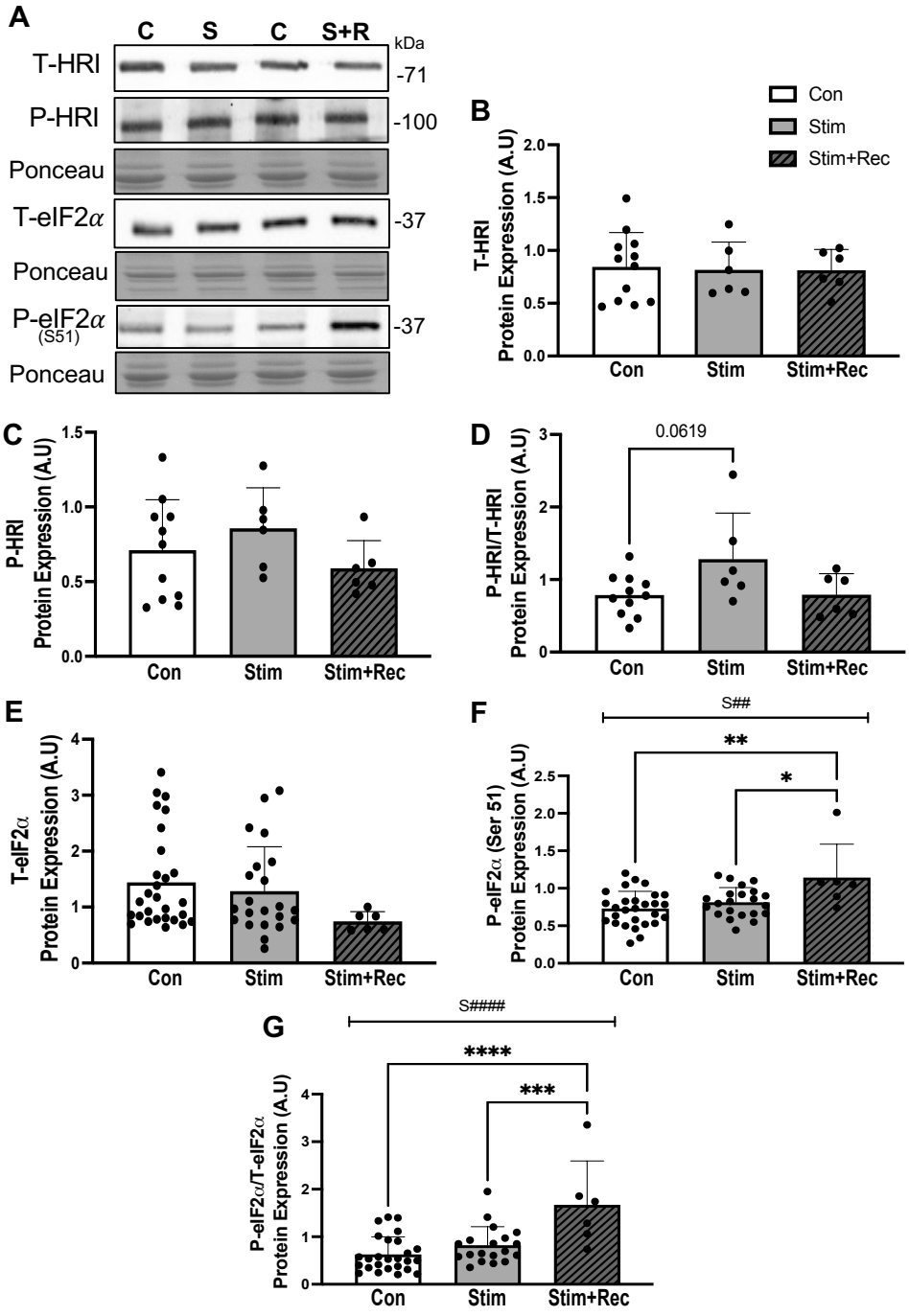

Figure 3: Effects of acute contractile stimulation and recovery on ISR upstream signaling, represented by HRI and eIF2α phosphorylation in whole muscle. A) Representative immunoblots of T-HRI, P-HRI, T-eIF2α and P-eIF2α, with the corresponding Ponceau stains. Quantifications of **B)** T-HRI, **C)** P-HRI, **D)** P-HRI/T-HRI, **E)** T-eIF2α, **F)** P-eIF2α, and **G)** P-eIF2α/T-eIF2α. The approximate molecular weights of proteins are indicated with a hash bar in kilodaltons (kDa). Con: n=11-12, 26-28; Stim: n=6, 19-22, Stim+Rec: n=6. S####P<0.0001, main effect of the stimulation conditions (including recovery), One-way ANOVA; Tukey's post-hoc analyses, Con vs. Stim, Stim vs. Stim+Rec, Con vs. Stim+Rec. Tukey's post-hoc: **P<0.01, ***P<0.001, ****P<0.0001. Con, Control; Stim, acute *in situ* stimulation; Stim+Rec, acute *in situ* stimulation followed by a 60-minute recovery period. Data are means ± SD.

Whole muscle protein expression of ATF4 and downstream targets were assessed in response to acute contractile activity. Due to the increases in ATF4 mRNA expression in response to acute contractile activity, we sought to determine whether this translates to enhancements in the protein expression of ATF4 and downstream targets (Figure 4A). However, neither ATF4 or ATF5 showed no change in protein expression across conditions (Figure 4B,C). In contrast, there was a main effect ($P<0.01$) of contractile activity on CHOP protein (Figure 4D), with 2-fold increases following stimulation ($P<0.05$), however, these levels we attenuated following recovery ($P<0.05$). Therefore, CHOP is highly responsive to cellular stress at both the mRNA and protein level.

Acute contractile activity stimulates the phosphorylation of the kinases JNK(1/2) and CaMKIIα. JNK is a stress kinase that is highly responsive to acute exercise and has been identified to be implicated in signaling during mitochondrial stress [48]. Evidence has shown that one of the ISR kinases, PKR, can induce the activation of JNK via its phosphorylation in response to mitochondrial proteotoxicity and elevations in ROS production [49]. Therefore, we assessed its extent of activation following our protocol as a further marker of ISR induction and contractile activity-induced stress. We detected two isoforms of JNK in muscle, JNK1 (~46 kDa) and JNK2 (~54 kDa), however, we only quantified JNK2 as it is the isoform activated following the induction of the ISR (Figure 5A). There was a main effect of stimulation ($P<0.0001$) on the ratio phosphorylated/total JNK2 protein expression (Figure 5B) with robust 6-fold increases immediately following the stimulation protocol ($P<0.0001$), however, this activation was attenuated following recovery ($P<0.001$). Since acute exercise has also been shown to stimulate the induction of the signaling kinases CaMKIIα, p38-MAPK, and AMPKα, we sought to evaluate the activation of these three key kinases in our model to confirm such exercise-induced molecular stress [50]. There was a main effect of contractile activity on the ratio of phosphorylated to total

CaMKIIα (Figure 5C, D), with a 6-fold increase in response to stimulation (P<0.0001). This activation was transient, returning to control levels during recovery (P<0.0001). Contrarily, there were no increases in the activation of p-38 MAPK (Figure 5E, F) or AMPKα (Figure 5G, H). These data further support the specific activation of the ISR in response to the contractile activity-induced stress imposed.

Acute contractile activity induces the nuclear translocation of ATF4. ATF4 is a transcription factor and therefore its translocation to the nucleus is required to impart its expressional regulation on target genes. This nuclear translocation is mediated by the targeting KKLKK signal (amino acids 280 to 284) located within the bZIP domain basic region of the ATF4 gene [51]. To evaluate this, we measured the subcellular localization of ATF4 in nuclear and cytosolic fractions isolated from muscle following contractile activity (Figure 6A). We observed a main effect of stimulation (P=0.05), with a stark 2-fold increase in the nuclear localization of ATF4 (Figure 6B).

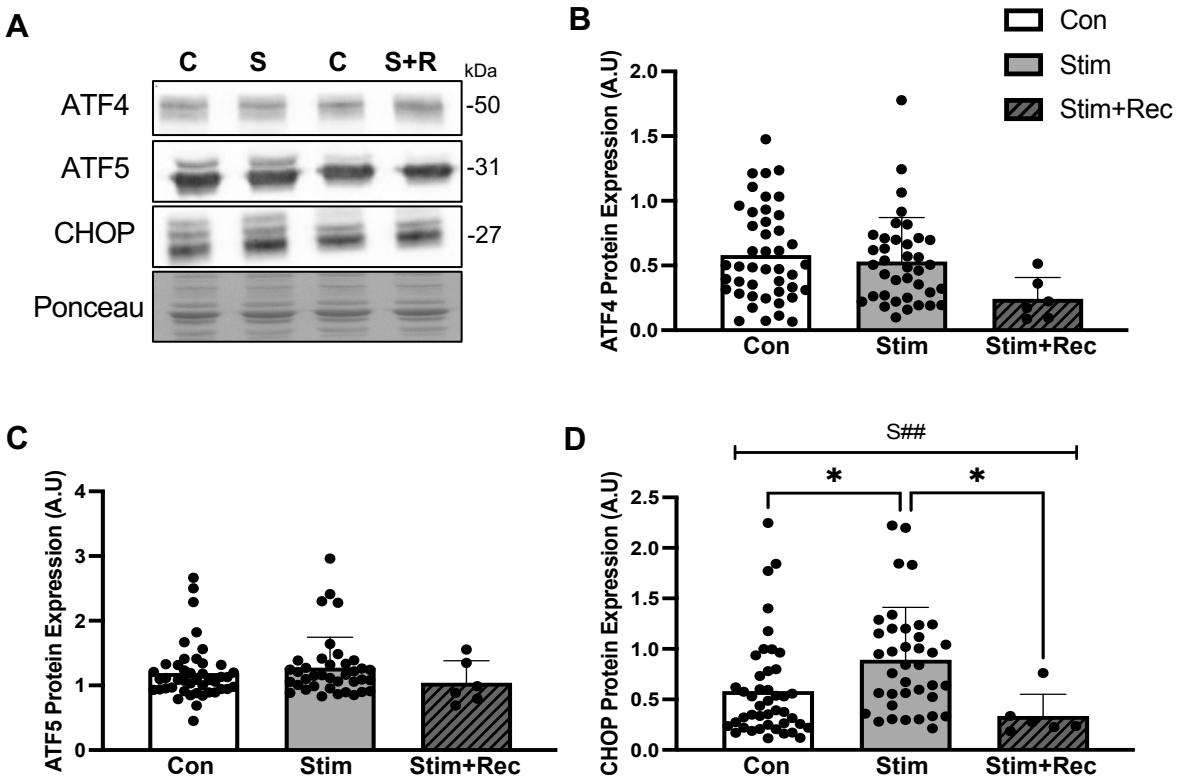

Figure 4: Downstream effects on the protein expression of ATF4 and direct targets following acute contractile stimulation in whole muscle. A) Representative immunoblots of ATF4, ATF5 and CHOP, with the corresponding Ponceau stain. Quantifications of **B)** ATF4, **C)** ATF5, and **D)** CHOP. The approximate molecular weights of proteins are indicated with a hash bar in kilodaltons (kDa). Con: n=44; Stim: n=38, Stim+Rec: n=6. S##P<0.01, main effect of the stimulation conditions (including recovery), One-way ANOVA; Tukey's post-hoc analyses, Con vs. Stim, Stim vs. Stim+Rec, Con vs. Stim+Rec. Tukey's post-hoc: *P<0.05. Con, Control; Stim, acute *in situ* stimulation; Stim+Rec, acute *in situ* stimulation followed by a 60-minute recovery period. Data are means ± SD.

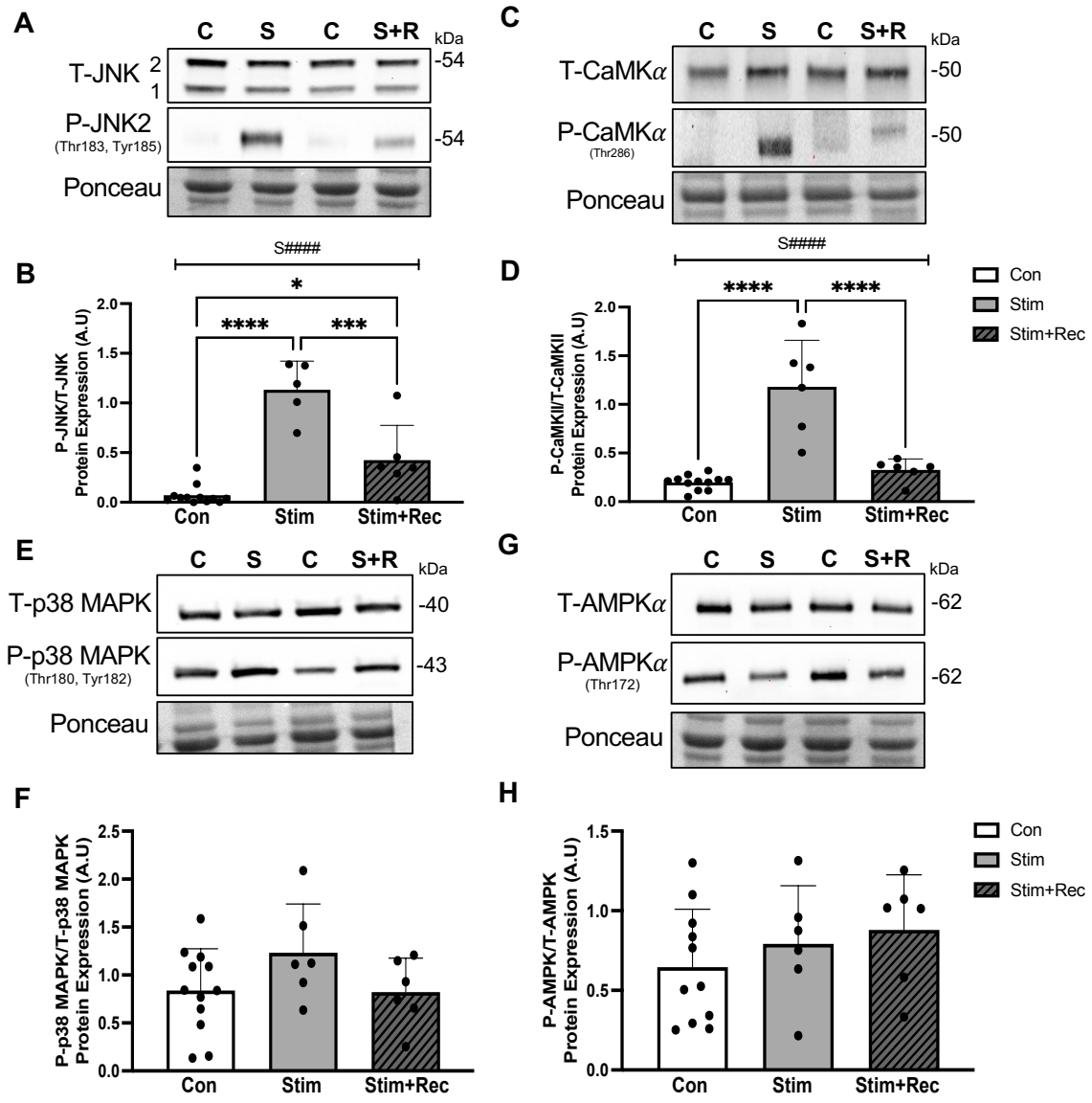

Figure 5: Effects of acute contractile stimulation on intracellular kinase signaling activation. A) Immunoblots of total and phosphorylated JNK2 with corresponding Ponceaus. **B)** Quantification of phosphorylated/total JNK2 protein in response to the acute contractile protocol and following the one-hour recovery. **C)** Immunoblots of total and phosphorylated CaMKIIα with the corresponding Ponceau Stains. **D)** Quantification of phosphorylated/total CaMKIIα in response to the acute contractile protocol and following the one-hour recovery. **E)** Immunoblots of total and phosphorylated p38-MAPK with the corresponding Ponceau Stains. **F)** Quantification of phosphorylated/total p-38 MAPK in response to the acute contractile protocol and following the one-hour recovery. **G)** Immunoblots of total and phosphorylated AMPKα with the corresponding Ponceau Stains. **H)** Quantification of phosphorylated/total AMPKα in response to the acute contractile protocol and following the one-hour recovery. The approximate molecular weights of proteins are indicated with a hash bar in kilodaltons (kDa). Con: n=11-12; Stim: n=5-6, Stim+Rec: n=6. S####P<0.0001, main effect of the stimulation conditions (including recovery), One-way ANOVA; Tukey's post-hoc analyses, Con vs. Stim, Stim vs. Stim+Rec, Con vs. Stim+Rec. Tukey's post-hoc: *P<0.05, ***P<0.001, ****P<0.0001. Con, Control; Stim, acute *in situ* stimulation; Stim+Rec, acute *in situ* stimulation followed by a 60-minute recovery period. Data are means ± SD.

ATF4 mRNA expression was increased following acute contractile activity, independent of promoter activity. Since we observed robust increases in the mRNA expression of ATF4 immediately following contractile activity (Figure 7A), we aimed to determine whether this was associated with a plausible enhancement in the transcriptional activation of ATF4. To evaluate this, we electrotransfected a 1.5-kb mouse ATF4 promoter-luciferase reporter into the gastrocnemius muscle prior the acute contractile protocol and assessed the luciferase activity following the completion of the protocol. There were no differences in the promoter activity of ATF4 in both control and stimulated conditions (Figure 7B).We then assessed the mRNA stability of ATF4 using an *in vitro* cell-free mRNA decay assay [52, 53]. Interestingly, ATF4 stability was significantly increased in stimulated muscle milieu compared to control muscle (Figure 7D, $P<0.05$), relative to the mRNA stability of the housekeeping gene GAPDH (Figure 7C). Additionally, the transcript (half-life) of ATF4 was increased following the acute contractile activity protocol (Figure 7E, $P<0.01$). Thus, the increase in mRNA expression seen with contractile activity is a product of enhanced mRNA/transcript stability and not its transcriptional activation.

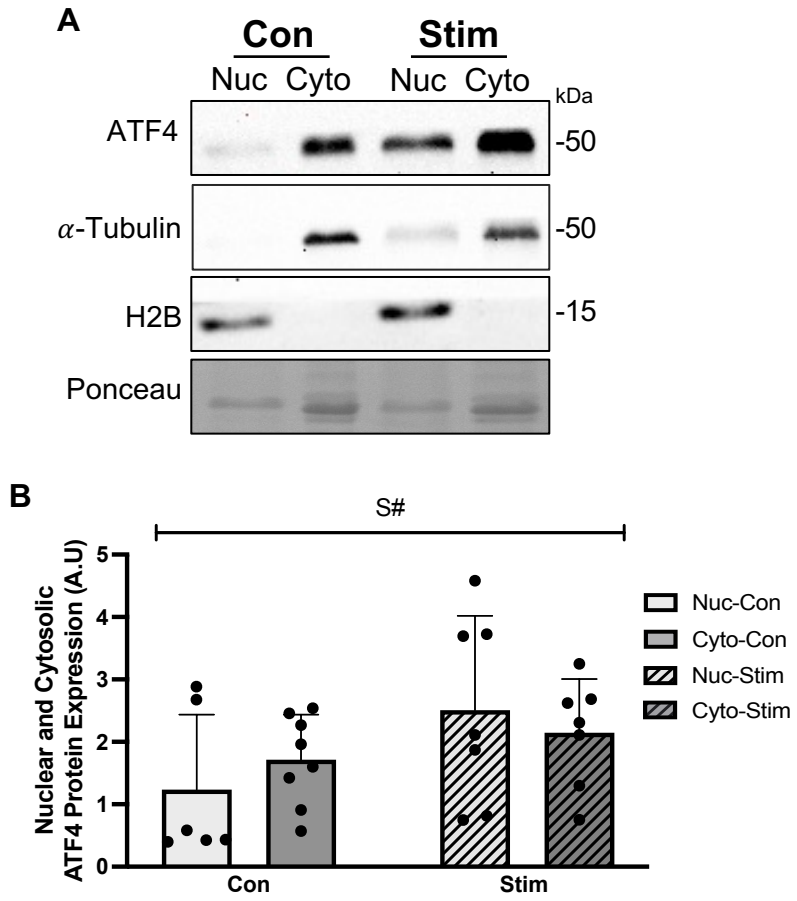

Figure 6: Cellular localization of ATF4 in control and acutely stimulated gastrocnemius samples. A) Representative immunoblots of ATF4 protein expression in Nuclear and Cytosolic fractions. Subcellular fractions were obtained from the gastrocnemius muscles of animals subjected to the acute *in situ* stimulation protocol and respective controls. Blots are shown with the corresponding Ponceau stain, α-tubulin and H2B as indicators of sample purity. Quantifications shown for **B)** Nuclear and Cytosolic ATF4 protein content corrected to Ponceau. The approximate molecular weights of proteins are indicated with a hash bar in kilodaltons (kDa). n=6-8. S#P=0.05, main effect of the stimulation conditions, One-way ANOVA. Con, Control; Stim, acute *in situ* stimulation; Nuc, Nuclear; Cyto, Cytosolic. Data are means ± SD.

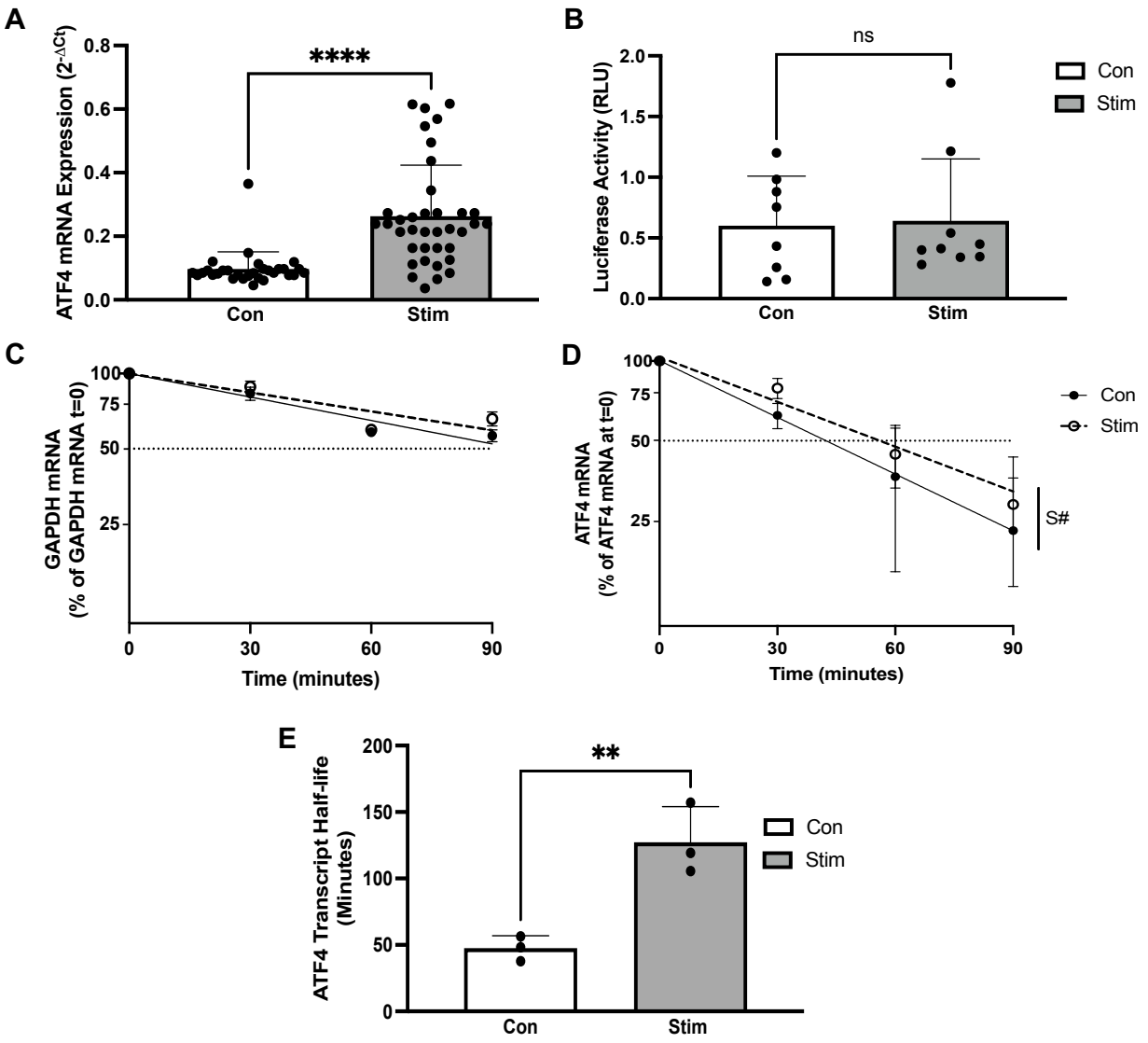

Figure 7: Effect of acute contractile activity on ATF4 transcription, steady-state mRNA content and mRNA stability. A) mRNA expression of ATF4 following the acute *in situ* contractile activity protocol (n=27-36). **B)** ~1.5-kb ATF4 upstream promoter driving firefly luciferase expression was electroporated bilaterally into the gastrocnemius muscles of young male mice in conjunction with a *renilla* luciferase reporter plasmid. Luciferase activity was corrected for *renilla* luciferase to control for transfection efficiency. Control/basal and acute contractile activity samples were assessed (n=9). Semilogarithmic quantification of the rate of mRNA decay of **C)** GADPH (housekeeping gene for qPCR), and **D)** ATF4 following incubation with cytosolic fractions from control or acutely stimulated muscle for 0, 30, 60 or 90 min (n=3, per group/gene). **E)** Half-life of ATF4 transcript (mRNA) levels in control and acutely stimulated samples, derived from the previous rate of decay non-linear regression analyses (n=3/group). S# $P<0.05$, main effect of the stimulation conditions, One-way ANOVA; Tukey's post-hoc analyses, Con vs. Stim (mRNA decay). Student's t-test; Unpaired, $P<0.01$**, $P<0.0001$****. Con, Control; Stim, acute *in situ* stimulation; Data are means ± SD.

DISCUSSION

Mitochondria are recognized as efficient energy hubs that can also coordinate a retrograde (mitochondria-nuclear) signaling response in the face of cellular stress [9-11]. This mito-nuclear communication is deemed functionally necessary as it provides a mechanism for mitochondria to monitor and maintain optimal functioning by inducing nuclear transcriptional programs in response to cellular perturbations [10, 14]. Recent evidence has elucidated that the Integrated Stress Response (ISR), and its effector ATF4, are novel components of the stress response required to maintain mitochondrial health [24-31]. Previous work from our laboratory has identified that ATF4 is responsive to contractile activity and that it has a role in maintaining mitochondrial function [45-47]. This suggests that contractile activity induces a transient increase in mitochondrial stress, which initiates the ISR and leads to the downstream activation of ATF4. However, no work has focused on elucidating the precise signaling events that elicit the induction of the ISR and the mechanism of ATF4 activation *in vivo*. Thus, in this study, we sought to investigate 1) whether the ISR was induced following acute contractile activity, and 2) how such activation correlates to the induction and activity of ATF4.

To understand whether contractile activity could initiate the signaling required to induce mitochondrial stress and the ISR, we subjected animals to a short, yet intense acute contractile activity protocol, with or without a 1-hr recovery period. We selected this paradigm as it induces the contractile activation of the gastrocnemius muscle, the depolarization of all motor units, and the recruitment of all fiber types. This protocol was able to induce significant muscle fatigue, as tetanic contraction force diminished by 40-85% during the stimulation period.

Acute contractile activity-induced stress elicits the activation (phosphorylation) of responsive kinases [55, 56]. Such activation is necessary to transduce cellular signaling and initiate

adaptive physiological responses. To confirm that our contractile activity paradigm was able to activate known exercise-responsive signaling pathways, we evaluated the phosphorylation of JNK2, CaMKIIα, AMPKα and p38-MAPK kinases immediately following the protocol and post-recovery. The phosphorylation of JNK2 and CaMKIIα were remarkably elevated immediately following the contractile activity protocol and returned to basal levels subsequent to the recovery period. This is in agreement with previous observations that have documented an enhancement in the signaling of JNK2 and CaMKIIα following acute exhaustive exercise [57], and moderate intensity exercise [58]. Along with the classical roles of JNK in mediating apoptosis, cell survival, and muscle growth, JNK can also serve as a link between contractile activity and stress response signaling [59]. In particular, it has been demonstrated that the JNK2 isoform is implicated in ISR signaling, lying downstream of the ISR kinase, PKR, and is thus responsive to mitochondrial proteotoxicity and ROS production [32, 59]. Thus, our findings confirm the induction of the ISR in response to our acute contractile paradigm. In addition, CaMKIIα was robustly activated by both acute and prolonged contractile activity in response to intracellular changes in Ca^{2+} and it has been shown to lead to the activation of various transcription factors, contributing to altered gene expression and cellular adaptations [60-62]. We have also previously shown that kinase activation is dependent on both the time and intensity of the contractile activity [55, 56]. Thus, it was interesting to observe that both AMPKα and p38-MAPK were not significantly phosphorylated under the conditions employed. Our observations indicate that our short, intense contractile activity protocol effectively dissociates the activation of specific stress kinases from one another, in favour of ISR signaling activation.

To further evaluate the activation of the ISR in response to acute contractile activity, we assessed the extent of phosphorylation of the ISR kinase, HRI, and the ribosomal eIF2α subunit.

Recent findings have demonstrated that the ISR is upregulated in response to mitochondrial stress via the OMA-DELE1-HRI axis [31, 63]. The activation of this axis requires the coordinated cleavage of the mitochondrial protein DELE1 from the mitochondrial stress-sensitive protease OMA1, producing small DELE1 fragments, which then interact with the HRI homodimer in the cytosol to induce its phosphorylation and catalytic activity [31, 63]. While these upstream events involving OMA1 and DELE1 were not assessed in this study, we observed a trending increase in the activation of HRI immediately following the contractile activity protocol, with levels returning to control in the recovery period. Despite the fact that the activation of HRI was not robust, our results indicate that its downstream target eIF2α was phosphorylated in a time-dependent manner, evident particularly in the recovery phase. This result is a direct indicator of ISR activation. These observations are in agreement with previous work which also showed an increase in its activation following an acute exhaustive bout of exercise in mice [57]. The data also suggest that potential pathway redundancies exist within the ISR kinases and their activation in response to mitochondrial stress [28, 64]. Future work will be designed to elucidate the precise triggering events that occur in response to acute exercise, notably involving either increases in mitochondrial ROS and/or protein aggregation.

Following the activation of the ISR in response to our contractile activity paradigm, we then investigated the regulation of the ISR effector, ATF4, and known downstream targets, ATF5 and CHOP, at the transcriptional and posttranslational levels. Research has shown that ATF4, ATF5, and CHOP are highly responsive to muscle contractile activity [45-47], and that ATF4 is induced following a wide-range of mitochondrial perturbations, consequently leading to the downstream activation of both ATF5 and CHOP [40-44]. ATF4 mRNA expression was elevated in response to contractile activity protocol, which increased further post-recovery. These results

are consistent with previous results from our group and others, indicating that ATF4 is highly responsive to the cellular stress provoked by acute contractile activity [45-47, 65-67]. CHOP mRNA expression was also drastically increased in response to contractile activity, which parallels findings from previous literature [45-47]. These data collectively support the induction of gene expression changes which are most often robustly observed during recovery [68, 69]. In contrast, the brief, intense nature of the contractile activity paradigm employed did not result in the induction of ATF5 or PGC-1α.

Given the brevity of the contractile activity stimulus, we did not anticipate that changes in the protein expression of ATF4, CHOP, and ATF5 would be evident, despite relatively rapid increases in ATF4 and CHOP mRNA levels, as well as an enhancement in the phosphorylation of eIF2α, responsible for mediating the translation of ATF4 mRNA at alternative upstream open reading frames [70]. However, it is not unreasonable to assume a likely delay in measurable protein production, indicating a lag between precursor (i.e, mRNA) and product (protein) synthesis. Surprisingly, this was not evident for CHOP, as CHOP protein was enhanced immediately post-contractile activity, likely reflecting different mRNA and protein turnover rates for ATF4 and CHOP within muscle.

ATF4 is capable of regulating the transcription of various cytoprotective genes in response to mitochondrial stress, thus, in conjunction with the activation of the ISR, we wished to examine the extent of ATF4 nuclear translocation following contractile activity. The ATF4 protein harbours a nuclear localization sequence in its bZIP domain at the C-terminus (amino acids 280 to 284), which regulates its organellar movement depending on the cellular environment [51]. A previous study confirmed that ATF4 is capable of translocating to the nucleus upon cellular stress [71]. Our data illustrate that contractile activity is also a potent stimulus that induces the nuclear

translocation of ATF4. These results indicate that, despite an unchanged protein content, ATF4 is active and can impart its transcriptional activity to downstream target genes, such as CHOP, contributing to its enhanced expression. Future work examining the DNA binding of ATF4 to the promoter region of target genes via ChIP analyses would be beneficial in understanding the extent of activation following acute contractile activity.

To delineate the mechanism underlying the robust increases in the mRNA expression of ATF4 in response to acute contractile activity, we first assessed the activity of the ATF4 promoter via the *in vivo* transfection of a 1.5-kb proximal mouse ATF4 promoter-luciferase construct. We hypothesized that the large increase in JNK2 activation observed with contractile activity would lead to the phosphorylation of regulatory proteins that have been proposed to induce the transcription of ATF4 [72]. Unexpectedly, ATF4 promoter activity in the gastrocnemius muscle following contractile activity remained unchanged in comparison to controls. Thus, our short, intense contractile activity regimen was insufficient to induce detectable transcriptional activation of the promoter, which may require a longer time, including the recovery period, to become evident.

The increase in ATF4 mRNA could also be the result of changes in mRNA degradation rate brought about by contractile activity. To evaluate this, we utilized a cell-free *in vitro* decay assay that has been well described by our laboratory [52,53,73,74]. We sought to compare the degradation rate of ATF4 mRNA in contracting, vs. resting muscle. Our observations indicate that ATF4 mRNA stability was increased immediately following contractile activity, which could account for the increase in ATF4 mRNA. These findings are in line with previous work which showed that contractile activity induces robust mRNA stabilization and the enhancement of nuclear RNA Binding Protein (RBP) expression [52, 53]. RBPs mediate the stability of (pre)

mRNAs primarily by interacting with the sequence elements found in the 3′-untranslated regions (UTRs) of transcripts [75, 76]. We intend to address whether contractile activity alters the expression and/or localization of well-characterized skeletal muscle related RBPs leading to ATF4 mRNA stabilization.

In conclusion, our results indicate that acute contractile activity is capable of eliciting 1) the induction of stress-kinase signaling pathways, 2) activation of the ISR, potentially responsive to changes in mitochondrial homeostasis, 3) an increase in both ATF4 and CHOP mRNA expression, 4) nuclear activation of ATF4 which contributes to the early expression of stress responsive genes, and 5) enhancements in the mRNA stability of ATF4. These findings collectively suggest a protective role of the ISR in maintaining cellular/mitochondrial homeostasis in the face of mechanical and molecular stress. This activation is an early response that may also be useful to further enhance the initial cellular adaptations in muscle responding to exercise-induced stress, contributing to improvements in the muscle phenotype. Further investigation is required to understand the precise mechanism of mitochondrial stress in activating the ISR and ATF4 in response to exercise, and how such induction can be beneficial in preserving the health of the muscle mitochondrial pool.

ACKNOWLEDGEMENTS

This work was supported by funding from the Natural Sciences and Engineering Research Council of Canada (NSERC) to D.A. Hood. D.A. Hood is also the holder of a Canada Research Chair in Cell Physiology. V. C. Sanfrancesco is a recipient of the Canada Graduate Scholarship-Master's (CGS-M) CIHR award.

REFERENCES

1. M. Rai, F. Demontis. (2016). Systemic nutrient and stress signaling via myokines and myometabolites, *Annu. Rev. Physiol*. 78, 85–107. https://doi.org/10.1146/annurev-physiol-021115-105305
2. Chen, C.C.W., Erlich, A.T. & Hood, D.A. (2008). Role of Parkin and endurance training on mitochondrial turnover in skeletal muscle. *Skeletal Muscle*, *10* (8). https://doi.org/10.1186/s13395-018-0157-y
3. A.E. Vincent, K. White, T. Davey, J. Philips, R.T. Ogden, C. Lawless, C. Warren, M. G. Hall, Y.S. Ng, G. Falkous, T. Holden, D. Deehan, R.W. Taylor, D.M. Turnbull, M. Picard. (2019). Quantitative 3D mapping of the human skeletal muscle mitochondrial network, *Cell Rep*. 26 996–-1009, https://doi.org/10.1016/j. celrep.2019.01.010
4. Romanello, V., & Sandri, M. (2022). Implications of mitochondrial fusion and fission in skeletal muscle mass and health. *Seminars in cell & developmental biology*, S1084-9521(22)00050-7. Advance online publication. https://doi.org/10.1016/j.semcdb.2022.02.011
5. Irrcher, I., Adhihetty, P. J., Joseph, A. M., Ljubicic, V., & Hood, D. A. (2003). Regulation of mitochondrial biogenesis in muscle by endurance exercise. *Sports medicine (Auckland, N.Z.)*, 33(11), 783–793. https://doi.org/10.2165/00007256-200333110-00001
6. O'Leary, M. F., & Hood, D. A. (2008). Effect of prior chronic contractile activity on mitochondrial function and apoptotic protein expression in denervated muscle. *Journal of applied physiology* (Bethesda, Md. : 1985), 105(1), 114–120. https://doi.org/10.1152/japplphysiol.00724.2007
7. Sanchez, A. M., Bernardi, H., Py, G., & Candau, R. B. (2014). Autophagy is essential to support skeletal muscle plasticity in response to endurance exercise. *American journal of physiology. Regulatory, integrative and comparative physiology,* 307(8), R956–R969. https://doi.org/10.1152/ajpregu.00187.2014
8. Hood D. A. (2001). Invited Review: contractile activity-induced mitochondrial biogenesis in skeletal muscle. *Journal of applied physiology (Bethesda, Md. : 1985)*, *90*(3), 1137–1157. https://doi.org/10.1152/jappl.2001.90.3.1137
9. Chandel N. S. (2015). Evolution of Mitochondria as Signaling Organelles. *Cell metabolism*, 22(2), 204–206. https://doi.org/10.1016/j.cmet.2015.05.013
10. Quirós, P. M., Mottis, A., & Auwerx, J. (2016). Mitonuclear communication in homeostasis and stress. Nature reviews. *Molecular cell biology, 17*(4), 213–226. https://doi.org/10.1038/nrm.2016.23
11. Matilainen, O., Quirós, P. M., & Auwerx, J. (2017). Mitochondria and Epigenetics - Crosstalk in Homeostasis and Stress. *Trends in cell biology*, 27(6), 453–463. https://doi.org/10.1016/j.tcb.2017.02.004
12. Couvillion, M. T., Soto, I. C., Shipkovenska, G., & Churchman, L. S. (2016). Synchronized mitochondrial and cytosolic translation programs. *Nature*, *533*(7604), 499–503. https://doi.org/10.1038/nature18015
13. Oliveira, A. N., & Hood, D. A. (2018). Effect of Tim23 knockdown in vivo on mitochondrial protein import and retrograde signaling to the UPRmt in muscle. *American journal of physiology. Cell physiology*, 315(4), C516–C526. https://doi.org/10.1152/ajpcell.00275.2017
14. Quirós, P. M., Langer, T., & López-Otín, C. (2015). New roles for mitochondrial proteases in health, ageing and disease. *Nature reviews. Molecular cell biology*, *16*(6), 345–359. https://doi.org/10.1038/nrm3984

15. Handschin, C., & Spiegelman, B. M. (2006). Peroxisome proliferator-activated receptor gamma coactivator 1 coactivators, energy homeostasis, and metabolism. *Endocrine reviews*, *27*(7), 728–735. https://doi.org/10.1210/er.2006-0037
16. Scarpulla, R. C., Vega, R. B., & Kelly, D. P. (2012). Transcriptional integration of mitochondrial biogenesis. *Trends in endocrinology and metabolism: TEM*, 23(9), 459–466. https://doi.org/10.1016/j.tem.2012.06.006
17. Scarpulla R. C. (2011). Metabolic control of mitochondrial biogenesis through the PGC-1 family regulatory network. *Biochimica et biophysica acta,* 1813(7), 1269–1278. https://doi.org/10.1016/j.bbamcr.2010.09.019
18. Hood, D. A., Adhihetty, P. J., Colavecchia, M., Gordon, J. W., Irrcher, I., Joseph, A. M., Lowe, S. T., & Rungi, A. A. (2003). Mitochondrial biogenesis and the role of the protein import pathway. *Medicine and science in sports and exercise*, 35(1), 86–94. https://doi.org/10.1097/00005768-200301000-00015
19. Hood, D. A., & Joseph, A. M. (2004). Mitochondrial assembly: protein import. *The Proceedings of the Nutrition Society*, *63*(2), 293–300. https://doi.org/10.1079/PNS2004342
20. Hoogenraad, N. J., & Ryan, M. T. (2001). Translocation of proteins into mitochondria. *IUBMB life*, *51*(6), 345–350. https://doi.org/10.1080/152165401753366096
21. Cordeiro, A. V., Peruca, G. F., Braga, R. R., Brícola, R. S., Lenhare, L., Silva, V. R. R., Anaruma, C. P., Katashima, C. K., Crisol, B. M., Barbosa, L. T., Simabuco, F. M., da Silva, A. S. R., Cintra, D. E., de Moura, L. P., Pauli, J. R., & Ropelle, E. R. (2021). High-intensity exercise training induces mitonuclear imbalance and activates the mitochondrial unfolded protein response in the skeletal muscle of aged mice. *GeroScience,* 43(3), 1513–1518. https://doi.org/10.1007/s11357-020-00246-5
22. Ogborn, D. I., McKay, B. R., Crane, J. D., Safdar, A., Akhtar, M., Parise, G., & Tarnopolsky, M. A. (2015). Effects of age and unaccustomed resistance exercise on mitochondrial transcript and protein abundance in skeletal muscle of men. American journal of physiology. *Regulatory, integrative and comparative physiology,* 308(8), R734–R741. https://doi.org/10.1152/ajpregu.00005.2014
23. Ogborn, D. I., McKay, B. R., Crane, J. D., Parise, G., & Tarnopolsky, M. A. (2014). The unfolded protein response is triggered following a single, unaccustomed resistance-exercise bout. *American journal of physiology. Regulatory, integrative and comparative physiology*, 307(6), R664–R669. https://doi.org/10.1152/ajpregu.00511.2013
24. Pakos-Zebrucka, K., Koryga, I., Mnich, K., Ljujic, M., Samali, A., & Gorman, A. M. (2016). The integrated stress response. *EMBO reports*, 17(10), 1374–1395. https://doi.org/10.15252/embr.201642195Anderson, N. S., & Haynes, C. M. (2020). Folding the Mitochondrial UPR into the Integrated Stress Response. *Trends in cell biology*, *30*(6), 428–439. https://doi.org/10.1016/j.tcb.2020.03.001
25. Dey, S., Baird, T. D., Zhou, D., Palam, L. R., Spandau, D. F., & Wek, R. C. (2010). Both transcriptional regulation and translational control of ATF4 are central to the integrated stress response. *The Journal of biological chemistry, 285*(43), 33165–33174. https://doi.org/10.1074/jbc.M110.167213
26. Castilho, B. A., Shanmugam, R., Silva, R. C., Ramesh, R., Himme, B. M., & Sattlegger, E. (2014). Keeping the eIF2 alpha kinase Gcn2 in check. *Biochimica et biophysica acta*, 1843(9), 1948–1968. https://doi.org/10.1016/j.bbamcr.2014.04.006

27. Mick, E., Titov, D. V., Skinner, O. S., Sharma, R., Jourdain, A. A., & Mootha, V. K. (2020). Distinct mitochondrial defects trigger the integrated stress response depending on the metabolic state of the cell. *eLife,* 9, e49178. https://doi.org/10.7554/eLife.49178
28. Bilen, M., Benhammouda, S., Slack, R., & Germain, M. (2022). The integrated stress response as a key pathway downstream of mitochondrial dysfunction. *Current Opinion in Physiology*, 27. https://doi.org/10.1016/j.cophys.2022.100555
29. Baird, T. D., & Wek, R. C. (2012). Eukaryotic initiation factor 2 phosphorylation and translational control in metabolism. *Advances in nutrition* (Bethesda, Md.), 3(3), 307–321. https://doi.org/10.3945/an.112.002113
30. Harding, H. P., Zhang, Y., Zeng, H., Novoa, I., Lu, P. D., Calfon, M., Sadri, N., Yun, C., Popko, B., Paules, R., Stojdl, D. F., Bell, J. C., Hettmann, T., Leiden, J. M., & Ron, D. (2003). An integrated stress response regulates amino acid metabolism and resistance to oxidative stress. *Molecular cell, 11(3), 619–633*. https://doi.org/10.1016/s1097-2765(03)00105-9
31. Guo X, Aviles G, Liu Y, Tian R, Unger BA, Lin YT, Wiita AP, Xu K, Correia MA, Kampmann M. (2020). Mitochondrial stress is relayed to the cytosol by an OMA1-DELE1-HRI pathway. *Nature.* 579(7799):427-432. doi: 10.1038/s41586-020-2078-2.
32. Rath, E., Berger, E., Messlik, A., Nunes, T., Liu, B., Kim, S. C., Hoogenraad, N., Sans, M., Sartor, R. B., & Haller, D. (2012). Induction of dsRNA-activated protein kinase links mitochondrial unfolded protein response to the pathogenesis of intestinal inflammation. *Gut*, *61*(9), 1269–1278. https://doi.org/10.1136/gutjnl-2011-300767
33. Chaveroux, C., Lambert-Langlais, S., Parry, L., Carraro, V., Jousse, C., Maurin, A. C., Bruhat, A., Marceau, G., Sapin, V., Averous, J., & Fafournoux, P. (2011). Identification of GCN2 as new redox regulator for oxidative stress prevention in vivo. *Biochemical and biophysical research communications*, *415*(1), 120–124. https://doi.org/10.1016/j.bbrc.2011.10.027
34. Ebert S. M., Rasmussen, B. B., Judge, A. R., Judge, S. M., Larsson, L., Wek, R. C., Anthony, T. G., Marcotte, G. R., Miller, M. J., Yorek, M. A., Vella, A., Volpi, E., Stern, J. I., Strub, M. D., Ryan, Z., Talley, J. J., & Adams, C. M. (2022). Biology of Activating Transcription Factor 4 (ATF4) and Its Role in Skeletal Muscle Atrophy. *The Journal of nutrition*, *152*(4), 926–938. https://doi.org/10.1093/jn/nxab440
35. Ameri, K., & Harris, A. L. (2008). Activating transcription factor 4. *The international journal of biochemistry & cell biology*, *40*(1), 14–21. https://doi.org/10.1016/j.biocel.2007.01.020
36. Celardo, I., Lehmann, S., Costa, A. C., Loh, S. H., & Miguel Martins, L. (2017). dATF4 regulation of mitochondrial folate-mediated one-carbon metabolism is neuroprotective. *Cell death and differentiation, 24*(4), 638–648. https://doi.org/10.1038/cdd.2016.158
37. Sorge, S., Theelke, J., Yildirim, K., Hertenstein, H., McMullen, E., Müller, S., Altbürger, C., Schirmeier, S., & Lohmann, I. (2020). ATF4-Induced Warburg Metabolism Drives Over-Proliferation in Drosophila. *Cell Reports, 31*(7), 107659. https://doi.org/10.1016/j.celrep.2020.107659
38. Zong, Y., Feng, S., Cheng, J., Yu, C., & Lu, G. (2017). Up-Regulated ATF4 Expression Increases Cell Sensitivity to Apoptosis in Response to Radiation. *Cellular physiology and biochemistry: international journal of experimental cellular physiology, biochemistry, and pharmacology, 41*(2), 784–794. https://doi.org/10.1159/000458742
39. Adams, C. M., Ebert, S. M., & Dyle, M. C. (2017). Role of ATF4 in skeletal muscle atrophy. *Current opinion in clinical nutrition and metabolic care, 20*(3), 164–168. https://doi.org/10.1097/MCO.0000000000000362

40. Sasaki, K., Uchiumi, T., Toshima, T., Yagi, M., Do, Y., Hirai, H., Igami, K., Gotoh, K., & Kang, D. (2020). Mitochondrial translation inhibition triggers ATF4 activation, leading to integrated stress response but not to mitochondrial unfolded protein response. *Bioscience reports*, *40*(11), BSR20201289. https://doi.org/10.1042/BSR20201289
41. Mahor, D., Pandey, R., & Bulusu, V. (2022). TCA cycle off, ATF4 on for metabolic homeostasis. *Trends in Biochemical Sciences*, *47*(7), 558–560. https://doi.org/10.1016/j.tibs.2022.03.006
42. Kasai S, Yamazaki H, Tanji K, Engler MJ, Matsumiya T, Itoh K. (2019). Role of the ISR-ATF4 pathway and its cross talk with Nrf2 in mitochondrial quality control. *J Clin Biochem Nutr.* 64(1):1-12. doi: 10.3164/jcbn.18-37.
43. Harding, H. P., Zhang, Y., Zeng, H., Novoa, I., Lu, P. D., Calfon, M., Sadri, N., Yun, C., Popko, B., Paules, R., Stojdl, D. F., Bell, J. C., Hettmann, T., Leiden, J. M., & Ron, D. (2003). An integrated stress response regulates amino acid metabolism and resistance to oxidative stress. *Molecular cell*, *11*(3), 619–633. https://doi.org/10.1016/s1097-2765(03)00105-9
44. Quirós, P. M., Prado, M. A., Zamboni, N., D'Amico, D., Williams, R. W., Finley, D., Gygi, S. P., & Auwerx, J. (2017). Multi-omics analysis identifies ATF4 as a key regulator of the mitochondrial stress response in mammals. *The Journal of Cell Biology*, *216*(7), 2027–2045. https://doi.org/10.1083/jcb.201702058
45. Memme, J. M., Sanfrancesco, V. C., & Hood, D. A. (2023). Activating transcription factor 4 regulates mitochondrial content, morphology, and function in differentiating skeletal muscle myotubes. American journal of physiology. *Cell physiology, 325*(1), C224–C242. https://doi.org/10.1152/ajpcell.00080.2023
46. Memme, J. M., Oliveira, A. N., & Hood, D. A. (2016). Chronology of UPR activation in skeletal muscle adaptations to chronic contractile activity. *American journal of physiology. Cell physiology*, *310*(11), C1024–C1036. https://doi.org/10.1152/ajpcell.00009.2016
47. Mesbah Moosavi, Z. S., & Hood, D. A. (2017). The unfolded protein response in relation to mitochondrial biogenesis in skeletal muscle cells. *American journal of physiology. Cell physiology*, *312*(5), C583–C594. https://doi.org/10.1152/ajpcell.00320.2016
48. Long, Y. C., Widegren, U., & Zierath, J. R. (2004). Exercise-induced mitogen-activated protein kinase signalling in skeletal muscle. *The Proceedings of the Nutrition Society*, *63*(2), 227–232. https://doi.org/10.1079/PNS2004346
49. Sud, N., Rutledge, A. C., Pan, K., & Su, Q. (2016). Activation of the dsRNA-Activated Protein Kinase PKR in Mitochondrial Dysfunction and Inflammatory Stress in Metabolic Syndrome. *Current pharmaceutical design*, *22*(18), 2697–2703. https://doi.org/10.2174/1381612822666160202141845
50. Combes, A., Dekerle, J., Webborn, N., Watt, P., Bougault, V., & Daussin, F. N. (2015). Exercise-induced metabolic fluctuations influence AMPK, p38-MAPK and CaMKII phosphorylation in human skeletal muscle. *Physiological reports*, *3*(9), e12462. https://doi.org/10.14814/phy2.12462
51. Cibelli, G., Schoch, S., & Thiel, G. (1999). Nuclear targeting of cAMP response element binding protein 2 (CREB2). *European journal of cell biology*, *78*(9), 642–649. https://doi.org/10.1016/S0171-9335(99)80049-1
52. D'souza, D., Lai, R. Y., Shuen, M., & Hood, D. A. (2012). mRNA stability as a function of striated muscle oxidative capacity. *American journal of physiology. Regulatory, integrative and comparative physiology*, *303*(4), R408–R417. https://doi.org/10.1152/ajpregu.00085.2012

53. Lai, R. Y., Ljubicic, V., D'souza, D., & Hood, D. A. (2010). Effect of chronic contractile activity on mRNA stability in skeletal muscle. *American journal of physiology. Cell physiology*, *299*(1), C155–C163. https://doi.org/10.1152/ajpcell.00523.2009
54. Parker L, Trewin A, Levinger I, Shaw CS, Stepto NK. (2017). The effect of exercise-intensity on skeletal muscle stress kinase and insulin protein signaling. *PLoS One;12*(2):e0171613. doi: 10.1371/journal.pone.0171613.
55. Ljubicic, V., & Hood, D. A. (2008). Kinase-specific responsiveness to incremental contractile activity in skeletal muscle with low and high mitochondrial content. *American journal of physiology. Endocrinology and metabolism*, *295*(1), E195–E204. https://doi.org/10.1152/ajpendo.90276.2008
56. Ljubicic, V., & Hood, D. A. (2009). Diminished contraction-induced intracellular signaling towards mitochondrial biogenesis in aged skeletal muscle. *Aging cell*, *8*(4), 394–404. https://doi.org/10.1111/j.1474-9726.2009.00483.x
57. Slavin, M. B., Kumari, R., & Hood, D. A. (2022). ATF5 is a regulator of exercise-induced mitochondrial quality control in skeletal muscle. *Molecular metabolism*, *66*, 101623. https://doi.org/10.1016/j.molmet.2022.101623
58. Brandt N, Dethlefsen MM, Bangsbo J, Pilegaard H. (2017). PGC-1α and exercise intensity dependent adaptations in mouse skeletal muscle. *PLoS One, 12*(10):e0185993. doi: 10.1371/journal.pone.0185993.
59. Aronson, D., Boppart, M. D., Dufresne, S. D., Fielding, R. A., & Goodyear, L. J. (1998). Exercise stimulates c-Jun NH2 kinase activity and c-Jun transcriptional activity in human skeletal muscle. *Biochemical and biophysical research communications*, *251*(1), 106–110. https://doi.org/10.1006/bbrc.1998.9435
60. Enslen, H., Tokumitsu, H., Stork, P. J., Davis, R. J., & Soderling, T. R. (1996). Regulation of mitogen-activated protein kinases by a calcium/calmodulin-dependent protein kinase cascade. *Proceedings of the National Academy of Sciences of the United States of America*, *93*(20), 10803–10808. https://doi.org/10.1073/pnas.93.20.10803
61. Chin E. R. (2005). Role of Ca2+/calmodulin-dependent kinases in skeletal muscle plasticity. *Journal of applied physiology (Bethesda, Md. : 1985)*, *99*(2), 414–423. https://doi.org/10.1152/japplphysiol.00015.2005
62. Combes, A., Dekerle, J., Webborn, N., Watt, P., Bougault, V., & Daussin, F. N. (2015). Exercise-induced metabolic fluctuations influence AMPK, p38-MAPK and CaMKII phosphorylation in human skeletal muscle. *Physiological reports*, *3*(9), e12462. https://doi.org/10.14814/phy2.12462
63. Fessler, E., Eckl, E. M., Schmitt, S., Mancilla, I. A., Meyer-Bender, M. F., Hanf, M., Philippou-Massier, J., Krebs, S., Zischka, H., & Jae, L. T. (2020). A pathway coordinated by DELE1 relays mitochondrial stress to the cytosol. *Nature*, *579*(7799), 433–437. https://doi.org/10.1038/s41586-020-2076-4
64. Zhang, G., Wang, X., Li, C., Li, Q., An, Y. A., Luo, X., Deng, Y., Gillette, T. G., Scherer, P. E., & Wang, Z. V. (2021). Integrated Stress Response Couples Mitochondrial Protein Translation With Oxidative Stress Control. *Circulation*, *144*(18), 1500–1515. https://doi.org/10.1161/CIRCULATIONAHA.120.053125
65. Kim K, Kim YH, Lee SH, Jeon MJ, Park SY, Doh KO. (2014). Effect of exercise intensity on unfolded protein response in skeletal muscle of rat. *Korean J Physiol Pharmacol*. 18(3):211-6. doi: 10.4196/kjpp.2014.18.3.211.

66. Kim KH, Kim SH, Min YK, Yang HM, Lee JB, Lee MS. (2013). Acute exercise induces FGF21 expression in mice and in healthy humans. *PLoS One, 8*(5):e63517. doi: 10.1371/journal.pone.0063517.
67. D'Hulst, G., Masschelein, E., & De Bock, K. (2022). Resistance exercise enhances long-term mTORC1 sensitivity to leucine. *Molecular metabolism*, *66*, 101615. https://doi.org/10.1016/j.molmet.2022.101615
68. Neufer, P. D., Ordway, G. A., & Williams, R. S. (1998). Transient regulation of c-fos, alpha B-crystallin, and hsp70 in muscle during recovery from contractile activity. *The American journal of physiology*, *274*(2), C341–C346. https://doi.org/10.1152/ajpcell.1998.274.2.C341
69. Saleem, A., & Hood, D. A. (2013). Acute exercise induces tumour suppressor protein p53 translocation to the mitochondria and promotes a p53-Tfam-mitochondrial DNA complex in skeletal muscle. *The Journal of physiology*, *591*(14), 3625–3636. https://doi.org/10.1113/jphysiol.2013.252791
70. Whitney ML, Jefferson LS, Kimball SR. (2009). ATF4 is necessary and sufficient for ER stress-induced upregulation of REDD1 expression. *Biochem Biophys Res Commun. 6;379*(2):451-5. doi: 10.1016/j.bbrc.2008.12.079.
71. Zhang C, Bai N, Chang A, Zhang Z, Yin J, Shen W, Tian Y, Xiang R, Liu C. (2013). ATF4 is directly recruited by TLR4 signaling and positively regulates TLR4-trigged cytokine production in human monocytes. *Cell Mol Immunol, 10*(1):84-94. doi: 10.1038/cmi.2012.57.
72. Matsuguchi, T., Chiba, N., Bandow, K., Kakimoto, K., Masuda, A., & Ohnishi, T. (2009). JNK activity is essential for Atf4 expression and late-stage osteoblast differentiation. *Journal of bone and mineral research : the official journal of the American Society for Bone and Mineral Research*, *24*(3), 398–410. https://doi.org/10.1359/jbmr.081107
73. Tryon LD, Crilly MJ, Hood DA. (2015). Effect of denervation on the regulation of mitochondrial transcription factor A expression in skeletal muscle. *Am J Physiol Cell Physiol*. 309(4):C228-38. doi: 10.1152/ajpcell.00266.2014
74. Freyssenet, D., Connor, M. K., Takahashi, M., & Hood, D. A. (1999). Cytochrome c transcriptional activation and mRNA stability during contractile activity in skeletal muscle. *The American journal of physiology*, *277*(1), E26–E32. https://doi.org/10.1152/ajpendo.1999.277.1.E26
75. Vlasova, I. A., Tahoe, N. M., Fan, D., Larsson, O., Rattenbacher, B., Sternjohn, J. R., Vasdewani, J., Karypis, G., Reilly, C. S., Bitterman, P. B., & Bohjanen, P. R. (2008). Conserved GU-rich elements mediate mRNA decay by binding to CUG-binding protein 1. *Molecular cell*, *29*(2), 263–270. https://doi.org/10.1016/j.molcel.2007.11.024
76. Yakubovskaya, E., Guja, K. E., Eng, E. T., Choi, W. S., Mejia, E., Beglov, D., Lukin, M., Kozakov, D., & Garcia-Diaz, M. (2014). Organization of the human mitochondrial transcription initiation complex. *Nucleic acids research*, *42*(6), 4100–4112. https://doi.org/10.1093/nar/gkt1360

FUTURE DIRECTIONS

1. Since the ISR is activated in response to our short contractile activity paradigm, it is worth investigating whether such activation is enhanced following an exhaustive bout of exercise. A hint towards this is shown in our RNA-seq (supplementary) findings, that show robust enhancement in ISR related genes following a bout of whole body exercise in mice. Such a project can also be done in a cell culture model via the use of our "exercise-in-a-dish" acute contractile protocol. Once the ISR has been successfully induced, it would also be worthwhile to examine the transient molecular adaptations that may exist and thereby contribute to an improvement in the mitochondrial pool. This can be accomplished by evaluating the drive for mitochondrial biogenesis and mitophagy, as well as mitochondrial respiration parameters.
2. Understanding the mechanism behind the induction of the ISR in response to acute contractile activity/exercise has not yet been investigated in the literature, thus, it would be beneficial to explore this in great depth. Evidence has indeed suggested that the ISR is responsive to mitochondrial ROS production, misfolded proteins aggregates and mutations in mtDNA, however, the precise mitochondrial stress that occurs with acute contractile activity has not yet been elucidated. To examine this, we can assess overall ROS emission via Oroboros or Clark Electrode analyses, evaluate the soluble and insoluble (protein aggregates) protein pool within the mitochondria, and/or assess the presence of unfolded proteins within mitochondria via the use of a Tetrephenulethene Maleimide (TPE-MI) fluorogenic dye or slot-blot analyses of beta-strand oligomers using the A11 Oligomer antibody.

3. To further validate the role of the ISR and thus ATF4 in maintaining mitochondrial homeostasis during acute exercise, a muscle-specific ATF4 knockout model can be employed. We have established our ATF4 knockout colony, and thus have the capacity to examine the differences between WT and ATF4 KO in their responsiveness to acute exercise induced mitochondrial stress, and the downstream consequences. As well, since ATF4 has been implicated in sarcopenia, it would be interesting to also identify how the absence of ATF4 contributes to not only the preservation of muscle, but the potential effects on mitochondrial health (age-related). Would these two parameters be contradicting? Lastly, with this ATF4 mKO colony, it would also be beneficial to evaluate the exercise training responsiveness, and if ATF4 is required to elicit beneficial mitochondrial adaptation to training, as observed in cell culture models.
4. The ISR has recently been suggested as the precursor pathway that is activated in response to mitochondrial stress and thereby induces the activation of the UPR^{mt}, however, no work has focused on elucidating how these two pathways coordinate their activation and cytoprotective transcriptional response. Thus, it worth investigating such relationship in response to exercise-induced mitochondrial stress. This can be examined in both animal and cell culture models. As well, it would be intriguing to determine the consequence of a double knockdown of the main effectors of both pathways (ATF4 and ATF5) and observe the corresponding effects that occur with respect to mitochondrial health and the ability to adapt to exercise-induced stress.

APPENDIX A: DATA AND STATISTICAL ANALYSIS

Table 1. % Force Production During the *in situ* Protocol.

	Force Production (% of initial force)		
N	3 Min	6 Min	9 Min
1	70.4	33.4	23.3
2	58.2	32.5	15.4
3	58.8	26.3	20.1
4	46.8	30.2	18.8
5	67.8	31.2	19.7
6	71.9	31.7	20.0
7	27.5	33.4	23.6
8	55.1	20.9	12.9
9	52.0	23.7	15.6
10	52.5	25.9	18.5
11	35.8	30.3	16.2
12	45.5	14.5	17.6
13	58.9	30.1	15.4
14	48.3	28.3	12.6
15	72.4	22.9	11.2
16	57.9	26.5	19.9
17	49.9	20.0	12.4
18	56.2	24.7	14.1
19	41.0	32.4	10.8
20	40.2	22.9	16.4
21	53.6	20.5	22.9
22	56.1	27.3	14.6
23	54.6	34.6	10.5
24	58.0	25.4	13.3
25	45.6	22.6	13.7
26	44.4	20.8	18.8
27	69.1	20.1	10.6
28	46.4	28.8	10.2
29	45.3	18.9	16.0
X	53.1	26.2	16.0
SD	10.8505039	5.233853	3.970567

1-Way ANOVA: Force Production (% of initial force)	
P value	<0.0001
P value summary	****
Signifcantly different (P>0.05?)	Yes

Post-Hoc Test					
Tukey's multiple comparisons test	Mean Diff.	95.00% CI of diff.	Below threshold?	Summary	Adjusted P Value
3 Mins vs. 6 Mins	27.04	22.48 to 31.61	Yes	****	<0.0001
3 Mins vs. 9 Mins	37.07	32.43 to 41.71	Yes	****	<0.0001
6 Mins vs. 9 Mins	10.03	5.425 to 14.63	Yes	****	<0.0001

Table 2A. ATF4 mRNA Expression.

	ATF4 mRNA Expression (2^-ΔCt)		
N	Con	Stim	Stim+Rec
1	0.1129662	0.61475	1.254
2	0.1203727	0.344523	1.247
3	0.1193048	0.106377	0.574
4	0.1478995	0.436847	0.224
5	0.084306	0.220433	0.639
6	0.075039	0.27161	0.588
7	0.068476	0.251534	
8	0.066144	0.122364	
9	0.061087	0.239021	
10	0.066636	0.2134	
11	0.078624	0.163046	
12	0.082139	0.272952	
13	0.084829	0.239021	
14	0.092612	0.2134	
15	0.077519	0.163046	
16	0.096732	0.272952	
17	0.084829	0.08454	
18	0.092612	0.11167	
19	0.077519	0.223005	
20	0.096732	0.036359	
21	0.084829	0.125796	
22	0.092612	0.071268	
23	0.077519	0.259645	
24	0.096732	0.239021	
25	0.084829	0.2134	
26	0.092612	0.163046	
27	0.077519	0.272952	
28	0.096732	0.239021	
29	0.046	0.2134	
30	0.365	0.163046	
31		0.272952	
32		0.065	
33		0.569	
34		0.495	
35		0.546	
36		0.603	
37		0.617	
X	0.096692073	0.262956676	0.754333333
SD	0.054354797	0.160762454	0.411613735

1-Way ANOVA: ATF4 mRNA Expression (2^-ΔCt)	
P value	<0.0001
P value summary	****
Signifcantly different (P>0.05?)	Yes

Post-Hoc Test					
Tukey's multiple comparisons test	Mean Diff.	95.00% CI of diff.	Below threshold?	Summary	Adjusted P Value
Con vs. Stim	-0.1663	-0.2665 to -0.06602	Yes	***	0.0005
Con vs. Stim+Rec	-0.7265	-0.8978 to -0.5553	Yes	****	<0.0001
Stim vs. Stim+Rec	-0.5603	-0.7284 to -0.3921	Yes	****	<0.0001

Table 2B. CHOP mRNA Expression.

	CHOP mRNA Expression (2^-ΔCt)		
N	Con	Stim	Stim+Rec
1	0.0437056	0.834503	0.86
2	0.0464162	0.425729	0.53
3	0.0768783	0.181323	0.51
4	0.3956068	0.280568	0.66
5	0.068873	0.150861	0.39
6	0.043782	0.282834	0.44
7	0.039414	0.23055	0.44
8	0.051075	0.22036	
9	0.060592	0.196336	
10	0.049831	0.182157	
11	0.059605	0.132491	
12	0.111261	0.627851	
13	0.073102	0.056941	
14	0.069872	0.073262	
15	0.051231	0.044555	
16	0.108007	0.020384	
17	0.052114	0.134345	
18	0.063558	0.187729	
19	0.1252	0.261452	
20	0.057924	0.256895	
21	0.037587	0.084686	
22	0.044364	0.185004	
23	0.026183	0.070797	
24	0.019814	0.353059	
25	0.073527	0.058032	
26	0.032841	0.069865	
27	0.052072	0.087892	
28	0.088968	0.004545	
29	0.075239	0.054983	
30	0.047982	0.050678	
31	0.046255	0.050867	
32	0.057433	0.088371	
33	0.034	0.039	
34	0.03	0.036	
35	0.031	0.044	
36	0.046	0.046	
37	0.079	0.067	
38	0.032	0.025	
39	0.047	0.044	
X	0.065367	0.16002321	0.54714286
SD	0.05907805	0.16968306	0.16327015

1-Way ANOVA: CHOP mRNA Expression (2^-ΔCt)	
P value	<0.0001
P value summary	****
Signifcantly different (P>0.05?)	Yes

Post-Hoc Test					
Tukey's multiple comparisons test	Mean Diff.	95.00% CI of diff.	Below threshold?	Summary	Adjusted P Value
Con vs. Stim	Con vs. Stim	-0.09211	-0.1631 to -0.02115	Yes	**
Con vs. Stim+Rec	Con vs. Stim+Rec	-0.4818	-0.6096 to -0.3540	Yes	****
Stim vs. Stim+Rec	Stim vs. Stim+Rec	-0.3897	-0.5177 to -0.2616	Yes	****

Table 2C. ATF5 mRNA Expression

	ATF5 mRNA Expression (2^-ΔCt)		
N	Con	Stim	Stim+Rec
1	0.0510545	0.055344	0.1
2	0.0623948	0.0797	0.083
3	0.0719377	0.079222	0.101
4	0.1074628	0.112217	0.036
5	0.106501	0.129766	0.025
6	0.121141	0.146131	0.028
7	0.135955	0.11706	0.022
8	0.0604	0.253879	
9	0.051558	0.06319	
10	0.070324	0.100789	
11	0.084647	0.080805	
12	0.038193	0.099762	
13	0.032609	0.031909	
14	0.043827	0.05452	
15	0.110245	0.045031	
16	0.02221	0.023581	
17	0.095579	0.053645	
18	0.074395	0.140933	
19	0.07551	0.076688	
20	0.032826	0.082634	
21	0.065397	0.062001	
22	0.07944	0.101983	
23	0.079587	0.065697	
24	0.076432	0.083116	
25	0.07738	0.085235	
26	0.110685	0.134398	
27	0.079681	0.103198	
28	0.033692	0.041098	
29	0.037767	0.024431	
30	0.07629	0.047861	
31	0.076771	0.078738	
32	0.043	0.101806	
33	0.032	0.037	
34	0.434	0.038	
35	0.026	0.665	
36	0.053	0.03	
37	0.022	0.041	
38	0.031	0.02	
39		0.029	
X	0.07586557	0.09272738	0.05642857
SD	0.0665266	0.10430258	0.03649136

1-Way ANOVA: ATF5 mRNA Expression (2^-ΔCt)	
P value	0.4868
P value summary	ns
Signifcantly different (P>0.05?)	No

Table 2D. PGC-1α mRNA Expression.

	PGC-1α mRNA Expression (2^-ΔCt)		
N	Con	Stim	Stim+Rec
1	0.2656155	0.390106	0.223
2	0.2850196	0.423098	0.344
3	0.2495429	0.291849	0.319
4	0.447101	0.651699	0.689
5	0.27357	0.314874	0.2
6	0.154222	0.347126	0.3
7	0.230413	0.439383	0.332
8	0.322195	0.527838	
9	0.357954	0.353759	
10	0.350202	0.401219	
11	0.321631	0.305867	
12	0.341227	0.304283	
13	0.375329	0.306286	
14	0.256716	0.218233	
15	0.130957	0.123011	
16	0.705517	0.29865	
17	0.22072	0.458856	
18	0.221408	0.229385	
19	0.231192	0.321183	
20	0.15712	0.258	
21	0.207139	0.242	
22	0.131884	0.393	
23	0.186367	0.394	
24	0.098358	0.265	
25	0.60375	0.247	
26	0.372442	0.397	
27	0.515748	0.592	
28	0.393658	0.324	
29	0.469001	0.35	
30	0.598153	0.229	
31	0.384407		
32	0.436906		
33	0.265		
34	0.292		
35	0.288		
36	0.364		
37	0.349		
38	0.274		
39	0.353		
X	0.320011923	0.346590167	0.343857143
SD	0.133919763	0.112501217	0.16181618

1-Way ANOVA: PGC-1α mRNA Expression (2^-ΔCt)	
P value	0.6773
P value summary	ns
Signifcantly different (P>0.05?)	No

Table 3A. Total-HRI Protein Expression.

	Total-HRI Protein Expression (A.U)		
N	Con	Stim	Stim+Rec
1	1.06181545	0.81441499	0.73227488
2	0.8526342	0.59553052	0.70275471
3	0.51199006	0.60675462	0.51152281
4	0.46712029	0.63526971	1.02300294
5	1.03029721	1.24742456	0.98122331
6	0.63856364	0.99770641	0.92451791
7	0.48315722		
8	0.52115643		
9	1.49258069		
10	0.92268324		
11	1.19600795		
12	0.94436758		
X	0.843531163	0.816183468	0.812549427
SD	0.326407698	0.262373985	0.197177285

1-Way ANOVA:Total-HRI Protein Expression (A.U)	
P value	0.969
P value summary	ns
Signifcantly different (P>0.05?)	No

Table 3B. Phosphorylated-HRI Protein Expression.

	Phosphorylated-HRI Protein Expression (A.U)		
N	Con	Stim	Stim+Rec
1	0.74971571	0.59847651	0.58942841
2	0.40593249	0.52500532	0.41965683
3	0.32631341	0.97778334	0.47679632
4	1.33214542	1.27510727	0.4957369
5	0.37890396	0.84564679	0.62533265
6	0.83788174	0.91756694	0.93262479
7	0.33886667		
8	1.05135059		
9	0.52150718		
10	0.93368388		
11	0.93451795		
12			
X	0.710074455	0.856597695	0.589929317
SD	0.338308363	0.272122563	0.1840423

1-Way ANOVA: Phosphorylated-HRI Protein Expression (A.U)	
P value	0.3018
P value summary	ns
Signifcantly different (P>0.05?)	No

Table 3C. Phosphorylated/Total-HRI Protein Expression.

	Phosphorylated/Total-HRI Protein Expression (A.U)		
N	Con	Stim	Stim+Rec
1	0.68163171	0.70191474	1.15124971
2	0.7786343	1.1239189	0.59715975
3	1.3189386	1.53122301	0.98683472
4	1.02381732	2.44668819	0.4845899
5	0.46433471	0.91650824	0.52284991
6	0.74073716	0.97162054	1.00876877
7	0.33124702		
8	0.84281697		
9	0.53148674		
10	0.9358303		
11	1.0108165		
12			
X	0.787299212	1.281978937	0.791908793
SD	0.283694088	0.634037675	0.289452945

1-Way ANOVA: Phosphorylated/Total-HRI Protein Expression (A.U)	
P value	0.3797
P value summary	ns
Signifcantly different (P>0.05?)	No

Table 3D. Total-eIF2α Protein Expression.

	Total-eIF2α Protein Expression (A.U)		
N	Con	Stim	Stim+Rec
1	2.01109371	1.47469581	0.84107525
2	1.5755305	0.93478042	0.59975707
3	2.81836916	2.41848849	0.58633636
4	3.04414907	3.08059682	0.60189686
5	0.86524802	0.25892866	1.00092511
6	0.78145257	0.6821428	0.83739441
7	1.51354137	1.56566706	
8	2.97752633	2.94952402	
9	1.38458202	0.96845457	
10	1.08034618	0.83065491	
11	2.7392243	1.80672587	
12	2.41465599	2.32598224	
13	0.6393995	0.42247489	
14	0.92026236	0.94085387	
15	1.606861	1.10365846	
16	3.40903137	1.72460849	
17	0.74213453	0.76723928	
18	0.76723928	0.6811589	
19	0.80435904	0.89818789	
20	0.6837854	0.6437807	
21	0.7418806	1.01243538	
22	1.09566087	0.77251211	
23	0.96958035		
24	0.84196122		
25	1.174716		
26	1.24626147		
27	0.85982574		
28	0.69881885		
X	1.443124886	1.284706893	0.744564177
SD	0.85269735	0.793266127	0.173211934

1-Way ANOVA: Total-eIF2α Protein Expression (A.U)	
P value	0.1524
P value summary	ns
Signifcantly different (P>0.05?)	No

Table 3E. Phosphorylated-eIF2α Protein Expression.

	Phosphorylated-eIF2α Protein Expression (A.U)		
N	Con	Stim	Stim+Rec
1	0.83311846	0.9572865	1.07964104
2	0.78376141	0.79727836	2.01139859
3	0.65492732	0.85695804	1.04841999
4	0.74306353	0.91740285	1.08680682
5	0.56763308	0.76808235	0.74038451
6	0.57943712	0.58167053	0.89025863
7	0.79841778	0.74855196	
8	0.610971	0.86114684	
9	0.79563126	0.89962141	
10	1.06844184	1.17233836	
11	0.95820262	1.13217867	
12	0.91063836	1.10133789	
13	0.45898285	0.82481409	
14	0.53257369	0.65435784	
15	0.49967945	0.64120705	
16	1.1159263	1.04468364	
17	1.04641982	0.92350543	
18	0.7866718	0.6611159	
19	0.73086981	0.54910137	
20	0.91382238	0.44212113	
21	0.82603297	0.70199792	
22	0.53386223	0.66355701	
23	0.52027467		
24	0.33907305		
25	0.63501636		
26	0.26813875		
27	1.20205311		
28	0.70970967		
X	0.729405382	0.813650688	1.142818263
SD	0.230328403	0.195564865	0.44636549

1-Way ANOVA: Phosphorylated-eIF2α Protein Expression (A.U)	
P value	0.0021
P value summary	**
Signifcantly different (P>0.05?)	Yes

Post-Hoc Test					
Tukey's multiple comparisons test	Mean Diff.	95.00% CI of diff.	Below threshold?	Summary	Adjusted P Value
Con vs. Stim	-0.08425	-0.2539 to 0.08539	No	ns	0.4599
Con vs. Stim+Rec	-0.4134	-0.6813 to -0.1456	Yes	**	0.0014
Stim vs. Stim+Rec	-0.3292	-0.6034 to -0.05494	Yes	*	0.015

Table 3F. Phosphorylated/Total-eIF2α Protein Expression.

	Phosphorylated/Total-eIF2α Protein Expression (A.U)		
N	Con	Stim	Stim+Rec
1	0.41426138	0.64914167	1.28364382
2	0.49745874	0.85290443	3.35368882
3	0.23237812	0.35433621	1.85355521
4	0.24409564	0.61134355	1.74185987
5	0.65603511	0.43669071	0.7397002
6	0.74148725	0.85271081	1.06312942
7	0.52751633	0.47810418	
8	0.20519416	0.97057516	
9	0.57463642	0.92892474	
10	0.90863628	1.41134224	
11	0.34980802	0.62664663	
12	0.37712965	0.47349368	
13	1.33641692	1.95233874	
14	0.57871941	0.6954936	
15	0.31096619	0.58098322	
16	0.3273441	0.60575119	
17	1.41001366	1.20367329	
18	0.93521991	1.0904302	
19	1.11343115	0.85896001	
20	0.48725134		
21	0.53659779		
22	0.40271813		
23	0.54057011		
24	0.21515449		
25	1.39801944		
26	1.01558461		
X	0.628332475	0.822833908	1.672596223
SD	0.37029684	0.388704901	0.92267488

1-Way ANOVA: Phosphorylated/Total-eIF2α Protein Expression (A.U)	
P value	<0.0001
P value summary	****
Signifcantly different (P>0.05?)	Yes

Post-Hoc Test					
Tukey's multiple comparisons test	Mean Diff.	95.00% CI of diff.	Below threshold?	Summary	Adjusted P Value
Con vs. Stim	-0.1945	-0.5343 to 0.1453	No	ns	0.3571
Con vs. Stim+Rec	-1.044	-1.554 to -0.5343	Yes	****	<0.0001
Stim vs. Stim+Rec	-0.8498	-1.377 to -0.3225	Yes	***	0.0009

Table 4A. ATF4 Protein Expression.

	ATF4 Protein Expression (A.U)		
N	Con	Stim	Stim+Rec
1	1.033169	0.386997	0.513391
2	0.070414	0.505202	0.223049
3	0.262576	0.190774	0.093593
4	0.282639	0.826914	0.17292
5	0.741664	0.19178	0.087893
6	0.29724	0.250798	0.360076
7	0.31583	0.291773	
8	0.613672	0.268906	
9	0.378443	0.159062	
10	0.252206	0.262121	
11	0.311408	0.098359	
12	0.352965	0.698949	
13	0.768499	0.737934	
14	0.912083	0.486076	
15	0.838162	0.5399	
16	0.932536	0.564356	
17	0.88946	0.403214	
18	0.24617	0.460743	
19	0.429794	0.182865	
20	0.501901	0.710411	
21	1.214864	0.321291	
22	0.174708	0.712497	
23	0.610994	0.432735	
24	0.375576	0.570376	
25	0.492116	0.221179	
26	0.112051	0.505239	
27	0.395662	0.697156	
28	0.664777	0.19413	
29	0.507291	0.354694	
30	0.609859	0.631619	
31	0.962788	0.221294	
32	0.472266	0.816822	
33	1.107777	0.91629	
34	1.033169	0.619119	
35	0.485222	1.06458	
36	0.47078	1.778236	
37	0.208308	0.664225	
38	1.235247	1.244832	
39	0.072455		
40	1.213127		
41	0.806436		
42	0.066589		
43	1.47517		
44	0.33261		
X	0.580243	0.531143	0.24182
SD	0.361715	0.339293	0.166433

1-Way ANOVA: ATF4 Protein Expression (A.U)	
P value	0.0824
P value summary	ns
Signifcantly different (P>0.05?	No

Table 4B. CHOP Protein Expression.

	CHOP Protein Expression (A.U)		
N	Con	Stim	Stim+Rec
1	0.336756	0.524724	0.761727
2	0.206108	2.199161	0.235977
3	0.620458	1.243433	0.2265
4	0.116391	0.280663	0.336946
5	1.176247	1.041893	0.274261
6	0.219462	0.556235	0.185846
7	0.220284	0.639853	
8	0.531016	1.236092	
9	0.236074	0.306105	
10	2.247023	1.844686	
11	0.257617	0.303462	
12	0.315449	0.562817	
13	0.935873	1.339548	
14	0.485593	1.201425	
15	0.263446	0.332122	
16	0.733145	1.005222	
17	0.594544	1.201207	
18	1.772476	2.221646	
19	0.376112	0.672127	
20	0.354156	0.564437	
21	0.780132	1.020228	
22	0.393646	0.758996	
23	0.207147	0.635664	
24	0.273687	0.360081	
25	0.556825	0.212808	
26	0.53578	0.840845	
27	0.169088	0.334499	
28	0.348575	0.296297	
29	0.529235	0.973796	
30	0.120369	0.440599	
31	0.57627	1.152918	
32	0.600277	1.287917	
33	0.96409	0.96267	
34	0.799864	0.597019	
35	0.436415	0.842611	
36	0.248341	1.117783	
37	1.842815	1.832043	
38	0.171261	0.949587	
39	0.998504		
40	0.161868		
41	1.400602		
42	0.188627		
43	0.996207		
44	0.321916		
X	0.582267	0.891927	0.336876
SD	0.485348	0.519491	0.214286

1-Way ANOVA: CHOP Protein Expression (A.U)	
P value	0.0042
P value summary	**
Signifcantly different (P>0.05?	Yes

Post-Hoc Test					
Tukey's multiple comparisons test	Mean Diff.	95.00% CI of diff.	Below threshold?	Summary	Adjusted P Value
Con vs. Stim	-0.3097	-0.5681 to -0.05121	Yes	*	0.0147
Con vs. Stim+Rec	0.2454	-0.2625 to 0.7533	No	ns	0.4847
Stim vs. Stim+Rec	0.5551	0.04238 to 1.068	Yes	*	0.0306

Table 4C. ATF5 Protein Expression.

	ATF5 Protein Expression (A.U)		
N	Con	Stim	Stim+Rec
1	1.232385	1.147011	0.88625
2	0.450053	2.961462	0.793596
3	0.881497	0.989669	1.348067
4	1.412139	1.334433	1.553769
5	1.669183	1.414003	0.987514
6	1.410501	1.156918	0.689439
7	1.340185	1.48508	
8	1.561423	1.388297	
9	1.181336	0.831434	
10	2.502043	2.279043	
11	0.946015	1.099994	
12	1.072074	1.114712	
13	1.192784	1.216744	
14	1.000156	1.384777	
15	1.130168	1.090667	
16	1.115492	1.207166	
17	0.891494	0.933364	
18	2.664924	2.411034	
19	0.97677	0.896392	
20	1.199745	1.262603	
21	0.939882	1.246307	
22	0.968468	1.057617	
23	1.313463	1.271594	
24	1.12784	1.08007	
25	0.841206	0.910357	
26	2.289246	2.302155	
27	0.890893	0.955226	
28	0.912114	1.061874	
29	0.847527	0.897317	
30	1.098278	1.166136	
31	0.943519	0.884426	
32	1.031949	1.24319	
33	1.088729	1.054109	
34	0.933117	0.86642	
35	0.788675	1.321068	
36	0.954129	1.642138	
37	1.820251	1.007415	
38	1.057794	0.852533	
39	1.319422		
40	1.209081		
41	1.328107		
42	1.080658		
43	1.085548		
44	0.689439		
X	1.190675	1.274336	1.043106
SD	0.435059	0.471749	0.337286

1-Way ANOVA: ATF5 Protein Expression (A.U)	
P value	0.4331
P value summary	ns
Signifcantly different (P>0.05?)	No

Table 5A. Phosphorylated/Total-JNK Protein Expression.

	Phosphorylated/Total-JNK Protein Expression (A.U)		
N	Con	Stim	Stim+Rec
1	0.04718777	1.3756579	0.45531627
2	0.04617908	1.19239952	0.34742457
3	0.18495586	1.00951731	0.28963093
4	0.03564866	0.69695425	1.07361829
5	0.34742457	1.38928822	0.35602
6	0.03759249		0.02080123
7	0.06345848		
8	0.00026683		
9	0.02247918		
10	0.04805733		
11	0.00181836		
12	0.00982413		
X	0.070407728	1.13276344	0.423801882
SD	0.099731653	0.288737944	0.350455066

1-Way ANOVA: Phosphorylated/Total-JNK Protein Expression (A.U)	
P value	<0.0001
P value summary	****
Signifcantly different (P>0.05?)	Yes

Post-Hoc Test					
Tukey's multiple comparisons test	Mean Diff.	95.00% CI of diff.	Below threshold?	Summary	Adjusted P Value
Con vs. Stim	-1.062	-1.372 to -0.7528	Yes	****	<0.0001
Con vs. Stim+Rec	-0.3534	-0.6442 to -0.06259	Yes	*	0.0158
Stim vs. Stim+Rec	0.709	0.3568 to 1.061	Yes	***	0.0002

Table 5B. Phosphorylated/Total-CaMKIIα Protein Expression.

	Phosphorylated/Total-CaMKIIα Protein Expression (A.U)		
N	Con	Stim	Stim+Rec
1	0.27928807	0.77180132	0.35483035
2	0.31850441	1.83009016	0.3793577
3	0.23101719	1.42454925	0.1108793
4	0.19840133	1.38035209	0.30863786
5	0.05003182	0.5048965	0.44167232
6	0.1904652	1.17311279	0.35862565
7	0.21283528		
8	0.22628555		
9	0.11454028		
10	0.20942889		
11	0.1120322		
12	0.22601878		
X	0.197404083	1.180800352	0.325667197
SD	0.074136404	0.478538818	0.113754514

1-Way ANOVA: Phosphorylated/Total-CaMKIIα Protein Expression (A.U)	
P value	<0.0001
P value summary	****
Signifcantly different (P>0.05?)	Yes

Post-Hoc Test					
Tukey's multiple comparisons test	Mean Diff.	95.00% CI of diff.	Below threshold?	Summary	Adjusted P Value
Con vs. Stim	-0.9834	-1.293 to -0.6734	Yes	****	<0.0001
Con vs. Stim+Rec	-0.1283	-0.4382 to 0.1817	No	ns	0.5588
Stim vs. Stim+Rec	0.8551	0.4972 to 1.213	Yes	****	<0.0001

Table 5C. Phosphorylated/Total-p-38 MAPK Protein Expression.

	Phosphorylated/Total-p-38 MAPK Protein Expression (A.U)		
N	Con	Stim	Stim+Rec
1	0.64782573	0.63457039	1.14797087
2	0.76938199	1.11094751	0.65539835
3	1.18922477	1.12449657	0.93070591
4	0.8433225	0.920947	0.25380309
5	0.83860047	2.0877492	0.73814233
6	0.48191535	1.5128365	1.20695259
7	1.0868209		
8	0.13496729		
9	1.5861768		
10	0.15453306		
11	1.08765583		
12	1.23672512		
X	0.838095818	1.231924528	0.82216219
SD	0.436455824	0.50814616	0.353241637

1-Way ANOVA: Phosphorylated/Total-p-38 MAPK Protein Expression (A.U)	
P value	0.1774
P value summary	ns
Signifcantly different (P>0.05?)	No

Table 5D. Phosphorylated/Total-AMPKα Protein Expression.

	Phosphorylated/Total-AMPKα Protein Expression (A.U)		
N	Con	Stim	Stim+Rec
1	0.76727528	0.75243142	0.33367015
2	0.50376361	0.95858854	1.01323662
3	0.52547855	0.21507219	0.58129181
4	0.83668127	0.87572163	1.07319877
5	0.25196532	1.31464099	1.01780517
6	0.34234458	0.63405884	1.25395363
7	0.25955138		
8	0.29289795		
9	1.10100124		
10	0.9213656		
11	1.30091502		
X	0.645749073	0.791752268	0.878859358
SD	0.363191757	0.365313857	0.34687301

1-Way ANOVA: Phosphorylated/Total-AMPKα Protein Expression (A.U)	
P value	0.4284
P value summary	ns
Signifcantly different (P>0.05?)	No

Table 6. ATF4 Protein Expression in the Nucleus and Cytosol.

	ATF4 Protein Expression (A.U)			
	Con		Stimulated	
N	Nuc	Cyto	Nuc	Cyto
1	2.88382745	2.45800622	3.69251326	2.68542549
2	0.43565798	2.5379969	4.58111003	2.11264686
3	0.42778818	1.42558017	1.87106153	2.3093576
4	2.67624299	1.59864084	3.7271671	3.25156949
5	0.3988755	1.96156554	0.74868808	2.6214913
6	0.58476783	2.26685035	2.11099425	1.29663244
7		0.57179455	0.81612659	0.7517029
8		0.90807631		
X	1.234526655	1.71606386	2.506808691	2.146975154
SD	1.200687854	0.722105482	1.51151875	0.859518942

2-Way ANOVA: ATF4 Protein Expression (Nuc/Cyto)			
Source of Variation	P value	P value summary	Significant?
Interaction	0.3238	ns	No
Stim	0.05	*	Yes
Nuc vs. Cyto	0.8854	ns	No

Post-Hoc Test					
Tukey's multiple comparisons test	Mean Diff.	95.00% CI of diff.	Below threshold?	Summary	Adjusted P Value
Con:Nuc vs. Con:Cyto	-0.4815	-2.119 to 1.156	No	ns	0.8486
Con:Nuc vs. Stim :Nuc	-1.272	-2.959 to 0.4148	No	ns	0.1881
Con:Nuc vs. Stim :Cyto	-0.9124	-2.599 to 0.7746	No	ns	0.4576
Con:Cyto vs. Stim :Nuc	-0.7907	-2.360 to 0.7786	No	ns	0.5175
Con:Cyto vs. Stim :Cyto	-0.4309	-2.000 to 1.138	No	ns	0.8726
Stim :Nuc vs. Stim :Cyto	0.3598	-1.261 to 1.981	No	ns	0.9271

Table 7A. ATF4 mRNA Expression in Control and Stimulated Samples.

	ATF4 mRNA Expression (2^-ΔCt)	
N	Con	Stim
1	0.1478995	0.436847
2	0.084306	0.220433
3	0.075039	0.27161
4	0.068476	0.251534
5	0.066144	0.122364
6	0.061087	0.239021
7	0.066636	0.2134
8	0.078624	0.163046
9	0.082139	0.272952
10	0.084829	0.239021
11	0.092612	0.2134
12	0.077519	0.163046
13	0.096732	0.272952
14	0.084829	0.08454
15	0.092612	0.11167
16	0.077519	0.223005
17	0.096732	0.036359
18	0.084829	0.125796
19	0.092612	0.071268
20	0.077519	0.259645
21	0.096732	0.239021
22	0.084829	0.2134
23	0.092612	0.163046
24	0.077519	0.272952
25	0.096732	0.239021
26	0.046	0.2134
27	0.365	0.163046
28		0.272952
29		0.065
30		0.569
31		0.495
32		0.546
33		0.603
34		0.617
35		0.603
36		0.617
X	0.094374759	0.274548528
SD	0.056906445	0.170009611

Unpaired T-test: ATF4 mRNA Expression (2^-ΔCt)	
P value	<0.0001
P value summary	****
Signifcantly different (P>0.05?)	Yes

Table 7B. ATF4-Protmoter Luciferase Construct Activity.

	ATF4 Promoter Luciferase Activity (RLU)	
N	Con	Stim
1	0.948935	1.213509
2	0.88109	0.449434
3	0.158333	0.412333
4	1.2015	0.54
5	0.257	1.7777
6	0.983	0.2806
7	0.432	0.346333
8	0.14	0.4
9	0.754667	0.340333
X	0.639613889	0.640026889
SD	0.3986853	0.510420231

Unpaired T-test: ATF4 Promoter Luciferase Activity (RLU)	
P value	0.9985
P value summary	ns
Signifcantly different (P>0.05?)	No

Table 7C. GAPDH mRNA Stability (*in vitro* cell-free assessment).

	GAPDH mRNA Expression (2^-ΔCt) FC Stability							
	Con				Stim			
Incubation Length (Min)	t=0	30	60	90	t=0	30	60	90
N								
1	6.317235018	4.473741594	3.37938711	0.622	6.317235018	5.348580835	3.524270619	3.113558056
2	0.657527906	0.613435455	0.37634993	0.330533923	0.657527906	0.644206842	0.403042937	0.39123291
3	0.761067259	0.590343468	0.4407032	0.454940135	0.761067259	0.630399692	0.459715874	0.562671551

	GAPDH mRNA Expression (% of t=0)							
	Con				Stim			
Incubation Length (Min)	t=0	30	60	90	t=0	30	60	90
N								
1	100	78.8180332	59.4947188	59.2867219	100	84.6664849	55.7881828	64.3003648
2	100	93.2942084	57.237104	50.2691855	100	97.9740687	61.2967045	59.5005788
3	100	77.5678445	57.9059463	59.7766006	100	82.8310094	61.6017163	73.9319087
X		83.22669537	58.2125897	56.44416933		88.490521	59.5622012	65.91095077
SD		8.741101587	1.15962441	5.353299384		8.264109166	3.271951896	7.349238807

	GAPDH:Non-Linear (Line of best fit) Regression Analysis	
Best-Fit values	Con	Stim
y-intercept	2	2
Slope	-0.003129	-0.002518
R-squared	0.8991	0.7655

Table 7D. ATF4 mRNA Stability (*in vitro* cell-free assessment).

	ATF4 mRNA Expression (2^-ΔCt) FC Stability							
	Con				Stim			
Incubation Length (Min)	t=0	30	60	90	t=0	30	60	90
N								
1	1.750	1.225	0.881	0.622	1.750	1.485	0.931	0.615
2	0.027254245	0.015517858	0.00352773	0.002467502	0.027254245	0.019474126	0.008634208	0.00327053
3	0.034683598	0.020824628	0.01612692	0.008361114	0.034683598	0.028003948	0.016844533	0.013583944

	ATF4 mRNA Expression (% of t=0)							
	Con				Stim			
Incubation Length (Min)	t=0	30	60	90	t=0	30	60	90
N								
1	100	69.985892	50.3212669	35.5299777	100	84.8597376	53.1604653	35.1245573
2	100	56.9373993	12.9437648	9.05364293	100	71.4535498	31.6802314	12.0000754
3	100	60.0417167	46.4972385	24.1068254	100	80.7411861	48.5662798	39.1653244
X		62.32166933	36.5874234	22.89681534		79.01815783	44.46899217	28.76331903
SD		6.816482116	20.5650855	13.27957714		6.867174647	11.31109794	14.65730884

2-Way ANOVA: ATF4 mRNA Expression (% of t=0)			
Source of Variation	P value	P value summary	Significant?
Time	<0.0001	****	Yes
Stim	0.0437	*	Yes
Time vs. Stim	0.1043	ns	No

Post-Hoc Test					
Tukey's multiple comparisons test	Mean Diff.	95.00% CI of diff.	Below threshold?	Summary	Adjusted P Value
0:Con vs. 0:Stim	0	-16.72 to 16.72	No	ns	>0.9999
0:Con vs. 30:Con	37.68	20.96 to 54.40	Yes	***	0.0008
0:Con vs. 30:Stim	20.98	4.264 to 37.70	Yes	*	0.0176
0:Con vs. 60:Con	63.41	46.69 to 80.13	Yes	****	<0.0001
0:Con vs. 60:Stim	55.53	38.81 to 72.25	Yes	****	<0.0001
0:Con vs. 90:Con	77.1	60.39 to 93.82	Yes	****	<0.0001
0:Con vs. 90:Stim	71.24	54.52 to 87.95	Yes	****	<0.0001
0:Stim vs. 30:Con	37.68	20.96 to 54.40	Yes	***	0.0008
0:Stim vs. 30:Stim	20.98	4.264 to 37.70	Yes	*	0.0176
0:Stim vs. 60:Con	63.41	46.69 to 80.13	Yes	****	<0.0001
0:Stim vs. 60:Stim	55.53	38.81 to 72.25	Yes	****	<0.0001
0:Stim vs. 90:Con	77.1	60.39 to 93.82	Yes	****	<0.0001
0:Stim vs. 90:Stim	71.24	54.52 to 87.95	Yes	****	<0.0001
30:Con vs. 30:Stim	-16.7	-33.41 to 0.02159	No	ns	0.0503
30:Con vs. 60:Con	25.73	9.016 to 42.45	Yes	**	0.0063
30:Con vs. 60:Stim	17.85	1.135 to 34.57	Yes	*	0.0374
30:Con vs. 90:Con	39.42	22.71 to 56.14	Yes	***	0.0006
30:Con vs. 90:Stim	33.56	16.84 to 50.28	Yes	**	0.0015
30:Stim vs. 60:Con	42.43	25.71 to 59.15	Yes	***	0.0004
30:Stim vs. 60:Stim	34.55	17.83 to 51.27	Yes	**	0.0013
30:Stim vs. 90:Con	56.12	39.40 to 72.84	Yes	****	<0.0001
30:Stim vs. 90:Stim	50.25	33.54 to 66.97	Yes	***	0.0002
60:Con vs. 60:Stim	-7.882	-24.60 to 8.837	No	ns	0.5251
60:Con vs. 90:Con	13.69	-3.027 to 30.41	No	ns	0.1122
60:Con vs. 90:Stim	7.824	-8.894 to 24.54	No	ns	0.5321
60:Stim vs. 90:Con	21.57	4.854 to 38.29	Yes	*	0.0154
60:Stim vs. 90:Stim	15.71	-1.012 to 32.42	No	ns	0.0652
90:Con vs. 90:Stim	-5.867	-22.58 to 10.85	No	ns	0.7782

	ATF4:Non-Linear (Line of best fit) Regression Analysis	
Best-Fit values	Con	Stim
y-intercept	2.001	2.015
Slope	-0.007132	-0.005636
R-squared	0.8885	0.8905

Table 7E. ATF4 mRNA Transcript Half-Life (*in vitro* cell-free assessment).

	ATF4:Non-Linear Decay Regression Analysis			
	Con		Stim	
N	Decay (k)	Half-life	Decay (k)	Half-life
1	0.01228	56.45	0.0005804	119.42
2	0.01836	37.76	0.004412	157.1
3	0.01434	48.32	0.006567	105.5
X	0.014993333	47.51	0.00385313	127.34
SD	0.003092205	9.371291266	0.00303218	26.69615703

Unpaired T-test: ATF4 mRNA Half-life	
P value	0.0082
P value summary	**
Signifcantly different (P>0.05?)	Yes

APPENDIX B: ADDITIONAL DATA
(STATISTIC TABLES NOT SHOWN)

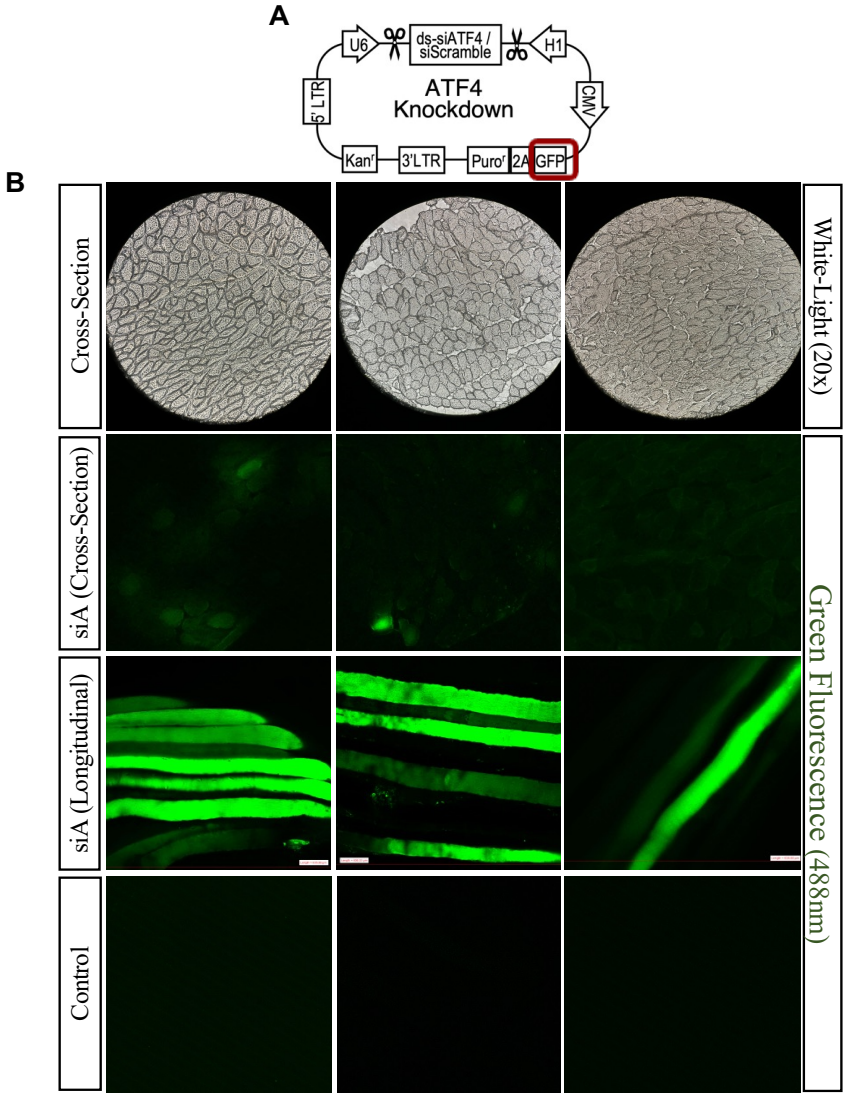

Supplementary Figure 1: *In vivo* knockdown of ATF4 in the Gastrocnemius muscle of mice using a siRNA vector DNA via electroporation. Briefly, a lentivector siRNA plasmid was amplified and isolated, as described in the Methods section. An injection containing 50μg of the plasmid in 0.9% saline was administered to the right hindlimb gastrocnemius, and was subsequently electroporated, as previously described. The left hindlimb gastrocnemius served as a control and received an injection only containing saline. Following 7 days of gene/plasmid amplification, both gastrocnemius muscles were excised and sectioned accordingly for experimentation, which included confocal microcopy (to evaluate plasmid uptake and expression into the muscle, confirmed via exogenous GFP presence/fluorescence), western blotting, and qPCR to evaluate the expression of ATF4 and downstream targets. **A)** Schematic of the ATF4 siRNA (Knockdown plasmid) used, which contains the GFP reporter-gene (exogenous expression detectable via fluorescence). **B)** Following 7 days of gene amplification, a small portion of the gastrocnemius muscle from both hindlimbs (Control and siA injected) was isolated and use immediately to be imaged with confocal microscopy (20x magnification, Green Fluorescent Laser). Both longitudinal and Cross-Sections of the muscle were imaged to observe the exogenous GFP expression. Representative white light imaging of the Cross-Sectional portion of the gastrocnemius is shown (not to scale). Control legs were imaged to evaluate endogenous GFP expression.

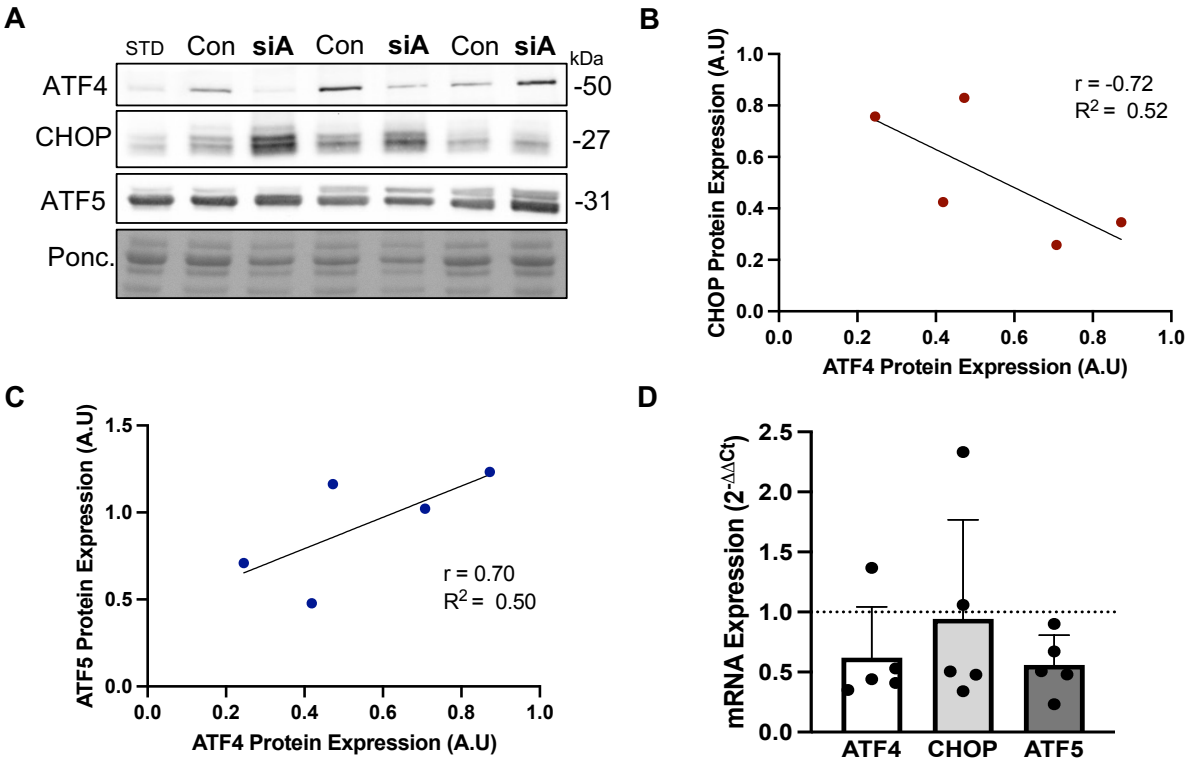

Supplementary Figure 2: Evaluation of the *in vivo* knockdown of ATF4 via a siRNA vector DNA plasmid in the Gastrocnemius muscle of mice. A) Representative immunoblots of ATF4, CHOP and ATF5 with the corresponding Ponceau (loading control). **B), C)** Quantification of ATF4, CHOP and ATF5 expressed as a correlation (relative to ATF4 protein expression) using linear regression and correlational analyses. **D)** mRNA expression of ATF4, CHOP and ATF5 in siA injected samples. mRNA levels are indicated as fold changes using the $2^{-\Delta\Delta Ct}$ values. Con, Control; siA, siRNA vector DNA against ATF4. Data are means ± SD.

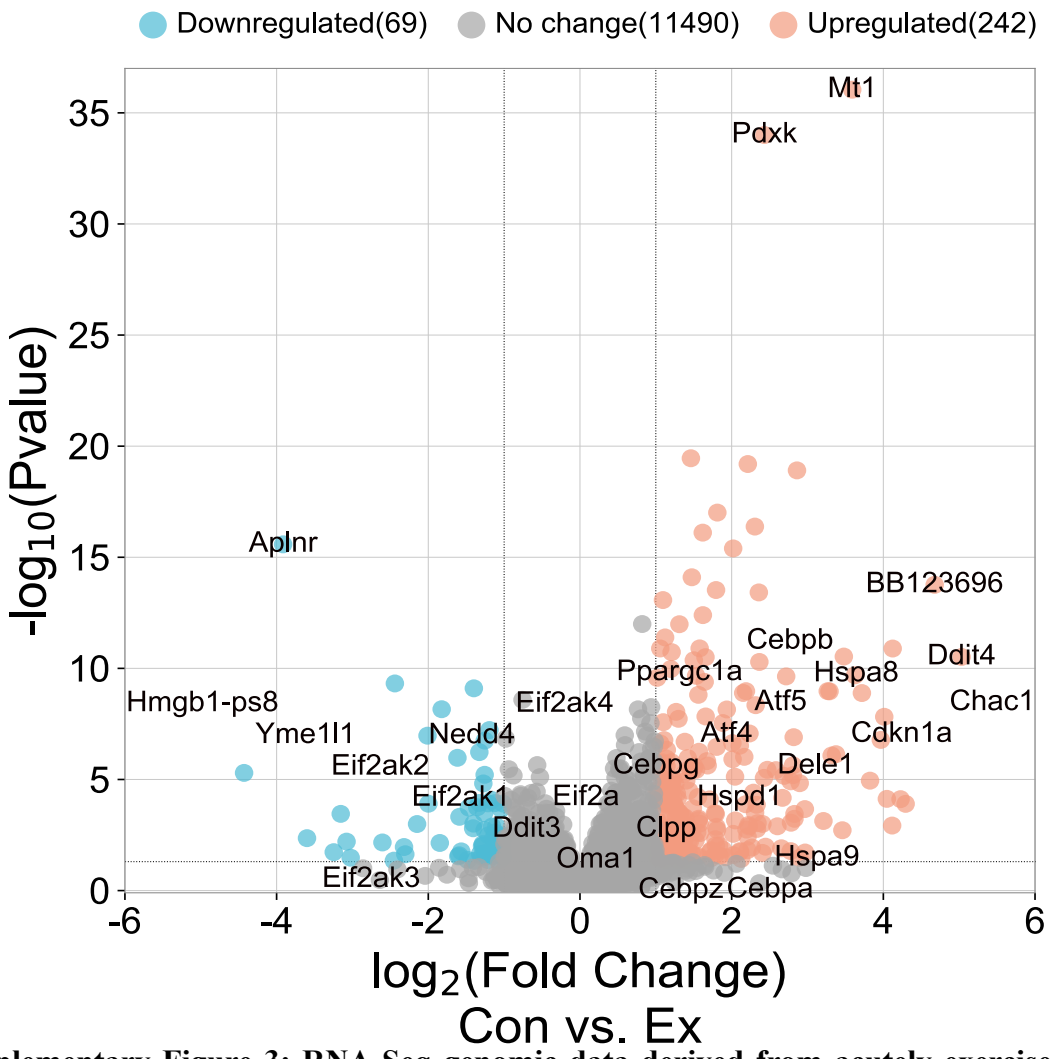

Supplementary Figure 3: RNA-Seq genomic data derived from acutely exercised Wild-Type mice. Total RNA from Wild-Type acutely exercise mice was isolated and used for RNA library preparation, sequencing, and pathway analysis were performed by the Toronto Centre for Applied Genomics (The Hospital for Sick Children). Exercised animals ran at a pace of 15 m/min for 60 min, followed by 18 m/min for 30 min (90 min total). Total RNA samples were processed at TCAG, accordingly. Briefly, NEBNext Ultra II Directional RNA libraries using poly-A selection were prepared. All 6 samples (three WT control and three WT Ex) were multiplexed on one lane of an SP flow cell and sequenced (paired end reads) on the Illumina NovaSeq 6000. Prior to performing RNA-Seq, the resulting DNA-free RNA samples were analyzed for quality on a 2100 Bioanalyzer System (Agilent Technologies). Differential gene expression analysis was performed with DESeq2 (version 1.26.0s; using R, version 3.6.1). Volcano plot of DESeq2 RNA-Seq data showing differential expression of all examined genes. The data are expressed as log2 fold change comparing control and acutely exercised (Ex) mice (enhanced gene expression, *red*; reduced gene abundance, *blue*; no change in gene expression, *white*; $P<0.05$). Genes of interest, related to ISR signaling and activation, and the most up- or down- regulated, were specifically identified illustrating their relative position on the plot.

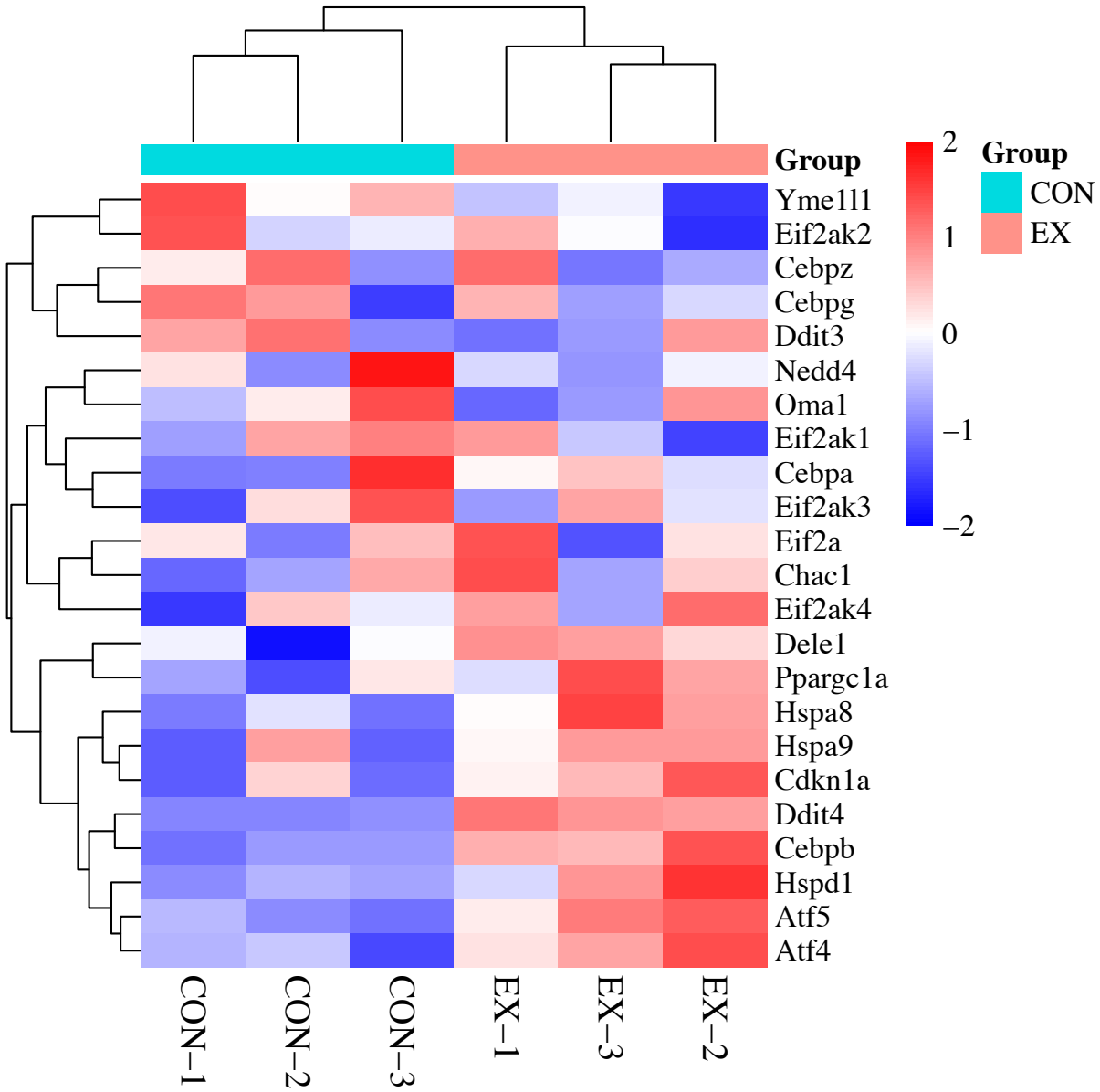

Supplementary Figure 4: Differential expression of select genes related to ISR activation and signaling in acutely exercise samples. Heat map of DESeq2 RNA-Seq data of specific ISR related genes showing the effect of an acute whole-body exercise protocol on relative differential gene expression. The data are expressed as log2 fold change comparing the acutely exercised samples with controls (n=3/group) (enhanced gene expression, *red*; reduced gene abundance, *blue*; no change in gene expression, *white*; P< 0.05).

APPENDIX C: LABORATORY METHODS AND PROTOCOLS

ISOLATING WHOLE MUSCLE PROTEIN EXTRACTS

Reagents:

1. Muscle Extraction Buffer (Sakamoto et al., JBC 277:11910, 2002)
    a. 20mM Hepes (ph 7.4) 2.383g/500ml
    b. 2mM EGTA 0.3804g/500ml
    c. 1% Trition-X100 5ml/500ml
    d. 50% Glycerol 10ml/500ml
    e. 50mM β-Glycerophosphate 5.4g/500ml

Volume up to 500ml with double distilled water (ddH_2O) pH to 7.4

2. Make extraction buffer with protease and phosphatase inhibitors:

In a 15ml tube, mix the following at the appropriate ratio as outlined below and keep on ice:

    a. 1 ml Sakamoto Muscle Extraction Buffer
    b. 10 ul Protease Inhibitor Stock (1 tablet in 500uL ddH_2O)
    c. 10 ul Cocktail 2 Phosphatase Inhibitor
    d. 10 ul Cocktail 3 Phosphatase Inhibitor

Procedure:

1. Add 100µl of Sakamoto Muscle Extraction Buffer to a set of Eppendorf tubes.
2. Weigh out 15-20mg of tissue into the first set of Eppendorf tubes and record the exact weight of each sample in a table.
3. Add the appropriate volume of buffer solution to each Eppendorf to produce 10x volume.
4. Insert a metal bead into each Eppendorf.
5. Place Eppendorfs in balanced manner in metal brackets (kept in freezer)
6. Insert brackets into TissueLyser and homogenize (shake) at 30 Hz for 1 min at a time.
7. Remove blocks, check for homogeneity and repeat if necessary (flip orientation of blocks for each cycle)
8. Remove beads with magnet and centrifuge at 14,000g for 10 minutes at 4°C.
9. Completely withdraw the supernatant and pipette the solution into the new pre-labeled Eppendorf tubes.
10. Store at -80°C

WESTERN/IMMUNOBLOTTING

SDS Polyacrylamide Gel Electrophoresis (SDS-PAGE) Protean Biorad System

Reagents:

1. Acrylamide/Bis-Acrylamide, 30% Solution 37.5:1 (BioShop 10.502)
    a. Store at 4°C
2. Under Tris Buffer
    a. 1M Tris, pH 8.8 (60.5g/500ml)
    b. Store at 4°C
3. Over Tris Buffer
    a. 1M Tris, pH 6.8 (12.1g/100ml)
    b. Bromophenol Blue (for colour)

c. Store at 4°C

4. Ammonium Persulfate (APS)
    a. 10% (w/v) APS in ddH_20 (1g/10ml)
    b. Stored at 4°C
5. Sodium Dodecyl Sulfate (SDS)
    a. 10% (w/v) in ddH_20 (1g/10ml)
    b. Store at room temperature
6. TEMED (Sigma T-9281)
7. Electrophoresis Buffer, pH 8.3 (10L)
    a. 25mM Tris 30.34g, 192mM Glycine 144g, 0.1% SDS 10g
    b. Volume to 10L with ddH_20
    c. Store at room temperature
8. 6X SDS
    a. Warm 100% glycerol in water bath at 65°C for 30 minutes.
    b. Combine 1.2g SDS, 0.06g Bromophenol Blue, 3mls of 1M Tris, pH 6.8 and 1ml of ddH_20 and stir at 4°C for 5 minutes.
    c. Add 3mls of 100% glycerol, stir and aliquot mixture.
    d. Store at -20°C
    e. Add 5% (v/v) ß-mercaptoethanol (Sigma M6250) to 6X SDS <u>just prior</u> to use.
9. *tetra*-Amyl alcohol ReagentPlus, 99% (Sigma 152463)

Procedure:

1. Prepare electrophoresis rack:
    a. Clean glass plates thoroughly with soap followed by 95% ethanol then ddH_20.
    b. Dry carefully with a kimwipe.
    c. Assemble glass plates as shown:
    d. Check the seal by adding a small volume of ddH_20 then pour off and let dry.

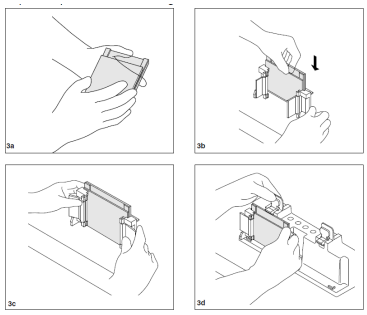

2. Prepare separating gels:
    a. Mini Protean 3 Bio-Rad System volumes:

	8%	**10%**	**12%**	**15%**	**18%**
Acrylamide	2.7 ml	3.3 ml	4.0 ml	5.0 ml	6.0 ml
ddH_20	4.1 ml	3.5 ml	2.8 ml	1.8 ml	0.8 ml
Under Tris	3.0 ml	3.0 ml	3.0 ml	3.0 ml	3.0 ml
SDS	100µl	100µl	100µl	100µl	100µl
APS	100µl	100µl	100µl	100µl	100µl
TEMED	10µl	10µl	10µl	10µl	10µl

    b. Mix the contents of the separating gel without adding APS or TEMED. Stir.
    c. Add APS and TEMED. Stir.
    d. Slowly pour the entire volume of the solution into the space between the two plates while keeping plates tilted to prevent bubble formation.
    e. Add *tert*-Amyl alcohol to coat top surface of gel solution.

f. Allow 30 minutes for gel polymerization.
g. Remove *tert*-Amyl alcohol by pouring it off and remove any remainder with a kimwipe. Rinse with ddH_20.

3. Prepare stacking gel:
   a. For a single mini gel use the following volumes:
   b. Add the contents of the stacking gel without adding APS or TEMED. Stir.
   c. Add APS and TEMED. Stir.
   d. Using a Pasteur pipette slowly add the entire volume from the beaker in between the plates.
   e. Add comb for desired number of wells.
   f. Allow 30 minutes for gel polymerization.

Acrylamide	500 µl
Over Tris	625 µl
ddH_20	3.75 ml
SDS	50 µl
APS	50 µl
TEMED	7.5 µl

4. Prepare samples:
   a. Turn on the block heater to 95ºC.
   b. Pipette required volume of sample into new Eppendorf with same amount of lysis buffer and 5 µl of sample dye. Keep samples on ice until all samples are prepared (use pipette plan).
   c. Briefly spin each sample to bring volume to the bottom of the Eppendorf.
   d. Incubate each sample at 95 ºC for 5 minutes in the heating block to denature the proteins.
   e. Briefly spin again to return volume to the bottom of the Eppendorf.

5. Assemble Mini-PROTEAN gel caster system:
   a. See images.
   b. If you are only running one gel a plastic rectangular pseudo plate must be clamped on the other side of the caster.
   c. Fill with electrophoresis buffer between the plates and outside of the plates in the chamber.
   d. Slowly remove the comb using both hands (one on each side) by pulling the comb straight upwards.
   e. Fix any wells that are deformed using a small spatula.
   f. Clean out the wells using a syringe filled with electrophoresis buffer.
   g. Withdraw the entire volume of the sample using a pipette. Dispense volume slowly into the bottom of the well.

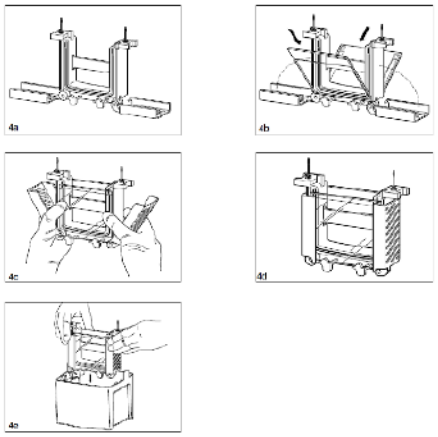

6. Gel electrophoresis
   a. Immediately after all samples are loaded place the lid on the gel chamber.
   b. Place positive and negative plugs into the power supply and turn on power supply.
   c. Set power supply to 120V. Gel will run for ~2 hours depending on percent gel made.

d. When the bromophenol blue has run off the bottom of the gel (or when gel has separated the desire amount) turn off the power supply. Remove plugs from power supply and remove lid.
e. Prepare for electrotransfer of proteins from the gel to nitrocellulose membrane.

Western Blotting Transfer and Immunodetection

Reagents:

1. Transfer Buffer
    a. 0.025M Tris-HCl pH 8.3 (12.14g)
    b. 0.15M Glycine (45.05g)
    c. 20% Methanol (800ml)
    d. Volume up to 4L with ddH_20
    e. Store at 4°C
2. Ponceau S stain
    a. 0.1% (w/v) Ponceau S
    b. 0.5% (v/v) Acetic Acid
    c. Store at room temperature
3. Wash Buffer
    a. Tris-HCl pH 7.5 (12g)
    b. NaCl (58.5g)
    c. 0.1% Tween (10ml)
    d. Store at room temperature
4. Blocking Solution
    a. 5% (w/v) skim milk power in wash buffer OR
    b. 5% (w/v) BSA in wash buffer
5. Enhanced Chemiluminescence Fluid (ECL; Santa Cruz sc-2048)

Procedure:

1. Transfer Procedure
    a. Remove electrophoresis plates from chamber and separate the plates.
    b. Cut away unnecessary parts of the gel using a spatula and measure remaining gel size.
    c. Using a paper cutter cut 6 pieces of Whatman paper per gel to the same size as the gel. Wearing gloves cut nitrocellulose membrane (GE Healthcare RPN303D) to the dimensions of the gel.
    d. Assemble Whatman paper, nitrocellulose membrane and gel as shown:
    e. Close the cassette and place in the transfer chamber with the black side of the cassette facing the back side of the chamber.
    f. Place ice pack in the chamber.
    g. Place lid on the chamber and connect the leads to the power supply.
    h. Turn on the power supply and run at 120V for 2 hours. This can vary depending on the size of the protein of interest.

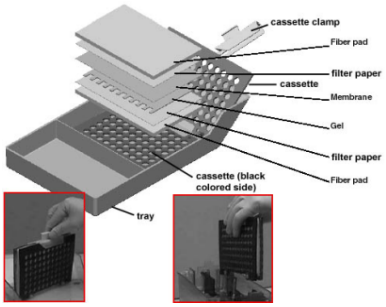

2. Removal of transfer membrane:
    a. Turn off the power supply and disconnect leads from the power supply then remove the lid from the chamber.
    b. Remove the cassette from the chamber.
    c. With gloves on, remove the Whatman paper and gel and place the nitrocellulose membrane in a plastic dish.
    d. Add Ponceau S stain on the membrane and gently swirl.
    e. Drain off the remaining Ponceau S and save for reuse.
    f. Rinse the membrane with ddH_20 to reduce the red background. Wrap membrane in saran wrap and scan image.
    g. Cut the membrane while protein bands are still visible at the desired molecular weight.
    h. Rotate membrane at room temperature in wash buffer until remaining Ponceau S has been removed.
    i. Incubate membrane for 1 hour with rotation in blocking solution.
    j. Incubate membrane with desired antibody diluted in blocking solution overnight at 4ºC. Membrane is placed face up into the solution on a glass plate covered in parafilm. To maintain a moist environment overnight, wet a small kimwipe and form it into a ball and place in each corner of the dish. Cover the dish with saran wrap.

3. Immunodetection
    a. Wash the blots in wash buffer with gentle rotation for 5 minutes 3X.
    b. Incubate the blots for 1 hour in room temperature with the appropriate secondary antibody diluted in blocking solution.
    c. Membrane is placed face up in solution on a glass plate covered with parafilm. Place moist kimwipes in each corner of the dish and cover the dish with saran wrap.
    d. Following the incubation, wash the membrane 3X for 5 minutes with wash buffer.

4. Enhanced Chemiluminescence Detection
    a. Mix ECL fluids “A” and “B” in a 1:1 ratio in a disposable Rohr tube.
    b. Place blots on saran wrap face up and apply ECL solution for 2 minutes.
    c. Dab off excess ECL on a kimwipe and place blots in Imager.
    d. Expose blot (time will vary depending on protein and antibody).

RNA ISOLATION

Reagents:
1. Tri-reagent (Trizol poly-phenol)
2. Chloroform
3. Isopropanol
4. 75% Ethanol (50 mL)
    a. 37.5 mL of Anhydrous Ethanol (-20°C)
    b. 12.5 mL sterile ddH_2O

Important:

1. Dispose test tubes and pipette tips that have come into contact with the tri-reagent in the phenol waste bags under the fume hood.
2. Change gloves frequently and sterilize them with 70% ethanol.
3. Use sterile pipette tips and Eppendorfs.
4. Make sure homogenizer and centrifuge are available for use.

Procedure:

Day 1:

1. In fume hood, pipette 1 mL of Tri-reagent into each pre-labeled 2mL Eppendorf with 1/3rd of the gastrocnemius muscle. Keep on ice.
2. Homogenize muscle in TissueLyser with sterile metal beads at 30 Hz for 1 min, twice, or until fully homogenized.
3. Remove blocks, check for homogeneity and repeat if necessary (flip orientation of blocks for each cycle).
4. Remove beads with magnet and let stand at RT for 5 mins.
5. Add 200μl chloroform to each Eppendorf.
6. Shake vigorously for 15secs under fumehood and observe colour change.
    a. Should look cloudy pink.
7. Let stand at RT for 2-3 mins.
8. Centrifuge at 16,000g for 15 mins at 4°C.
9. Transfer upper aqueous phase (clear) to 1.5mL Eppendorf tubes.
    a. Ensure you do not disturb the other phases (affects RNA purity).
10. Add 500μl isopropanol to each Eppendorf.
11. Shake vigorously for 15secs and store at -20°C overnight.

Day 2:

12. Let stand at room temperature for 10 minutes.
13. Spin at max speed (16,000g) for 10 minutes at 4°C.
14. Discard Supernate by pouring into waste container, remover the remaining volume using a p200.
15. Add 700μL of 75% Ethanol to each sample. Wash by lightly pipetting along the wall to lift the pellet, take extra precaution to NOT resuspend the pellet.
16. Spin at max speed (16,000g) for 10 min at 4°C.
17. Discard Supernate and remove excess liquid with p200 pipette.
18. Carefully leave pellets to air dry for 25-40 minutes.
    a. Place Eppendorfs with their lids open facing upside down on Kim-wipe.
    b. Cover with top with Kim-wipe.
19. Dissolve pellet in 10-30μl st. dd H_2O (dependent on pellet size) by gently pipetting up and down.
20. Measure RNA concentration using the Nano Drop.

MEASURING [RNA] USING THE NANO DROP

Notes: Always sterilize your hands and pipettes with Ethanol and use sterilized pipette tips.

Blank the System

1. Open the Nano Drop 2000 program on the desktop.
2. Click Nucleic Acid.
3. In the top right change:
    i. "Type:" from "DNA" to "RNA"; and
    ii. "Conc:" to "ug/uL" Blank the System
4. Open the Nano Drop lid and add 1 uL of molecular grade sterile H20 to the Close lid carefully.
5. Click Blank (in top left corner).
6. Wait for message "Load your sample and press measure button."
7. Type Blank 1 in "Sample ID:" field.
8. Open the Nano Drop lid and add 1 μL of molecular grade sterile H_2O to the small metal test platform.
    i. Close lid carefully.
9. Click Measure (in the top left corner).
    i. Wait for message "Load your sample and press measure button."
    ii. Take 3-4 measurements.
    iii. Values should be 0.00_ _
10. Clear "Sample ID:" field and type in Blank 2.
11. Open the Nano Drop lid and add 1 μL of molecular grade sterile H20 to the small metal test platform.
12. Click Measure (in the top left corner) and once again take 3 readings.
    i. Values should once again be at 0.00_ _

Measuring Sample Concentrations

13. In the "Sample ID:" field, input the name/description of your first sample.
14. Open Nano Drop lid and add 1 μL of Sample 1 onto the small metal test platform.
15. Click Measure and wait for the reading to appear.
    i. Take 3-4 readings per sample and ensure that readings are within 1/100th of the others.
16. Repeat for all samples. Export Data.
17. In Excel, calculate average of the 3-4 "Nucleic Acid Conc." values for each sample.
18. NOTE: take note of the 260/280 and 260/230 columns. The value should be ~2.00 in each of these columns. Values that are drastically different than 2.00 are considered less pure.

REVERSE TRANSCRIPTION OF CDNA (FIRST STRAND CDNA SYNTHESIS)

Reagents:

1. Master Mix 1 (MM1):
    a. 1ul Oligo(dt) 20
    b. 1ul 10mM dNTP
    c. Keep on ice
2. Master Mix 2 (MM2):
    a. 4ul 5x first-strand buffer
    b. 1ul 0.1M DTT
    c. Keep on ice

3. RNase OUT
    a. Store at -20°C (temperature sensitive)
4. SuperScript III RT
    a. Store at -20°C (temperature sensitive)

Procedure:

1. Place all reagents related to cDNA preparation to thaw on ice, except for the temperature sensitive 'RNase OUT' and 'SuperScript III RT' reagents.
2. Prepare your working cDNA samples (pipette plan) by following the order of sterile water, then your extracted RNA, and finally the correct volume of MM1 and mix well.
3. Keep samples on ice.
4. Use the thermal cycler to initiate the amplification stage of the procedure.
    a. 65°C for 5 mins
5. Let samples stand on ice for 1 min.
6. Add the 5ul of MM2 to each tube and transfer to the thermal cycler.
7. Work with the temperature-sensitive reagents one at a time.
    a. Add 1ul RNase OUT to each Eppendorf.
    b. Add 1ul SuperScript III RT to each Eppendorf.
8. Run the appropriate file in the thermal cycler.
    a. 50°C for 50 mins
    b. 72°C for 20 mins
9. Dilute samples (in new tubes) to a 1:40 concentration.
    a. 1µL cDNA stock
    b. 39µL sterile water
10. Store both stock and working concentrations at -20°C until ready for qPCR.

REAL-TIME QPCR

Reaction settings:

- 25µL reaction volume.
- Initial holding stage (95°C for 10 min).
- Amplification cycles (40x: 60°C for 1 min, 95°C for 15 secs).

DNA INJECTION AND ELECTROPORATION INTO MOUSE HINDLIMB MUSCLE

Materials:

- 29 gauge insulin syringe, ½" needle (Ultrafine, Becton Dickson)
- Forceps (sterile)
- Plasmid DNA: 50µg plasmid of interest + 1µg of pRL-CMV plasmid (use NanoDrop to determine DNA concentration)
- ECM 830 Electroporation system (BTX)
- 0.7cm tweezertrodes (BTX)
- Conductive Gel

DNA preparation:
DNA is prepared to produce plasmids inserted with the promoter of interest (ATF4) upstream of the luciferase gene. The DNA plasmid is stored via stab cultures, in glycerol, at -80°C for long-term storage. DNA was isolated using a MaxiPrep isolation kit (Qiagen, HiSpeed Plasmid Maxi Kit) following the manufacturer's instructions. Transfection efficiency is determined through the co-transfection of the pRL-CMV (renilla luciferase) plasmid, assuming the cells were transfected with the pRL-CMV plasmid.

Injection preparation:
Sample calculation:
[1.5Kb ATF4 + pGL3] = 2.20µg/µl (measured after isolation via NanoDrop)
∴ 50µg of [1.5Kb ATF4 + pGL3] = 50/2.20=22.72µl of plasmid DNA

[pRL-CMV]=1.00µg/µl (stock solution is kept at this concentration, measured via NanoDrop)
∴ 1µg of [pRL-CMV] = 1/1 = 1µl of plasmid DNA

Volume up to 30µl with 0.9% sterile saline or PBS.

22.72ul of plasmid DNA [1.5Kb Tfam+pGL3] + 1µl of plasmid DNA [pRL-CMV] +6.28µl sterile saline/PBS = 30µl to be injected into muscle

Injection procedure:
1. Animals are anesthetized using isoflourane.
2. Set the appropriate parameters on the electroporator (100 V/cm^2, 20ms pulse duration, 200ms interval, 10 pulses, unipolarity).
3. Both hindlimbs near the gastrocnemius muscle are shaved (to remove fur).
4. The injection site is sterilized by applying iodine (Providine solution) and ethanol.
5. A prefilled syringe (containing 50µg of plasmid DNA of the gene of interest, 1µg of plasmid DNA of the control plasmid in a 30µl solution with 0.9% sterile saline) is used for injection into the muscle, with the animal on its back.
6. Insert the needle of the syringe no more than 1-3mm into the muscle, and ensure injection takes place along 3 sites of the muscle.
7. Remove the needle from the muscle very slowly, and observe if there are any leaks from the injection site.
8. Apply conductive gel to the Tweezertrodes, and position them over the skin, and on either side of the muscle in a direction parallel to the muscle fiber orientation.
9. Pulse the muscle (10x) and observe contraction of the muscle.
10. Switch the polarity by reversing the orientation of the electrodes and pulse the muscle again.
11. Repeat steps 5-9 on the contralateral hindlimb.
12. Remove the isoflurane anesthetic and allow the animal to recover for 7 days without any further handling.
13. Perform the *in situ* contractile activity protocol and harvest the gastrocnemius muscle for promoter activity analysis using a luciferase assay.

GASTROCNEMIUS MUSCLE PREPARATION FOR LUCIFERASE ASSAY

Reagents:

- 5X Passive Lysis Buffer
- 1X Passive Lysis Buffer (800µl ddH_2O, 200µl 5X Passive Lysis Buffer)
- ddH_2O

Procedure:

1. Add 200µl of 5X passive lysis buffer (PLB) into 800µl of ddH_2O to dilute 5-fold.
2. Add 150µl of this now diluted 1X PLB into 1.5ml Eppendorfs.
3. Pound a portion of the gastrocnemius muscle at the temperature of liquid nitrogen into a fine powder using a mortar and pestle.
4. Weigh 30mg of this powdered tissue into the 1.5ml Eppendorfs already containing 150µl of 1X PLB to make a 5X dilution of tissue.
5. Mix samples by flicking the Eppendorfs briefly and sonicate samples 3 X 3 seconds on ice.
6. Centrifuge at 16,100g in centrifuge for 10 minutes at 4°C.
7. Retain supernate and transfer them to new 1.5ml Eppendorfs. Use these supernate for a luciferase assay on the same day.

LUCIFERASE ASSAY

Promega "Dual-Luciferase® Reporter Assay System"
Product#E1910
Store at 4°C

Reagents:

- 10ml Luciferase Assay Buffer II (LARII).
- 1 vial Luciferase Assay Substrate (Lyophilized Product).
- 10ml Stop & Glo® Buffer.
- 200µl Stop & Glo® Substrate, 50X.
- 30ml Passive Lysis Buffer, 5X.

Reagent Preparation:

1. 1X PLB: Add 1 volume of 5X Passive Lysis Buffer (PLB) to 4 volumes of distilled water. Mix well.
    a. Store at 4°C (≤1 month).
2. LAR II: Resuspend the lyophilized Luciferase Assay Substrate in Luciferase Assay Buffer II
    a. Store at –20°C (≤1 month) or –70°C (≤1 year).
3. Stop & Glo® Reagent:
    a. To the required amount of Stop & Glo® Buffer, add 50X Stop & Glo® Substrate to a final 1X concentration.
        i. For example, add 20.4ul of 50X Stop & Glo® Substrate to 979.59ul of Stop & Glo® Buffer to make a 1X solution of Stop & Glo® Reagent.)

Measurement of Luciferase activity: (shown beside)

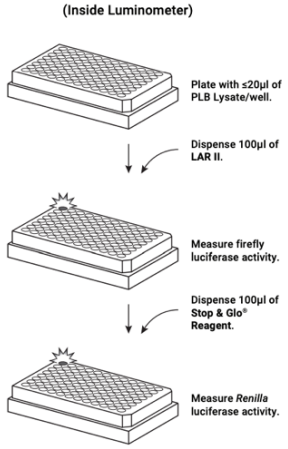

1. Using an opaque white 96-well plate, load 100ul of LARII reagent into required wells.
    a. Samples require triplicate readings; thus, 9-wells must be loaded for background control, control and stimulated samples, respectively.
2. Add 20ul of 1x PLB (background control), control and stimulated samples.
3. READ: measure firefly luciferase activity.
4. immediately add the 1X solution of Stop & Glo® Reagent into the same wells to quench the firefly luciferase activity and initiate renilla luciferase activity.
5. READ: quench and read.
6. Correct firefly Luciferase values to renilla luciferase reading and average triplicates per sample.

NUCLEAR AND CYTOPLASMIC EXTRACTION

Thermo-Scientific "NE-PER Nuclear and Cytoplasmic Extraction Reagents"
Product# 78835
Store at 4°C.

Notes:

- Fresh cells/tissue samples.
- Inhibitors (protease and phosphatase) required (l:l00 for each)
- Centrifuge at 4°C.
- Keep all samples and extracts on ice.

Reagents:

- Protease inhibitors (cocktail 2 and 3), phosphatase inhibitor.
- Phosphate-buffer-saline (PBS - 0.1M phosphate, 0.15M NaCl. pH 7.2)
- CERI, CERII, NER (comes in kit).

Tissue preparation:

1. Place fresh tissue (gastrocnemius portion weighing ~40 mg) into a 1.5 mL Eppendorf containing PBS and inhibitors (100:1).
    a. Keep on ice until use.
2. Cut tissue into small pieces and place into a 20mL homogenizing tube using 400Ul of CERI.
3. Homogenize with a Dounce homogenizer.
    a. Go all the way to bottom and move up and down, slowly.
    b. Ensure you do not leave the solution and create an air bubble (keep pestle submerged).
    c. ~2-5 minutes.
4. Pour resultant suspension into l.5mL Eppendorf.

Cytoplasmic and nuclear protein extraction:

1. Vortex on highest setting for 15 seconds to suspend the tissue. Incubate on ice for 10 minutes.
2. Add ice-cold CERII (22ul) to the tube.
3. Vortex the tube for 10 seconds on the highest setting. Incubate on ice for 1 minute.
    a. Shake while vortexing.
4. Vortex the tube for 15 seconds on the highest setting. Centrifuge the tube for 10 minutes at maximum speed in a microcentrifuge (16,000g).
5. Immediately transfer the supernatant (cytoplasmic extract) to a clean pre-chilled tube. Place on ice until storage or use.
6. Wash pellet- suspend in PBS and spin at max for 30 seconds – 3X.
7. Suspend the pellet m NER (200uL).
8. Sonicate (3x3) at 30% power.
9. Vortex for 15 seconds and place on ice for 10 minutes - X4 (total of 40 minutes).
10. Centrifuge at max (16,000g) for 10 minutes.
11. Immediately transfer the supernatant (nuclear extract) to a clean, pre-chilled tube.
    a. Both the liquid and semi-solid phase.
12. Use immediately or store at -80°C.

IN VITRO mRNA DECAY ASSAY

Reagents:

1. Tri-reagent (Trizol poly-phenol)
2. Chloroform:Isopropanol mixture
3. Isopropanol

Preparation of cytosolic (S15) extracts:

1. Centrifuge the previously isolated cytosolic fraction supernate at 4°C for 15 minutes at 15000 g and transfer the resulting postmitochondrial supernate (S15) to a sterile 1.5ml Eppendorf.
2. Determine the protein concentration of the S15 fractions using the Braford total protein assay. These extracts can be used immediately in the assay, or store at -20°C.

***in vitro* decay reaction:**

1. Incubate total RNA (35µg) and S15 extract (20µg) in a sterile 700µl Eppendorf. Volume up the reaction to a 100µl with sterile water and incubate in a water bath set to 37°C.
2. A baseline control must be made, which allows for an estimation of the amount of RNA present in the sample not exposed to the S15 extract.
    a. This sample consists of total RNA (35µg) and 5ul homogenization buffer, volumed up to 100µl.
    b. Add 200µl Trizol to this reaction immediately, shake vigorously (~15 seconds) and set aside on ice.
3. Remove aliquots after selected time points (30, 60 and 90 minutes) and add 200µl of Trizol to stop the decay of the mRNA substrate.
    a. Shake vigorously (~15 seconds) and place on ice.
4. Once all samples have been collected at all time points, add 150µl of the Chloroform:Isopropanol mixture.

    a. Shake vigorously (~15 seconds) and rest at room temp for 2-3 minutes.
5. Centrifuge samples at 16,000g for 15 minutes at 4°C.
6. Immediately transfer the aqueous phase to a sterile 1.5ml Eppendorf.
7. Add 150µl of Isopropanol and shake vigorously (observe bubbles).
8. Precipitate samples at -20°C overnight.
9. The next day, let samples stand at room temperature for 10 minutes.
10. Centrifuge samples at 4°C for 10 minutes (16,000g).
11. Wash and resuspend the pellet with 700µl of 75% ethanol and spin in a tabletop centrifuge at 16,000g for 10 minutes (4°C).
12. Pour off the supernate, and air dry the pellets.
13. Resuspend the pellet in 10-20µl of sterile water.
14. Measure [RNA] and store samples at -80°C.

APPENDIX D: OTHER CONTRIBUTIONS TO THE LITERATURE

PEER-REVIEWED PUBLICATIONS

1. Memme, J.M., **Sanfrancesco, V. C**., & Hood, D. A. (2023). ATF4 regulates mitochondrial content, morphology, and function in skeletal muscle cells. *American Journal of Physiology, Cell Physiology.* 10.1152/ajpcell.00080.2023. Advance online publication.

2. Richards, B. J., Slavin, M., Oliveira, A. N., **Sanfrancesco, V. C**., & Hood, D. A. (2022). Mitochondrial protein import and UPR^{mt} in skeletal muscle remodeling and adaptation. *Seminars in cell & developmental biology*, S1084-9521(22)00004-0.

PUBLISHED ABSTRACTS AND CONFERENCE PROCEEDINGS

1. **Sanfrancesco V.C.,** Slavin M., & Hood D. A. (May 2023). The transcription factor ATF4 is responsive to mitochondrial stress following an acute bout of contractile activity. *Proceedings of Muscle Health Awareness Day*, 14th edition. Toronto, ON, Canada. May 19, 2023.

2. Gorman, R.A., Yakobov, S., Polidovitch, N., Debi, R., **Sanfrancesco, V.C.**, Hood, D.A., Lakin, R., & Backx., P.H. (May 2023). The Effects of Exercise Dose on Cardiac Responses and Atrial Fibrillation. *Proceedings of Muscle Health Awareness Day*, 14th edition. Toronto, ON, Canada. May 19, 2023.

3. Khemraj, P., **Sanfrancesco, V. C**., Oliveira, A. N., Gorman, R. A., Backx, P. H., &Hood, D. A. (May 2023). Investigating NLRP3 Inflammasome Activation in response to Chronic Denervation and Exercise Training. *Proceedings of Muscle Health Awareness Day*, 14th edition. Toronto, ON, Canada. May 19, 2023.

4. **Sanfrancesco V.C.**, Memme J.M., & Hood D.A. (November 2022). The role of ATF4 in mediating skeletal muscle function during acute contractile activity. CSEP. *Journal of Applied Physiology, Nutrition and Metabolism*. In Press, 2022. Fredericton, New Brunswick, Canada.

5. Memme J.M., **Sanfrancesco V.C.**, & Hood D.A (May 2022). ATF4 preserves mitochondrial function and remodeling during myotube differentiation and contractile activity. *International Biochemistry of Exercise Conference*. In Press, 2022. Toronto, Ontario, Canada.

6. Memme J.M., **Sanfrancesco V.C.**, & Hood D.A. (April 2022). Determining the role of ATF4 in the regulation of mitochondrial remodeling during myotube differentiation and contractile activity. *Experimental Biology*. FASEB Journal. In press, 2022. Philadelphia, PA, USA.

ORAL PRESENTATIONS

1. The role of ATF4 in mediating skeletal muscle function during acute contractile activity. KAHS Graduate Seminar 2023. York University, Toronto, ON., Canada. January 2023.